

2017

Understanding Pregnancy Centered Medications: Characterizing the Interactions of a Series of Sulfonylurea Analogs and the ATP Binding Cassette Transporter Proteins, P-Glycoprotein and Breast Cancer Resistance Protein

Samuel D. Bell
University of Rhode Island, sbell@chm.uri.edu

Follow this and additional works at: https://digitalcommons.uri.edu/oa_diss

Terms of Use

All rights reserved under copyright.

Recommended Citation

Bell, Samuel D., "Understanding Pregnancy Centered Medications: Characterizing the Interactions of a Series of Sulfonylurea Analogs and the ATP Binding Cassette Transporter Proteins, P-Glycoprotein and Breast Cancer Resistance Protein" (2017). *Open Access Dissertations*. Paper 747.
https://digitalcommons.uri.edu/oa_diss/747

This Dissertation is brought to you by the University of Rhode Island. It has been accepted for inclusion in Open Access Dissertations by an authorized administrator of DigitalCommons@URI. For more information, please contact digitalcommons-group@uri.edu. For permission to reuse copyrighted content, contact the author directly.

UNDERSTANDING PREGNANCY CENTERED
MEDICATIONS: CHARACTERIZING THE
INTERACTIONS OF A SERIES OF SULFONYLUREA
ANALOGS AND THE ATP BINDING CASSETTE
TRANSPORTER PROTEINS, P-GLYCOPROTEIN AND
BREAST CANCER RESISTANCE PROTEIN

BY

SAMUEL D BELL

A DISSERTATION SUBMITTED IN PARTIAL FULFILLMENT OF THE
REQUIREMENTS FOR THE DEGREE OF
DOCTOR OF PHILOSOPHY
IN
CHEMISTRY

UNIVERSITY OF RHODE ISLAND

2017

DOCTOR OF PHILOSOPHY DISSERTATION

OF

SAMUEL D BELL

APPROVED:

Dissertation Committee:

Major Professor William Euler

Brian Bronk

Niall Howlett

Nasser H. Zawia
DEAN OF THE GRADUATE SCHOOL

UNIVERSITY OF RHODE ISLAND
2017

ABSTRACT

The oral hypoglycemic agent Glyburide has been shown to be actively transported from various biological tissues through a pronounced interaction with the ATP binding cassette (ABC) active transport proteins. Specifically, Glyburide is actively transported by the ABC proteins, P-glycoprotein (Pgp), Breast Cancer Resistance Protein (BCRP), and the Multidrug Resistance Proteins (MRP). This active transport occurs at various locations throughout the body but has been identified as being responsible for Glyburide's unique placental transport behavior. Glyburide has been shown to not cross the placental barrier to any appreciable effect and will leave the placental barrier against the concentration gradient. Understanding this active transport creates the possibility of medicines designed specifically for pregnant women. The objective of this thesis is to investigate the activity of Glyburide and a series of sulfonylurea analogs against these two ABC transporter proteins.

The transport of Glyburide and a series of sulfonylurea analogs in the presence of P-glycoprotein (Pgp) and breast cancer resistance protein (BCRP) was investigated in cell-based transport assays using two stably transfected Madin-Darby Canine Kidney cell lines, one overexpressing Pgp and the other overexpressing BCRP genes. The results of the transport studies confirm that both Pgp and BCRP play a role in the transport of the sulfonylureas. Further, in addition to Glyburide, the molecules Glimepiride, Glisoxepide, and Gliquidone were confirmed as Pgp and BCRP substrates, all of which has not previously been reported.

Subsequently, the sulfonylurea transport activity with both Pgp and BCRP were used as the basis to build quantitative structure activity relationship (QSAR) and

pharmacophore models. These models suggest that there are core molecular features necessary for the Pgp and BCRP activity, specifically that the arylsulfonyleurea and benzamido ligands are required for both activities. We also found that increased hydrophobic character and increased bulky groups are key to both activities. The main differences in the activities were surrounding the sulfonyleurea and amide moieties, with positive charge increasing the BCRP activity, and negative charge increasing the Pgp activity. Overall, the results of this research serve to provide improved knowledge for the design of pregnancy centered medications.

ACKNOWLEDGMENTS

Foremost I would like to thank my advisor, Prof. William Euler. The only reason this thesis work was possible was due to his kind mentoring, patience, flexibility, and the occasional jab to keep me moving. I will always be grateful for your time, and the mentoring and guidance you have given me over the years. And, I truly could not have asked for a better PhD advisor – thank you for everything.

I am forever indebted to Brian Bronk – colleague and friend. Your patience to allow me to grow into this body of work and complete it on my time has been an invaluable growth opportunity for me. Thank you for the discussions, listening to the crazy ideas, honing it down to one crazy idea, and finally for the all the guidance through the writing and defense. Your support and encouragement has meant more than you know.

To my committee members, David Rowland and Niall Howlett, thank you both so very much for taking the time to guide me through this process. The time you spent, and the schedules you had to rearrange to make this all happen was not lost on me - thank you for making this happen.

I would also like to Robert Chapin and Douglas Spracklin for the long discussions and guidance you provided me along the way. I look back fondly at the times we spent together, and sincerely thank you for being a part of this journey.

I am also incredibly grateful to Pfizer Global Research, for my time spent there and the opportunities I was given. To my supervisors and mentors, Amy Antipas and Marc Tesconi for the wonderful support and encouragement over the years; Ken Waterman for his wonderful support and for suggesting I start this journey to begin with. And to my colleagues and friends who helped me along the way, from the cell transport

assays, through many discussions on the theory - Matthew Troutman, Ayman el Kattan, James Federico, Charles Rotter, Carrie Whitney-Picket, and Ralph Davidson- thank you all so very much.

Also, I am incredibly grateful to my colleagues at Boehringer-Ingelheim and the encouragement that I was always given. To Loic le Hir de Fallois and the rest of the DISCO team, I will always be thankful for the encouragement, support, and excitement you showed me as I was finishing this journey.

To my family, for always believing in me and allowing me the time to make this happen. To my four beautiful ladies, my wife Renee and my three girls, Abby, Kaity Bell, and Gracie – your support over the years has meant the world to me, and I love you all so much. I could not have done this without you, and thank you so, so much for sacrificing so much to let me complete this dream.

And finally, for Jesus, in whom all things are possible. Amen.

PREFACE

This dissertation is submitted for the degree of Doctor of Philosophy at the University of Rhode Island. The research described herein was conducted under the supervision of Professor William Euler in the Department of Chemistry, University of Rhode Island, between August 2009 and December 2017.

This work is to the best of my knowledge original, except where acknowledgements and references are made to previous work. Neither this, nor any substantially similar dissertation has been or is being submitted for any other degree, diploma, or other qualification at any other university.

This thesis is presented in Manuscript formatting.

TABLE OF CONTENTS

ABSTRACT.....	ii
ACKNOWLEDGMENTS	iv
PREFACE	vi
TABLE OF CONTENTS.....	vii
LIST OF TABLES	x
LIST OF FIGURES	xi
CHAPTER 1	1
Manuscript Submission Statement.....	1
INTRODUCTION AND REVIEW OF LITERATURE	2
Sulfonylureas for Type II Diabetes	5
Similarities Between Type II Diabetes and Gestational Diabetes States.....	6
Challenges of Gestational Diabetes Treatment to Mother and Fetus.....	9
Transporter Story	11
Problem Statement and Summary of Remaining Sections of Thesis.....	13
CHAPTER 2	16
Manuscript Submission Statement	16
QSAR MODELS OF SULFONYLUREA AND Pgp/BCRP ACTIVITY	16
Abstract.....	17
Introduction	18
Materials and Methods	21
Cell Cultures	22

Transporter Assay Procedures	23
LC-MS Analysis	24
Data Analysis	24
Cell Assay Materials.....	25
Computational Modeling	26
Experimental	30
Mathematical Models	34
QSAR Discussion	35
Pgp 2D QSAR Modeling Discussion.....	40
BCRP 2D QSAR Modeling Discussion.....	46
Pgp 3D QSAR Modeling Discussion	53
BCRP 3D QSAR Modeling Discussion.....	59
Pharmacophore Modeling Discussion	64
Sulfonylurea-Pgp Pharmacophore Discussion.....	67
Sulfonylurea-BCRP Pharmacophore Discussion.....	69
Pharmacophore Discussion	70
General Discussion	71
Conclusion	79
CHAPTER 3	82
Manuscript Submission Statement	82
COMPARISON OF Pgp AND BCRP MODELS.....	82
Abstract	83
Introduction.....	84

Data Set	86
Conformational Hunt and Alignment of Molecules	87
Activity Atlas Modeling.....	88
Activity Cliff Modeling	89
Average of Actives Modeling	90
Results	91
Electrostatics Average Summary	98
Hydrophobics Average Summary	100
Shape Summary	102
Discussion	103
Conclusion	107
CHAPTER 4	109
Manuscript Submission Statement	109
Designing Pregnancy Centered Medications: Insights and Recommendations.....	110
APPENDICES	
APPENDIX I Sulfonilyrea Structures and Representative Pgp Activity	117
APPENDIX II Sulfonilyrea Structures and Representative BCRP Activity	120
APPENDIX III VLifeMDS® Molecular Descriptors	127
BIBLIOGRAPHY	143

LIST OF TABLES

TABLE	PAGE
Table 1. Statistical results of 2D QSAR kNN Model 58 for the Sulfonylurea-Pgp activity.....	41
Table 2. Molecular Descriptors used in Pgp 2D QSAR Study	42
Table 3. 78 Molecules used in Pgp Study with experimental, predicted, and residual activity values.....	44
Table 4. Comparison of the 3-6-9 nearest neighbors Models for Pgp	45
Table 5. Statistical results of BCRP 2D QSAR MLR model.....	47
Table 6. Molecular Descriptors used in the BCRP 2D QSAR Study.	49
Table 7. 54 Molecules used in the BCRP study with experimental, predicted, residual activity values.....	51
Table 8. Descriptors shared by both Pgp and BCRP 2D QSAR Models	52
Table 9. The Pgp 3D QSAR Model statistical parameters and values.....	54
Table 10. 78 Molecules used in the Pgp study with experimental, predicted, residual activity values.....	58
Table 11. The BCRP 3D QSAR Model statistical parameters and values	60
Table 12. 54 Molecules used in the BCRP study with experimental, predicted, residual activity values.....	64

LIST OF FIGURES

FIGURE	PAGE
Figure 1. Sulfonylurea backbone structure.....	2
Figure 2. Representative structures of the first-generation sulfonylurea hypoglycemic agents.	3
Figure 3. Representative structures of the second-generation sulfonylurea hypoglycemic agents	4
Figure 4. Biding Site of SUR1 protein and 1 st and 2 nd generation SUs structural map	5
Figure 5. The mechanism of glucose dependent insulin release in pancreatic β - cells.	6
Figure 6. Structures of two categories of ABC transporters, Pgp (ABCB1-MDR1) and MRPs are shown on top, BCRP (ABCG2) shown on bottom.	13
Figure 7. Modulation of insulin by the sulfonylureas, reproduced from Tahrani et al.	19
Figure 8. Structures of the Glyburide and the sulfonylurea backbone.....	20
Figure 9. Cell Transport Assay Monolayer insert setup for Pgp and BCRP assays....	24
Figure 10. Molecular Overlay of MMFF94 energy minimized molecules.....	28
Figure 11. Glyburide molecule with the sulfonylurea backbone template (highlighted in red).	28
Figure 12. Energy minimized MMFF94 structure of Glyburide.....	29

Figure 13. Bar graphs showing asymmetric absorption and efflux of Glyburide, Glimepiride, Gliquidone, and Glisoxepide. <i>Note: A denotes A-B transport; B denotes B-A transport</i>	32
Figure 14. Map of all 78 compounds and the respective log P _{app} activity.....	33
Figure 15. Map of all 53 compounds and the respective log BCRP P _{app} activity	34
Figure 16. Graphical representation of predicted Pgp activity vs. experimental activity for the training and test sets for kNN Model 58.....	41
Figure 17. Predicted BCRP activity vs. experimental activity for the training and test sets for model 89	48
Figure 18. Graph depicting 2D QSAR variables and % contributions	50
Figure 19. Graphical representation of predicted Pgp activity vs. actual activity for the training and test sets for MLR Model 10.....	55
Figure 20. Steric and Electrostatic descriptors contributions for the 3D QSAR modeling of Pgp activity for 3D QSAR del re energy minimization.....	56
Figure 21. Glyburide molecule showing the points of 3D model.	56
Figure 22. Graphical representation of predicted BCRP activity vs. actual activity for the training and test sets for MLR Model 65.....	60
Figure 23. Steric and Electrostatic descriptors contribution plots for the 3D QSAR modeling of BCRP activity for 3D QSAR Model 65 Gasteiger- Marsili energy minimization.....	61
Figure 24. Field point model detailing steric and electrostatic descriptors for the 3D QSAR modeling of BCRP	62

Figure 25. Glyburide Pharmacophore features.....	65
Figure 26. Glyburide-Pgp Pharmacophore detailing the 5 points of interest.....	68
Figure 27. Sulfonylurea-BRCP Pharmacophore denoting the para position of the arylsulfonylurea ring.....	68
Figure 28. Glyburide-BCRP Pharmacophore detailing the 5 points of interest.....	69
Figure 29. Simple diagrams of key pharmacophore features of the Pgp (left) and BCRP (right) models, superimposed on the molecule Glyburide. Key: green aromatic, blue hydrogen acceptor, red hydrogen donator, and orange hydrophobic	75
Figure 30. Core structure of sulfonylurea with the potential ligands that can increase or decrease the activity for both Pgp and BCRP	76
Figure 31. Representative binding sites on SUR1, tolbutamide and glyburide presented as examples, reproduced from Vila-Carriles <i>et al</i>	78
Figure 32. Key features in Glyburide-Pgp interaction, reproduced from Bessadock. Key: green is aromatic red is hydrogen donating, blue is hydrogen accepting groups.....	79
Figure 33. Glyburide, Glipizide, and Gliclazide structures	85
Figure 34. Activity map of the sulfonylurea analogs tested in the Pgp and BCRP efflux assays.....	92
Figure 35. Pgp (left) and BCRP (right) pharmacophores.....	93
Figure 36. 3D field points describing model space for Pgp and BCRP Pharmacophores.....	94

Figure 37. Activity cliff summary maps describing the sulfonylurea-Pgp (top) and sulfonylurea-BCRP (bottom) activity.	96
Figure 38. Summary of electrostatics activity for sulfonylurea interaction with Pgp (top) and BCRP (bottom).....	98
Figure 39. Summary of hydrophobics activity for sulfonylurea interaction with Pgp (left) and BCRP (right).....	100
Figure 40. Summary of shape activity for sulfonylurea interaction with Pgp (left) and BCRP (right).	102
Figure 41. Summary of Activity Atlas modeling for the Pgp and BCRP models on Glyburide.	106
Figure 42. Core structures highlighting the arylsulfonylurea (dark blue) and the benzamido (light blue) ligand.....	112
Figure 43. Summary of Activity Atlas modeling for the Pgp and BCRP models on Glyburide.	113
Figure 44. Glyburide low energy conformation used in our research.....	114

CHAPTER 1

Review of the Sulfonylurea Hypoglycemic Agents Unique Placental Transport due to
the ATP Binding Cassette Proteins

by

Samuel D Bell¹ ; Brian Bronk² ; William Euler³

is submitted to Current Opinion in Pharmacology

¹ PhD Candidate, Department of Chemistry, The University of Rhode Island, Kingston, RI 02881. Email: sbell@chm.uri.edu

² Adjunct Professor, Department of Chemistry, The University of Rhode Island, Kingston, RI, 02881. Email: brian.bronk@sanofi.com

³ Professor, Department of Chemistry, The University of Rhode Island, Kingston, RI, 02881. Email: weuler@chm.uri.edu

INTRODUCTION

Glyburide (generic, glibenclamide) is a small molecule sulfonylurea used for the treatment of hyperglycemia. Glyburide is the most prescribed small molecule for the first line of defense or the treatment of Type II Diabetes due to its very attractive pharmacological profile.¹ The sulfonylurea compounds were first discovered by Janbon *et al.*; when researching sulfonamides in patients with typhoid fever, the team noted hypoglycemic results, leading to introduction of sulfonylureas to treat hyperglycemia into the US commercial market in 1955.² The sulfonylureas have evolved over two generations, though each generation shares the same core sulfonylurea backbone as presented in Figure 1.

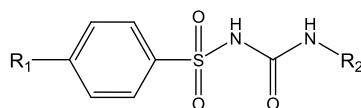


Figure 1. Sulfonylurea backbone.

Sulfonylureas development has been sixty years in the making, with the first-generation molecules developed in 1950-1980's, and the second-generation molecules developed during the 1980-1990's. The two generations of sulfonylureas differ in the physical-chemical attributes, and subsequent pharmacokinetic/pharmacodynamic (PK/PD) parameters, with the latter generation having an increased safety and efficacy.³ The improvements to the physical-chemical and PK/PD parameters are due to the structural changes at the para position on the central aryl ring (R_1) and functional group R_2 attached to the remote urea position, as detailed in Figure 1. The first-generation

sulfonylureas have smaller molecular weights, with more polar and hydrophilic substituents. The second-generation sulfonylureas have larger molecular weights, containing more non-polar lipophilic substituents. This increased lipophilic character allows for easier membrane permeability, and therefore an increased potency. This is an important point to discuss as the target protein, the sulfonylurea receptor (SUR1), is membrane bound protein, and having molecules with an increased hydrophobicity allows for the molecules to penetrate the membrane more readily, reaching the receptor more efficiently.⁴ The commercial sulfonylurea structures are presented in Figures 2 and 3.

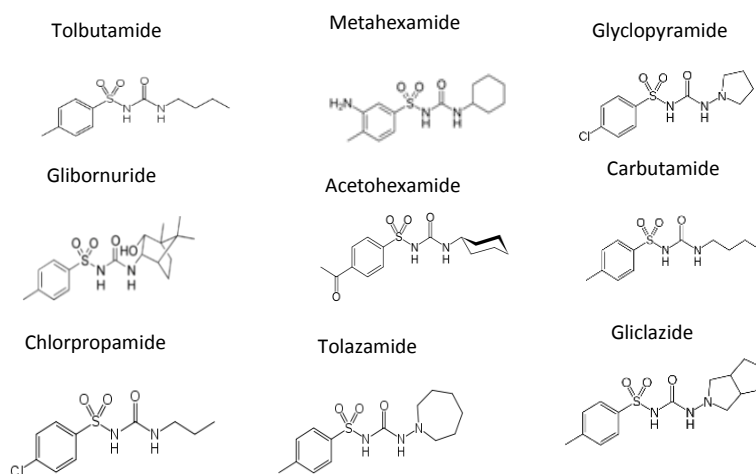


Figure 2. Representative structures of the first-generation sulfonylurea hypoglycemic agents.

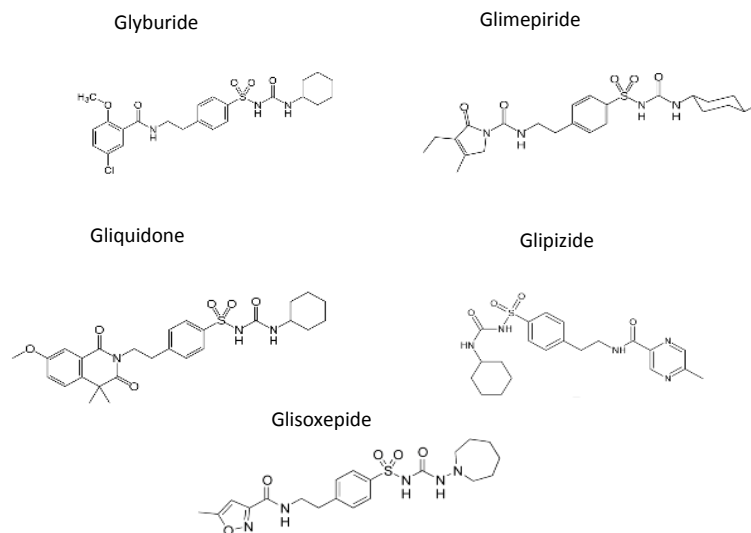


Figure 3. Representative structures of the second-generation sulfonylurea hypoglycemic agents.

As expected, the similarity of the core structure of the first and second-generation sulfonylureas allow for a similar response to reducing hyperglycemia.⁵ This can be explained in the structure activity relationship research performed for the development of the sulfonylureas, as demonstrated by an increase in binding affinity for the sulfonylurea receptor 1 (SUR1). The SUR1 receptor is an active transporter that has been shown to have multiple binding sites, A and B, with the more potent second-generation molecules believed to bind to both the A and B sites. For reference, the molecules tolbutamide (1st gen) and glyburide (2nd gen) and the representative binding sites of SUR1 are presented in Figure 4.⁶ This increased structure activity relationship (SAR) work also presents as a longer half-life, higher lipophilicity, and increased plasma protein binding adding to the increase in efficacy and safety.⁷

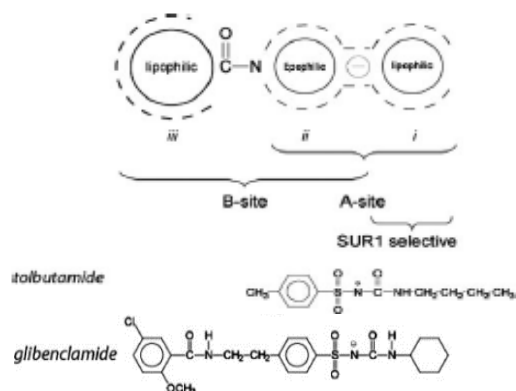


Figure 4. Binding Site of SUR1 protein and 1st and 2nd generation SUs structural map.⁸

SULFONYLUREAS FOR TYPE II DIABETES

The sulfonylurea chemical class has been widely used in the treatment of hyperglycemia for more than sixty years and is now a popular choice for a first line of treatment in diabetes care. Specifically, the sulfonylureas have become an integral treatment option for those patients who have not maintained or achieved adequate glycemic control through diet and exercise alone.^{9,10,11} The sulfonylureas work by binding to the SUR1 receptor, which triggers the cascade of two signal pathways that release insulin in the pancreatic β -cell. The first pathway is the ATP-sensitive potassium channel (K_{ATP}) pathway and is the link between glucose metabolism and the stimulation of insulin production. The second pathway is a glucose signaling pathway and augments the insulin release due to the increase in the Ca^{2+} concentration.¹² In this respect, the sulfonylureas are insulin secretagogues, meaning that the mode of action is similar to that of insulin, stimulating the ATP sensitive Potassium (K_{ATP}) channels within the pancreatic β - cells.¹³ In summary, this action stimulates the insulin release via the occupation of the β -cell membrane SUR1.^{14,15,16} In response to an increase in blood

glucose concentrations, the enhanced rate of glucose metabolism causes the changes in concentrations of the adenosine diphosphate (ADP) and adenosine triphosphate (ATP), driving the closure of the pore. The depolarization of the cell membrane is due to a decrease in the K^+ permeability into the cell and an opening of the Ca^{2+} channels. This enhancement of the Ca^{2+} influx across the cell membrane is the final step of the cascade and triggers the release of insulin.¹⁷ The dual pathway mechanism of insulin release in the pancreatic beta cells is depicted in Figure 5.

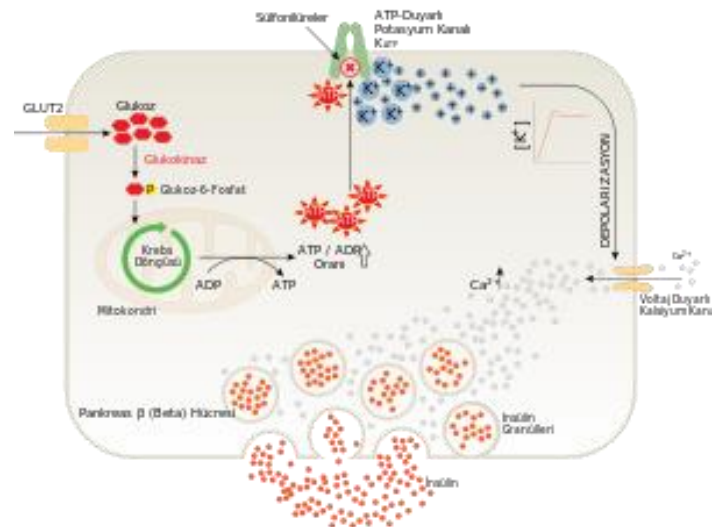


Figure 5. The mechanism of glucose dependent insulin release in pancreatic β - cells.¹⁸

SIMILARITIES BETWEEN T2D AND GESTATIONAL DIABETES MELLITUS STATES

As part of normal function, the body needs to regulate insulin production as a direct response to the increase or decrease in blood sugar levels after food consumption. There are two states of blood sugar levels, hyperglycemia and hypoglycemia, which represent too much and too little blood sugar, respectively. Hyperglycemia can be a chronic

condition in which the body's inability to produce any or enough insulin causes elevated levels of glucose in the blood, and are known as Type I and Type II Diabetes, respectively.¹⁹ Both types of Diabetes are characterized by an insulin resistance and a resultant insulin deficiency. In general terms, Type I diabetes is an autoimmune disorder leading to the destruction of pancreatic beta cells and hence the body's inability to produce insulin; and Type II Diabetes is primarily a problem of progressively impaired glucose regulation due to the dysfunction of the pancreatic beta cells and general insulin resistance.^{20, 21} . Also, Type II diabetes is influenced by many genetic and environmental factors, such as obesity and overweight contributing to the insulin resistance, compounding the issue.²² Researchers have found that the occurrence rate of Type 1 vs Type 2 Diabetes is approximately 10% and 90%, respectively, regardless of country or population.²³

Type I diabetes has only one treatment option, daily injections of insulin to directly manage blood sugar levels. Type II diabetes, however, has multiple treatment options available, including diet, exercise, pharmacological treatment, or a mix of all three. The bulk of the Type II case are treatable with diet and exercise changes alone, with only approximately 30% of Type II patients requiring pharmacological treatment.²⁴

This inability to control blood glucose levels occurs in pregnant women and is referred to as pregnancy induced gestational diabetes mellitus (GDM). The definition of GDM is carbohydrate intolerance resulting in hyperglycemia, with the onset or recognition occurring during pregnancy.²⁵ GDM is a well characterized disease affecting a large portion of the population and has been widely linked to the weight gain associated with pregnancy.²⁶ Although the exact cause of GDM is not known, there are some theories

that may explain the condition and why it occurs. During pregnancy, the placenta supplies the fetus with nutrient and water, and produces hormones to maintain the pregnancy throughout gestation. Some of these hormones produces a contra-insulin effect, blocking the normal function of insulin. As the gestational period goes on, the placenta grows, produces more hormones, and the increase of insulin resistance becomes greater. Under normal circumstances, and normal pancreatic function, there would simply be an increase in insulin production to compensate for the state of insulin resistance. However, when the production of insulin is somehow blocked by the effect of the placental hormones, GDM can occur. GDM occurs in up to 20% of all pregnancy globally, depending on country, population demographic and lifestyle, though approximately 30-40% requiring pharmacological treatment.^{27, 28, 29, 30}

Type II and GDM are characterized by insulin resistance and a subsequent insulin deficiency, and numerous studies have demonstrated that the rate of occurrence within a population of GDM to Type II Diabetes are similar.³¹ However, the one real difference between Type II and GDM is that pregnancy is a state of increasing insulin resistance, as the need to provide a constant supply of nutrients to the fetus. This pathological increase in insulin resistance, diminished sensitivity and impaired insulin secretion due to various conditions of pregnancy, which runs counter to the need of the developing fetus and produces a serious condition of hyperglycemia in the mother.³² So, the goal of any Diabetes-related management during pregnancy is to maintain blood glucose as close to normal as possible.

CHALLENGES OF GDM TREATMENT TO MOTHER AND FETUS

As noted, GDM occurs in a significant number of pregnancies globally, and is considered a risk factor for Type II Diabetes for the mother. There is a great deal of evidence that proves the treatment of GDM is far better than not treating GDM. In fact, common conditions are drastically reduced through treatment options, saving the mother and fetus from hypertension, preeclampsia, urinary tract infections, development of Type II diabetes later in life in mothers and child, as well as macrosomia, neonatal hypoglycemia, and childhood obesity.³³ Leaving these conditions untreated will potentially cause harm to the mother and fetus, and requires chronic maintenance through proper diet, exercise and pharmacological treatment.³⁴

Therefore, to be a successful medication for GDM, the need to control blood glucose in a similar manner to insulin, while maintaining the safety of the mother and fetus paramount. Prescribing drugs in pregnancy represents an unusual situation that must be constantly monitored. Drugs that will help the mother can deform or kill the fetus.³⁵

This is well characterized that there are a small group of drugs that are known to cause adverse events or birth defects in humans, but the safety or harm to the fetus must not be exaggerated. Today, the importance of monitoring the pregnant woman and fetus for harm is well understood, but initially, the placenta was thought to be a barrier, protecting the fetus from harm and the mother's blood, and delivering only what's needed, for example essential nutrients. The Thalidomide disaster of the 1950's demonstrated that the placenta was a very leaky barrier, and that precautions must be taken when treating pregnant women with medicines, as it is now understood that many substances will cross the placenta.³⁶ Treatment conditions of the mother quickly accounts for how much harm

will be done to the fetus, and that can be determined by the rate and extent of the of the drug concentration that crosses the placenta, and at what gestational stage.³⁷

For those patients that cannot manage the hyperglycemia with diet and exercise alone, the preferred pharmacological treatment option for diabetes has been insulin. The same approach is taken for GDM, with insulin as the first line of treatment due to its high efficacy, safety, and the fact that the higher molecular weight insulin cannot cross the placenta barrier.^{38,39} Insulin treatment however, suffers from compliance issues and in some countries the cost is prohibitive.⁴⁰ Specific to pregnant women, the insulin route of administration and the schedule of treatments present numerous difficulties.⁴¹ Due to the similarities in GDM and Type II conditions, and the ease of treatment for oral medications, doctors have explored treating GDM with the small molecule sulfonylureas.^{42,43}

In order for the sulfonylureas to be effective in the treatment of diabetes, the patient needs to have retained some level of pancreatic insulin-releasing function.⁴⁴ This holds true for GDM based on the similarities of the pathophysiology with Type II, the sulfonylurea compounds are an excellent choice for treating either condition.^{45,46} In fact, there is a growing acceptance of Glyburide as a treatment option for GDM, based on the attractive pharmacological response and low potential adverse side effects (i.e., neonatal hypoglycemia), making the sulfonylurea(s) a viable option based on compliance, and overall mother and fetal outcomes.^{47,48,49}

Considerable data exists suggesting that Glyburide is a safe alternative to insulin for treatment of GDM.⁵⁰ Numerous clinical studies, and five retrospective studies, have been performed on thousands of pregnant women who were taking Glyburide. These

studies have been performed to understand the pharmacokinetics and pharmacodynamics of Glyburide during pregnancy, and many interesting results have been demonstrated. In these multiple, large, randomly controlled clinical studies, Glyburide has been shown to be as safe and effective as insulin in pregnant women.^{51, 52, 53, 54, 55} Further, placental drug transport studies have demonstrated two key findings: Glyburide does not cross the placenta to any appreciable extent, and Glyburide will leave the placental barrier against the concentration gradient.^{56, 57, 58, 59, 60} This represents an ideal situation for treating pregnant women and has garnered much excitement.

TRANSPORTER STORY

The placental transport studies have demonstrated that Glyburide is a substrate for active transport by the ATP Binding Cassette (ABC) transporter proteins specifically P-glycoprotein (Pgp), Breast Cancer Resistance Protein (BCRP), and the Multiple Resistance Protein (MRP) family.^{61, 62, 63, 64, 65} The ABC transporter proteins are part of a larger class of drug transporters, with a primary function to transport nutrients and endogenous substrates (sugars, amino acids, vitamins), and to protect the body from dietary and environmental toxins.⁶⁶ As the transporters are designed to transport substrates of a wide physiologic background, drugs that are similar in structure to the physiological substrate can also be transported. It is in this functionality and the ability to transport a broad range of substrates that the drug transporters play a significant role in the bioavailability, efficacy and PK of most drugs.⁶⁷

Transport of drugs can be classified in a variety of ways, with the main characterizations being directional (efflux vs influx), and through energy vs non-energy dependent (active

or passive) means. For the context of the work reported here, we will focus on the efflux by active transport systems, which have been further classified into two main categories, primary and secondary. The primary systems utilize ATP hydrolysis to drive the transport and include the ABC transporters. The secondary systems are ones that utilize multiple driving forces such as ion concentration gradients, and electric potential difference across the cell membrane, an example is the Solute Carrier transporters (SLC).^{68, 69}

The ABC proteins of the human genome comprise a family of 49 proteins, and based on their amino acid sequence, are divided into roughly 7 sub-families. As ABC transporters serve a protection function, they are found in most tissues at barrier locations throughout the body, such as brain, testes, heart, liver, kidney, and gastrointestinal tract. Transporter proteins are membrane-bound proteins whose primary function is to facilitate the flux of molecules in and out of cells, protecting from toxins.^{70,71, 72} The ABC drug transporters have a diverse substrate pool; as such, many molecules that bear structural similarities to the endogenous compounds may be recognized and transported. This diverse set of substrates covers molecules that are nonpolar, weakly amphiphilic, and encompass a diverse group of compounds from anti-cancer drugs to natural products.^{73, 74, 75}

As illustrated in Figure 4, all ABC Transporter proteins share similar structural components, consisting of 4 different domains: two transmembrane and two cytosolic domains. The transmembrane domains (TMD) consist of alpha helices (in groups of 5-6) embedded in the membrane bilayer, with the ability to recognize and transport a broad range of substrates by changing conformations. The nucleoside binding domains (NBD)

is the location of the binding of ATP that drives the transport mechanism, containing the Walker A and B motifs for this function.⁷⁶ A complete transporter structure is considered a homo-dimer or a fully functional transporter, example of which are Pgp, MRP, and OATP. The exception to this requires the two smaller monomer structures to pair together to form a homodimer, an example of this is BCRP.

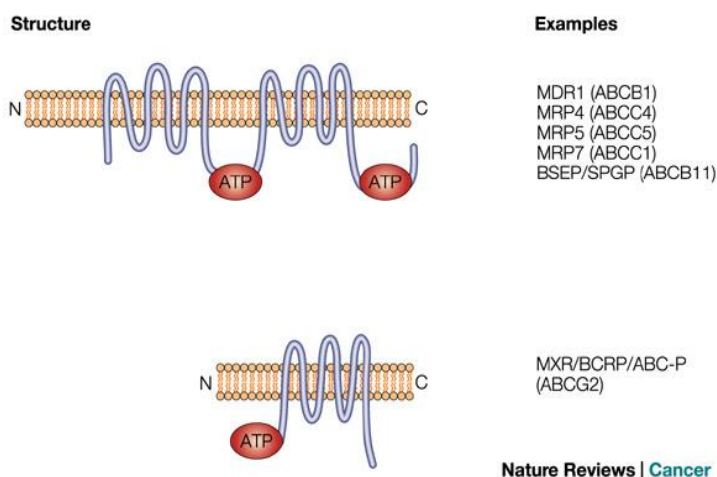


Figure 6. Structures of two categories of ABC transporters, Pgp (ABCB1-MDR1) and MRPs are shown on top, BCRP (ABCG2) shown on bottom.⁷⁷

PROBLEM STATEMENT AND SUMMARY OF REMAINING SECTIONS OF THESIS

The ABC transporters described above in Figure 6 hold the key to the unique placental transport of Glyburide. As discussed, the oral hypoglycemic sulfonylurea molecule Glyburide has been shown to be actively transported through a pronounced interaction with the ATP binding cassette (ABC) active transporter proteins. This unique placental transport behavior is largely due to the primary transport resulting in the efflux of

Glyburide by Pgp and BCRP, minimizing the effect of the drug on the fetus.

Specifically, the small molecule Glyburide has been shown to not cross the placental barrier to any appreciable effect; and, Glyburide will leave the fetal compartment against the concentration gradient (active efflux).⁷⁸ The research presented here will focus on understanding this unique placental transport to design medications for pregnant women that are safe and effective, without presenting harm to the mother or fetus.

There is a great deal of research detailing the mechanism of action of the sulfonylureas, the PK/PD of the sulfonylureas during pregnancy, and even the specific ABC transporter proteins responsible for the unique placental transport behavior. However, there has been no research to date to explain the nature of the interaction with the ABC transporter proteins to better design pregnancy centered drugs. The research presented here will look to explain the interactions of a series of sulfonylurea analogs and two of the main ABC proteins responsible for active drug transport, BCRP and Pgp. The work described in this body of work was performed in cell-based transport assays using cell lines that overexpress Pgp or BCRP, and molecular modeling software packages to build structure activity models based on the transport activity.

In the coming chapters we will explore the interaction of the sulfonylureas with the two transporters, individually, building quantitative structure activity relationships (QSAR), and then complete the body of work with molecular modeling highlighting the molecular descriptors/features that drive the affinity to one transporter or the other. In Chapter 2 we will evaluate the sulfonylurea analogs using Madin-Darby Kidney Cells (MDCK) that overexpress Pgp and BCRP proteins, ultimately building 2D, 3D-QSAR and pharmacophore models using the molecular dynamics modeling software VLifeMDS®

to explain the molecule-protein interaction. And finally, in Chapter 3, we will detail and explain the similarities and differences between the two molecule-protein interactions, using the molecular modeling software Cresset Group Forge®. The outcome of this research will be to characterize the molecular features driving the interactions with the ABC transporter proteins, in the hope that this knowledge will help design novel pregnancy centered medications.

CHAPTER 2

Quantitative Structure Activity Relationship for a Series of Sulfonylurea Analogs and two ATP Binding Cassette Proteins, P-glycoprotein and Breast Cancer Resistance Protein

by

Samuel D Bell⁴; Brian Bronk⁵; William Euler⁶

is submitted to Molecular Pharmaceutics

⁴ PhD Candidate, Department of Chemistry, The University of Rhode Island, Kingston, RI 02881. Email: sbell@chm.uri.edu

⁵ Adjunct Professor, Department of Chemistry, The University of Rhode Island, Kingston, RI, 02881. Email: brian.bronk@sanofi.com

⁶ Professor, Department of Chemistry, The University of Rhode Island, Kingston, RI, 02881. Email: weuler@chm.uri.edu

**Quantitative Structure Activity Relationship for a Series of Sulfonylurea Analogs
and two ATP Binding Cassette Proteins, P-glycoprotein and Breast Cancer
Resistance Protein**

ABSTRACT

Sulfonylureas used in the treatment of Type II diabetes have been shown to interact with the ATP binding cassette (ABC) active transporters, P-glycoprotein (Pgp) and Breast Cancer Resistance Protein (BCRP). Starting from a series of sulfonylurea compounds, two and three-dimensional quantitative structure activity relationship (QSAR) studies were performed to determine the essential molecular features responsible for the Pgp and BCRP mediated transport. For the both the 2D and 3D QSARs, numerous models were developed and evaluated in an effort to correlate the physico-chemical features of the sulfonylureas with the biological interaction with Pgp or BCRP. In our studies, the 2D Pgp QSAR model with the best prediction capability was found to be a k-Nearest Neighbor (kNN) model for substrate activity with a $q^2 = 0.7152$, and a $r^2 = 0.8150$. For the 3D Pgp QSAR model with the best prediction capability, a multiple regression model for substrate activity performed best, with an $r^2 = 0.8304$, a cross-validation $q^2 = 0.7501$. In contrast, the 2D BCRP QSAR model with the best prediction capability was a multiple linear regression (MLR) model for substrate activity with a $q^2 = 0.8690$, and a $r^2 = 0.8131$. Similarly, the 3D BCRP QSAR model with the best prediction capability was a multiple regression model for substrate activity with an $r^2 = 0.9063$, a cross-validation $q^2 = 0.7789$. All models were cross validated with an autonomous set of compounds not used in the training or test sets.

As previously reported, Glyburide has been shown to be a substrate for numerous ABC transporters, but this is the first comprehensive QSAR study designed to understand the interaction driving the active transport of the entire class of sulfonylureas specifically with the two ABC transporters, Pgp and BCRP. The physico-chemical properties and molecular descriptors of the sulfonylureas were used to build three-dimensional pharmacophores to further understand the interactions with Pgp and BCRP. Each pharmacophore model contained five features found to be essential for identification as a Pgp or BCRP substrate: one hydrogen bond donor, two hydrogen bond acceptors, and two aromatic rings. For both Pgp and BCRP pharmacophores, the active sites focused on the benzamido and arylsulfonylurea ligands. However, the two pharmacophore models differed in the location of the fifth active site, with Pgp activity needing an unsubstituted, and the BCRP activity needing the substituted, benzamido ligand. This work confirms Glyburide as a substrate for both Pgp and BCRP, and details the oral hypoglycemic agents Glimepiride, Glisoxepide, and Gliquidone as Pgp substrates; with Glimepiride and Glisoxepide confirmed as BCRP substrates not previously reported.

INTRODUCTION

The oral hypoglycemic sulfonylurea molecule Glyburide has been shown to be actively transported from various biological tissues through a pronounced interaction with the ATP binding cassette (ABC) active transporter proteins.^{79, 80, 81, 82, 83, 84, 85} Specifically, Glyburide is actively transported by the ABC proteins, P-glycoprotein (Pgp), Breast Cancer Resistance Protein (BCRP), and the Multidrug Resistance Proteins (MRP).^{86, 87} This active transport occurs at various locations throughout the body but has been

identified as responsible for unique transport behavior of Glyburide at the placenta barrier. Glyburide has been shown to not cross the placental barrier to any appreciable effect, and will leave the placental barrier against the concentration gradient, attributed to the active transport by the ABC proteins. Harnessing the unique placental transfer by the ABC proteins and understanding what molecular features drive the drug-protein interaction, creates the possibility of designing medications specifically for pregnant women. Glyburide is a second-generation sulfonylurea hypoglycemic agent, widely used in the treatment of Type II diabetes.^{88, 89, 90} The sulfonylurea molecule class are insulin secretagogues, stimulating the ATP sensitive Potassium (K_{ATP}) channels within the pancreatic β -islet cells.⁹¹ Stimulation of the K_{ATP} channel triggers the insulin release via the occupation of the ABC sulfonylurea receptor (SUR1) in the β -cell membrane.^{92, 93} In order for this mechanism to work, patients need to have retained some level of pancreatic β -cell function, as shown in the cascade of events presented in Figure 7.

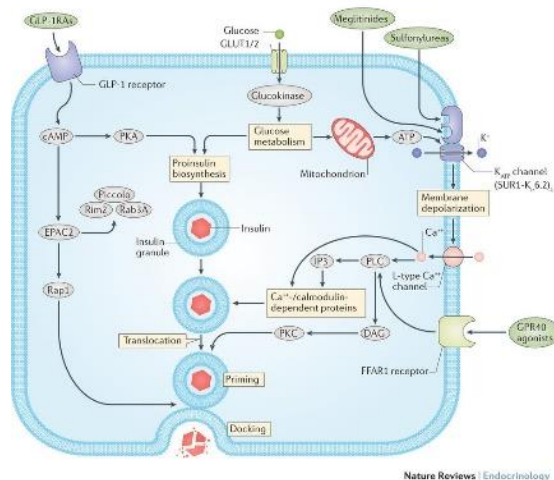


Figure 7. Modulation of insulin, reproduced from Tahrani et al.⁹⁴

In general terms, Type II Diabetes is primarily a condition of progressively impaired glucose regulation due to the dysfunction of the pancreatic beta cells and general insulin resistance.^{15, 95} This impaired glucose regulation can also occur in pregnant women and is commonly referred to as pregnancy induced gestational diabetes mellitus (GDM). GDM occurs in up to 20% of all pregnancy globally, with approximately 90% of those diagnosed as treatable Type II diabetes, and roughly 30-40% requiring pharmacological treatment.^{4, 96, 97, 98}

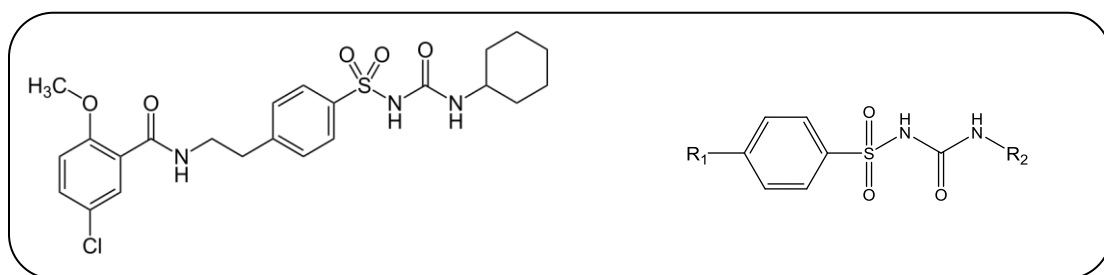


Figure 8. Structures of the Glyburide and the sulfonyleurea backbone.

For both Type II and GDM, insulin has been the gold standard of treatment; however, with the availability and ease of treatment of oral hypoglycemic medications, doctors have recently attempted to treat GDM with small molecule therapeutics.^{99, 100, 101} The similarities of the pathophysiology of both the Type II and GDM indicate that the oral hypoglycemic sulfonyleureas are appropriate, and numerous studies have been performed to understand the pharmacokinetics and pharmacodynamics of Glyburide during pregnancy.^{1, 16} In multiple clinical studies, Glyburide has been shown to be as safe and effective as insulin in pregnant women.^{102, 103, 104, 105, 106} Further, studies evaluating the fetal pharmacokinetics of Glyburide have demonstrated two remarkable findings: that Glyburide does not cross the placenta to any appreciable extent as compared to other

sulfonylureas (Glyburide 3.9%, Glipizide 6.6%, Tolbutamide 21.5%, and Chlorpropamide 11%) and Glyburide will leave the placenta barrier against the concentration gradient.¹⁰⁷ As previously mentioned, this unique placental transport behavior has been demonstrated to be ABC transporter mediated. Evaluation of this unique transport has been performed *in vitro*, and repeatedly demonstrated in cell lines and in placenta-like models (vesicles, perfused placenta, etc.), confirming Glyburide as a substrate for active transport, and demonstrating that the mechanism of placenta transport can be studied *in vitro*.^{108, 109, 110, 111}

Understanding the sulfonylurea and ABC transporter interactions and the unique placental transport serves as an example for the design of pregnancy center drugs. To further investigate this unique interaction of the sulfonylureas with the ABC transporter proteins, Glyburide and a series of sulfonylurea analogs were tested in *in vitro* cell-based transport assays using a Madin-Darby kidney cell (MDCK) lines overexpressing either the Pgp or BCRP proteins. From the measured transporter activity, we developed both 2D and 3D quantitative structure activity relationship (QSAR) models to account for the Pgp and BCRP substrate activity for the sulfonylurea compounds. To accompany this work, we have performed a two-step computational study to generate the 3D pharmacophore to aid in describing the parts of the molecule responsible for the Pgp and/or BCRP activity.

MATERIALS and METHODS

A set of 78 sulfonylurea compounds were acquired for this study, selected via a compound similarity search against Glyburide in both the Pfizer internal and publicly available external databases. The compounds for the study were further selected based on

the Tanimoto searching criteria of >70% similarity, which allowed for the selection of molecules based on the structural similarities to Glyburide. The sulfonylurea analogs were divided into two groups, the commercial sulfonylureas (molecules 1-14) and the sulfonylurea analog series (molecules 15-78). The structures of all molecules studied are presented in Appendix I and II.

CELL CULTURES

The Madin-Darby Canine Kidney cell line stably transfected with the Pgp gene (MDCK-MDR) or the BCRP gene (MDCK-BCRP) were used in the present study and have been thoroughly characterized.^{112,113, 114} The MDCK-MDR cells were initially received from Pier Borst and the National Cancer Institute (NCI), Netherlands, and maintained by the PDM labs, Pfizer Global Research and Development, Groton, CT.^{115, 116, 117, 118} The MDCK-BCRP cell line are a stably transfected cell line, developed and maintained at the Pfizer PDM labs Groton CT.¹¹⁹ Briefly, the stably transfected MDCK-MDR or MDCK-BCRP cells were cultured in Dulbecco's minimum essential media (MEM) with supplements, in 75cm² tissue culture T-flasks were incubated at 37°C with 95% and 5% CO₂ and passaged every 4 days after achieving 90% confluence. The cells were then harvested with trypsin and plated for a density of 2 x 10⁶ cells/cm in Falcon/BD 96 well insert plates with a 1µm pore polyethylene terephthalate filter. Seeded inserts were then placed into prefilled Falcon/BD feeder trays containing 37mL growth medium and incubated at 37°C with 95% and 5% CO₂ for 4 days. Immediately prior to performing the assay, each well of the plates were assessed for uniform barrier functionality of the polarized cell monolayers. The integrity of the MDCK-MDR or MDCK-BCRP cell

monolayers were evaluated by measuring the trans-epithelial electrical resistance, and only those cell monolayers with a measurement with of at least $320\Omega\text{cm}^2$ were used.¹²⁰

TRANSPORT ASSAY PROCEDURES

The cell transport assays are the most direct assay for performing drug transfer studies across a cell monolayer, and to determine a transporters function. The transport assays have been standardized in that the cell lines are widely shared between research labs or are commercially available. All transport assays were performed as per standard procedures, and as previously described.^{121,122, 123, 124} Briefly, the assays were performed in Hanks' balanced salt solution with 10mM HEPES and 25mM D-glucose, 1.25mM CaCl_2 , and 0.5mM MgCl_2 at pH 7.4. Assays were performed with set drug concentrations (2-100 μM) and performed in triplicate to generate statistically sound data. Transport studies were performed by adding the compounds pre-dissolved in dimethyl sulfoxide (DMSO)/transport buffer to the donor wells and measuring the appearance of drug in the receiver wells after 2.5 hours at 37°C. For all of the transport studies performed, the drug was added to the donor compartment A, or the apical side. And the analysis was completed by measuring the compartment A concentration against the receiver compartment B, or the basolateral side. Figure 9 depicts an example insert and transport directions used in the present study.

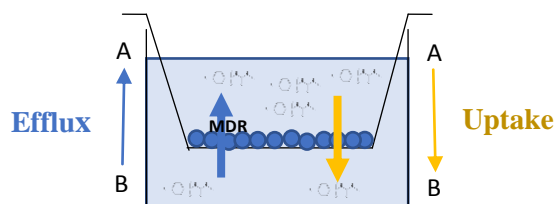


Figure 9. Typical cell monolayer setup for Pgp and BCRP assays.

LC-MS ANALYSIS

The LC-MS analysis was conducted according to internal procedures, and as previously described by L. Di *et al*, Feng *et al*, and Varma *et al*.^{125, 126, 127} Briefly, samples of 25µL were injected on a Sciex API-5500-Electrospray LC system comprising an Optimize Technologies SP Small Molecule Trap column, an Apricot/Sounds Analytics ADDA autosampler, Jackso PU-1580 HPLC pump, and a quadrapole MS detector using the multiple reaction monitoring (MRM) detection mode. Mobile phase A was 95% 2mM ammonium acetate/5% 50/50 acetonitrile/methanol and mobile phase B was 90% 50/50 acetonitrile/methanol/ 10% 2 mM ammonium acetate, at a flow rate of 1.5mL/min. The AUC was integrated using Analyst 1.5.1/DiscoveryQuantAnalyze software, version 2.1.0.14 and compared to standards for each compound in cell culture media for the quantification of concentrations.

DATA ANALYSIS

For these studies, the apparent permeability (P_{app}) was calculated for each compound according to equation 1:

$$P_{app} = \left(\frac{1}{area * C_{D(0)}} \right) * \frac{dM_t}{dt} \quad \text{Equation 1}$$

Where the area is the surface area of the cell monolayer (0.625cm²), C_{D(0)} is the concentration of compound in the donor chamber, t is the time, M_t is the mass of the compound, and $\frac{dM_t}{dt}$ is the flux of compound across the cell monolayer. The P_{app} was calculated in both apical to basolateral and basolateral to apical directions to determine the efflux ratio as shown in Equation 2.

$$ER = \frac{P_{app \ A \rightarrow B}}{P_{app \ B \rightarrow A}} \quad \text{Equation 2}$$

where A→B and B→A denote the direction of transport. In order for a compound to be characterized as a Pgp substrate, the value of the efflux ratio (ER) would exceed a value of 2.5. The value of 2.5 was determined through internal data analysis and has been demonstrated to minimize the false-positive and false-negative results in the assay as tested by the appropriate internal control molecules for each cell line. The efflux ratio is a way to rank order and predict ABC transporter activity, with the larger efflux ratio meaning substrate activity.

CELL ASSAY MATERIALS

The 14 commercial sulfonylureas (molecules 1-14 in Appendix 1) were purchased from Sigma Aldrich, WI, or donated from Pfizer Global R&D, Groton CT. The sulfonylurea analogs (molecules 15-78 in Appendix I and II) were donated from Pfizer Global R&D,

Groton CT. Cell culture media reagents, transport buffer (including Hanks balanced salt solution, HEPES, d-glucose, 1.25mM CaCl₂ and 0.5mM MgCl₂) were purchased from Invitrogen, Carlsbad CA. All organic solvents were purchased from Sigma Aldrich, WI and used as is.

COMPUTER MODELING

All computational studies were performed on an HP, Intel i5 processor running Windows 7 Professional Office, with VLifeMDS® software (version 4.6).¹²⁸ In order to minimize variability and difficulty interpreting the results, it is important to establish a statistically significant correlation between the molecular descriptors and the biological activity. This correlation starts with the molecular alignment of the molecules across the test, training, and validation data sets.¹²⁹ Due to the well documented Glyburide ABC substrate activity, and the common sulfonylurea backbone of the molecules in the present study, Glyburide was used as the template molecule.

As the x-ray crystal structures of the compounds or the ABC transporter proteins were not available, the 2D structures were obtained from Chemaxon® Marvin Sketch and ChemDraw® 15.1.^{130, 131} The sulfonylurea molecules are all flexible with many rotatable bonds which required energy minimization prior to modeling. The minimization was carried out in the ChemDraw® 3D 15.1 suite utilizing the Merck Molecular force field (MMFF94).^{132, 133, 134, 135} The energy minimizations were carried out using 1000 iterations to eliminate any change in conformations. The RMS gradient was set to 0.100, the dielectric constant was set to 1.0 and exact calculation, and the Van der Waals calculation was set to exact. To maximize the modeling, 1000 calculations were

performed to eliminate any variability in the lowest energy conformations. The RMS and van der Waals calculations are parameters that can be adjusted to enhance the threshold interactions. For our modeling efforts described here, the RMS and van der Waals parameters were left as recommended by the software. The Figure 4 shows the overlay of the MMFF94 energy minimized molecules.

The total energy of the molecular conformation was calculated using the MMFF94 relationship presented in Equation 3:

$$E_{\text{total}} = E_{\text{B}} + E_{\text{A}} + E_{\text{BA}} + E_{\text{OOP}} + E_{\text{T}} + E_{\text{vdW}} + E_{\text{elec}} \quad \text{Equation 3}$$

where,

- E_{B} = bond stretching energy
- E_{A} = angle bending energy
- E_{BA} = bond stretching and angle bending energy
- E_{OOP} = out of plane bending energy
- E_{T} = torsion energy
- E_{vdW} = van der Waals energy
- E_{ELEC} = electrostatic energy

As shown in the energy equation, the MMFF94 energy calculation has multiple energy terms to capture all potential molecular motions. The total energy of the system is calculated as the sum of individual energy terms defined for a force field.¹³⁶

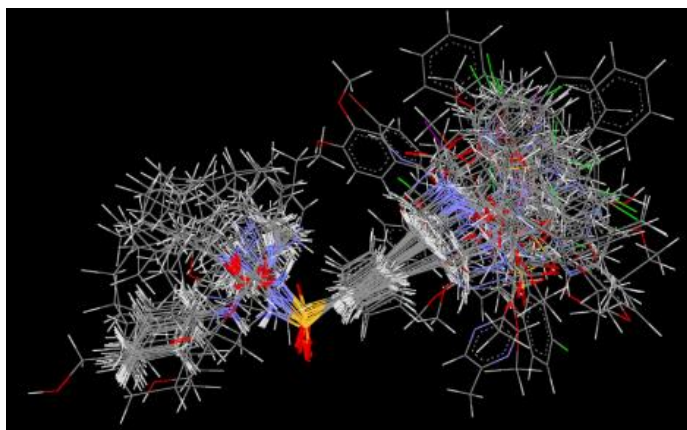


Figure 10. Molecular Overlay of MMFF94 energy minimized molecules.

After energy minimization, the molecules were loaded into the VLifeMDS® software and aligned to a set conformation using the VLifeEngine® module. To correctly overlay the molecules for quality QSAR modeling, the alignment was performed using the modules' atom-based approach. This approach allowed for the selection of the central arylsulfonylurea section of the Glyburide template molecule. Figure 9 depicts the molecule overlay of the energy minimized molecules, with Figure 11 showing the sulfonylurea backbone chosen for molecule conformer alignment template (highlighted in red).

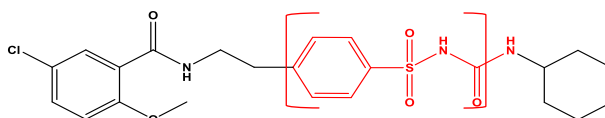


Figure 11. Glyburide molecule with the sulfonylurea backbone template (highlighted in red).

As mentioned previously, with not all crystal structures of the compounds available, the lowest energy conformations were calculated for each compound using ChemDraw® 15.1. Yuriev *et al* evaluated previous glyburide structure analysis and modeled glyburide to determine the three-relevant energy minimized structures - crystal, *in vacuo*, and *in solution*.¹³⁷ Previous work L. Lin *et al*, S.R. Byrn *et al*, W. Grell *et al*, and T.J. Hou explain the various Glyburide energy minimization work in detail.^{138, 139, 140, 141} In summary, the Glyburide SD file was loaded into ChemDraw, and the MMFF94 energy minimization calculations were performed as described. The Lin *et al* published lowest energy confirmations for Glyburide in solution was chosen as the most representative conformation for our studies.

These findings demonstrate the viability of energy minimization modeling in absence of crystal structures. The MMFF94 energy minimization for the sulfonylurea analogs matched the Lin low energy solution model very closely and was used in the present study, as presented in Figure 12. Future work will evaluate different energy minimizations and docking, and how that influences the QSAR modeling.

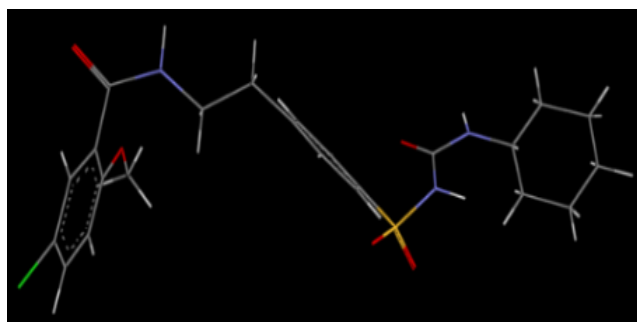


Figure 12. Energy minimized MMFF94 structure of Glyburide.

EXPERIMENTAL

The experimental work was divided into two main sections, (1) assessing the commercial sulfonylureas as Pgp or BCRP substrates, and (2) then screening a large series of analogs for activity to better understand the molecular features responsible for the Pgp or BCRP activity. The initial experiments were designed to determine if any of the 14 commercial sulfonylureas (shown in Figure 1) demonstrated Pgp or BCRP activity, and to what extent. The second set of experiments reported here was designed to determine the two and three dimensional molecular descriptors of a series of sulfonylurea analogs responsible for the Pgp or BCRP transporter activity. The molecular descriptors are described in Appendix IV.

The initial evaluation of the commercial sulfonylureas was run at a standard concentration, and all compounds were run in at least triplicate. Traditionally, transport assays evaluating the sulfonylureas have been performed with concentrations ranging from 1-500 μ M, depending on the substrate or inhibitor function.¹⁴² Accounting for this range, our studies were performed at a nominal concentration of 2 μ M for the sulfonylurea analogs due to ease of screening and to not saturate the transport mechanism for Pgp or BCRP activity. Also, to make sure our cell monolayers were performing as expected, compounds with well documented Pgp or BCRP activity were used as the controls. The negative control was the molecule antipyrine, which demonstrates unilateral crossing of the MDCK-MDR and MDCK-BCRP cell monolayers (antipyrine efflux ratio = 0.99); the positive control for the MDCK-MDR cells was vinblastine which is a well-documented substrate/inhibitor of Pgp (vinblastine efflux ratio =6.42); and the positive control for the MDCK-BCRP cells was novobiocin which is a well-documented

substrate/inhibitor of Pgp (novobiocin efflux ratio =8.65). From this group of commercial sulfonylureas, four molecules demonstrated high Pgp substrate activity (Glyburide, Glimepiride, Glisoxepide, and Gliquidone), and one molecule was borderline (Glipizide). Only three of these molecules demonstrated BCRP substrate activity (Glyburide, Glimepiride, and Glisoxepide). These molecules are similar to Glyburide, and are also second-generation sulfonylureas, exhibiting a better safety profile, increased potency, and higher binding affinity to the Sulfonylurea 1 (SUR1) protein.¹⁴³

Having determined the Pgp activity of the commercial sulfonylureas, the next step of the evaluation was to test the various concentrations of the four compounds to confirm Pgp activity as a function of the concentration. Glyburide, Glimepiride, Glisoxepide, and Gliquidone were dosed over a concentration range of 2-100 μM . As Glipizide did not show Pgp activity in the initial screening study, it was not included in the second round of testing. Compared to therapeutic doses of Glyburide of approximately 0.202 μM , this concentration range represents an approximately 10-500 times increase in concentration and is used to ensure a reproducible measurement. All four compounds demonstrated an asymmetric transport across the concentration range, with the absorption of each compound increased with concentration, whereas the efflux slightly increased with increasing concentrations. Figure 13 depicts the asymmetric relationship of Glyburide, Glimepiride, Glisoxepide, and Gliquidone.

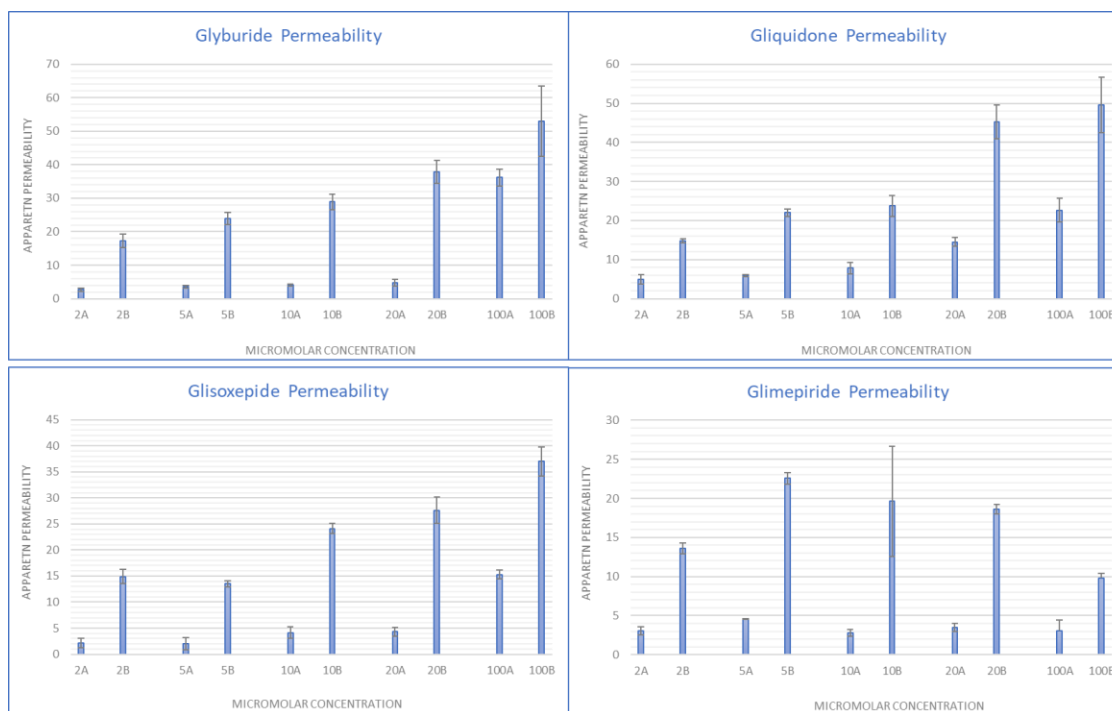


Figure 13. Bar graphs showing asymmetric absorption and efflux of Glyburide, Glimepiride, Gliquidone, and Glisoxepide. *Note: A denotes A-B transport; B denotes B-A transport.*

As shown in the bar graphs of Figure 13, the lower concentrations of the compounds demonstrated the active transport out of the cells from the basolateral to apical. In the lower concentration ranges (2-20 μM) the rate of efflux exceeded the rate of absorption by the following values: approximately 6-8 times for Glyburide, 5-6 times for Glimepiride, 3-4 times for Gliquidone, and 5-7 times for Glisoxepide. At the highest concentration tested (100 μM), the transport was nonlinear, and the transport started to balance out, especially for the Glyburide assay. This is an effect of the inhibitory nature of the compounds at the 100 μM concentration, as discussed in literature.¹⁴⁴ These findings demonstrate the transport is a carrier mediated process from the basolateral to

apical compartment for each of the compounds represented. These results were expected based on the known Pgp-Glyburide interaction, and the molecular similarities of the four compounds. Also, the non-Pgp activity of Gliclazide was expected as the only reported Gliclazide Pgp activity found in literature was at very high concentrations.¹⁴⁵

The bulk of the experimental work reported in this paper was performed to evaluate a large series of sulfonylurea analogs as substrates of the ABC transporters (Pgp and/or BCRP), and to use this information to build 2D and 3D QSAR models. Based on the initial experiments, and internal procedures, all the sulfonylurea analogs cell transport assays were performed at 2 μ M and measured in triplicate. It is well understood that the work reported describes local models for both Pgp and BCRP, as all the compounds used in the study were sulfonylureas, though containing structurally diverse R₁ and R₂ groups (described in Appendix I). However, even though structurally similar, the 78 sulfonylurea analogs spanned approximately 3 logs of Pgp activity and 2 logs of BCRP activity, as shown in Figures 14 and 15.

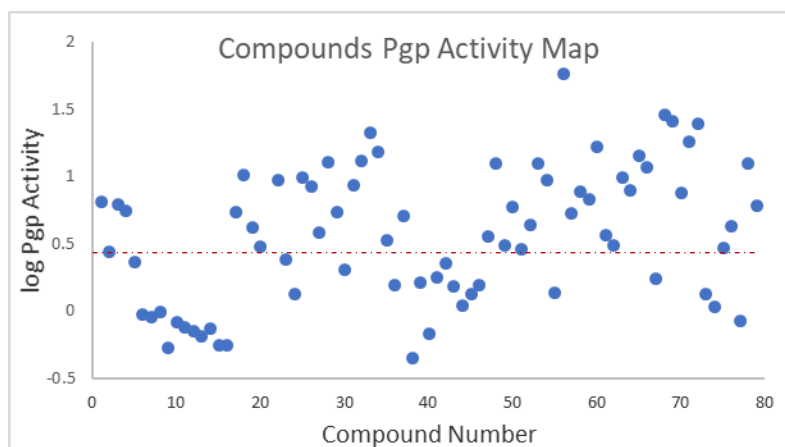


Figure 14. Map of all 78 compounds and the respective log Papp activity. *Note: red dotted line represents the activity cutoff value of 0.4 (ER value =2.5).*

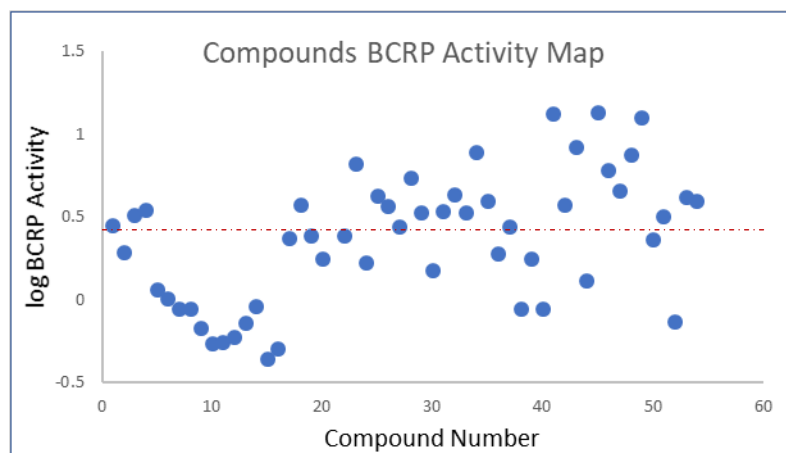


Figure 15. Map of all 53 compounds and the respective log BCRP P_{app} activity. *Note: red dotted line represents the activity cutoff value of 0.4 (ER value = 2.5).*

The compound activity maps in Figures 13 and 14 represent the range of activities for the molecules used in our research. As you can see, the log normalized range of activity for all of the compounds was between -0.5 to 2.0. Based on the cutoff values from both of the transport assays of 2.5 for substrate activity, the cutoff for activity is 0.40 as shown by the red dotted line in both Figures 13 and 14. The log scale of the activities represents the activity values from 0 to 56, with negative numbers simply representing the log calculations of activities less than 1.

MATHEMATICAL MODELS

Molecular dynamics modeling was performed using the VLifeMDS®, version 4.6 software package to evaluate the physico-chemical properties of sulfonylurea molecules against the biological activity of Pgp efflux. The basic assumption of QSAR and molecular modeling is that the interactions of the aligned molecules to a probe or model molecule will provide the necessary features to explain the biological activity. The most

important assumption then, is that any change in biological activity is directly related to the changes in the molecular properties. The VLifeMDS® software package has multiple modeling algorithms available, but only the models used in the present study will be discussed and explained in more detail here. However, the available modeling algorithms in the VLifeMDS software package are nearest neighbor (kNN), partial least squares regression (PLSR), and multiple linear regression (MLR), techniques. An initial screening of the activity data and each model was performed to determine the best statistical modeling algorithm to use for our research. For the Pgp work, the kNN and MLR demonstrated the best model predictions for the 2D and 3D QSAR, respectively. For the BCRP work, the MLR demonstrated the best model predictions for both the 2D and 3D QSAR.

Developing QSAR models is an iterative approach, and hundreds of modeling simulations were performed to evaluate the necessary parameters and build the most representative models defining each sulfonylurea and ABC transporter activity. The models presented here represent the most appropriate to define the sulfonylurea-protein interactions, and the most predictive, and will be discussed individually here.

QSAR DISCUSSION

A QSAR model is a regression or classification model that relates a set of predictor variables (x) to the potency of a response variable (y). The QSAR model is defined by the two and three-dimensional descriptors that make up the space surrounding the molecule, and are important tools to describe the correlation of a biological activity to the molecular features responsible for the activity. To explain the interaction of the sulfonylureas with

the Pgp and BCRP proteins, we developed both 2D and 3D QSAR models that will be described in more depth here.

The 2D QSAR models require calculating molecular descriptors and matching the molecular descriptors to a biological activity. The 2D modeling and descriptors are the most widely used, based on their simple nature of employing a direct math algorithm that is highly reproducible and requires minimal compute time consumption.¹⁴⁶ In contrast, the 3D QSAR models are more in-depth and require more computational time to complete the analysis. In the VLifeMDS® software, there are approximately 1300 molecular descriptors used for the 2D QSAR models, whereas the 3D QSAR models use steric (S) and electrostatic (E) descriptors that specify the region where the structural feature variation between the test and training set of compounds leads to an increase or decrease in activity.¹⁴⁷ VLifeMDS® comes equipped with numerous statistical modeling algorithms for both 2D and 3D QSAR modeling, including partial least squares (PLS), k-nearest neighbor (kNN), and multiple linear regression (MLR). All modeling studies were performed with the stepwise forward and backward variable selection methods which resulted in hundreds of models in 2D and 3D space for each protein. The stepwise forward and backward variable selection is a technique of choosing the predictive variables that are carried out by the software. The fundamental difference between the forward and backward selection methods is the use of descriptors (backward) or no descriptors (forward) to build the model.¹⁴⁸ The Pgp and BCRP models with the greatest predictive ability were achieved with MLR or kNN regression analysis and will be described here in more depth.

The kNN method adopts a nearest neighbor principle for generating the relationship between the molecular descriptors and a given biological activity. The basic principle of the kNN classification model is that the compounds are assigned to a class membership of its nearest neighbors in a common rectangular grid, taking into account the weighted similarities between a compound and its nearest neighbors.^{149, 150} The kNN statistical methodology is represented by points of the grid in the form of

$$Y = (\text{point}) (\text{value}) (\text{point1}) (\text{value1}) \quad \text{Equation 4}$$

where: y is the dependent variable (activity), and the points and values represent descriptors, or steric/electrostatic spaces on the grid.

Also included in the VLifeMDS® software are numerous regression methods to calculate the best for the data, with the Multiple Linear Regression (MLR) methodology demonstrated the greatest predictive ability for the sulfonylurea and ABC transporter protein interactions.¹⁵¹ The MLR methodology relates the dependent variable (activity) to a number of independent variables (molecular descriptors) through linear equations. The MLR analysis estimates the values of regression by applying least squares curve fitting methods.^{152, 153} The MLR equation takes the form:

$$Y = b_1 * x_1 + b_2 * x_2 + b_3 * x_3 + c \quad \text{Equation 5}$$

where: Y is the dependent variable (activity), b's are the regression coefficients of the corresponding x's (molecular descriptors), and c is the regression constant (intercept). Simply stated, the points and values represent molecular descriptors surrounding the molecule on the grid in 2-dimensional space or the steric and electrostatic descriptors of the 3-dimensional space.

The predictive ability of the both the 2D and 3D models was evaluated by the cross-validation (q^2) term, employing the leave one out (LOO) methodology. The LOO principle is a method that computes the statistics for the left-out value, allowing for faster computation time.^{154, 155} Simply, in the LOO principle, one data point is selected from the test set, and the model is built around the remaining points, with the model cross-validated against the error on the single point held out of the model. This process is then repeated for each point of the training set and averaging the results in the final model.

The leave one out equation is presented as equation 6 here:

$$q^2 = 1 - \frac{\sum(y_i - \hat{y}_i)^2}{\sum(y_i - y_{\text{mean}})^2} \quad \text{Equation 6}$$

The predictive ability of all the QSAR models was confirmed by the predicted r^2 ($pred_r^2$) and the external validation test data set. One final point used in the evaluation is the standard error of estimation for the cross-validated q^2 and the predicted r^2 , with a low standard error signifying that the models are statistically significant. In summary, the VLifeMDS® software program calculates the best model based on the squared correlation coefficient (r^2) which defines the linearity, the cross validated coefficient (q^2)

which is a measure of quality of the fit, and the predicted r^2 value. The low standard of error for each of the terms shows the quality of the fitness of the model, and the F_{test} values demonstrate the variance due to the error of the models, with high F test values indicating that the models are statistically significant. As there were hundreds of modeling attempts made, the q^2 and pred r^2 values were the main factors governing the selection of the optimal models.

For the modeling work described here, all models were generated using the 70:20:10 approximation; 70% of the molecules were used as the training set, 20% as the test set, and the remaining 10% as the independent set used for the external validation of the model. An important note is that the VLifeMDS® program randomly selects the training, test, and independent set molecules for each model built. For all the sulfonylurea-Pgp models, this amounted to a training set of 54 compounds, a test set of 15 compounds and validated with an independent set of 9 compounds. In comparison, all of the sulfonylurea-BCRP models used a training set of 38 compounds, a test set of 11 compounds, and 5 compounds used as the independent set to validate the model.

Finally, all the models generated for each protein in both the 2D and 3D space were evaluated for acceptable performance against linearity, cross-validation, standard error, and the predictability of the model to identify substrates not in the training or test set. Many models succeeded in one or two of the criteria, but the models chosen to describe the behavior had the best balance of high linearity and cross-validation values, low standard error, and high ability to predict substrate behavior.

Pgp 2D QSAR DISCUSSION

Of the 200 models run, the optimum model to describe the sulfonylurea-Pgp interaction within the 2D space was obtained in Model 58, using the kNN methodology with sphere exclusion.¹⁵⁶ The sphere exclusion technique represents a simple clustering method whereby molecules are clustered together based on a defined similarity score, continuing until all molecules are grouped.¹⁵⁷ Model 58 parameters are shown in Table 2 and proved very robust and an excellent cross validation (q^2), with the predicted r^2 and externally validated r^2 very close in value, but not over-predicting. This is an important point as over-predicting models can lead to false predictions, allowing the model to incorrectly label molecules as substrates/non-substrates for activity. The external predictability of Model 58 was determined by the predicted r^2 ($pred_r^2$) value, which was 0.8150, meaning that the model has a prediction rate of 81.5%. This prediction rate is right in line with the observed Pgp activity data for Glyburide, Glimepiride, Glipizide, Glisoxepide, and Gliquidone with the model ability to select 4 out of 5 molecules' activity. Table 1 summarizes the kNN QSAR Model 58.

Statistical Parameter	2D kNN QSAR Model 58
n	3
k	54
deg. of free	46
q^2	0.7151
q^2 se	0.2536
Predicted r^2	0.8150
Predicted r^2 se	0.2705
ext val r^2	0.8288
ext val r^2 se	0.2261

Table 1. Statistical results of 2D QSAR kNN Model 58 for the Sulfonylurea-Pgp activity.

Graphing the predicted vs. the experimental Pgp activity is also a good way to assess model performance. Model 58 shows good linear correlation between the two data sets, as presented in Figure 16.

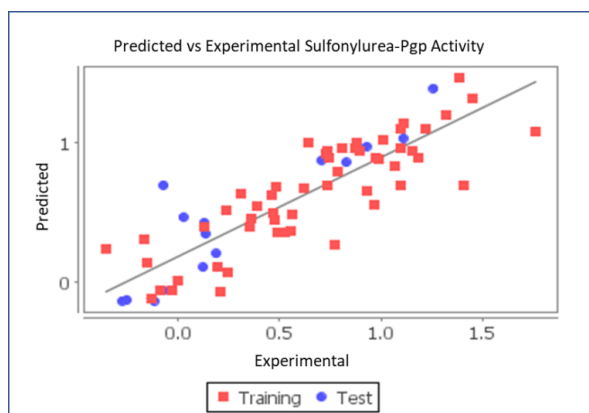


Figure 16. Graphical representation of predicted Pgp activity vs. experimental activity for the training and test sets for kNN Model 58.

Table 2. Molecular Descriptors used in 2D QSAR Study

Model	Molecular Descriptor	Description
58	DipoleMoment	DipoleMoment signifies the dipole moment calculated from the partial charges of the molecule
	6chaincount	6chaincount signifies the total number of six membered rings in a compound
	Chi4	Chi4 signifies atomic valence connectivity index (order 4)
	K3alpha	K3alpha signifies the third alpha modified shape index
	SaaaCcount	SaaaCcount signifies the total number of carbons connected with three aromatic bonds
	SAMostHydrophobic	SAMostHydrophobicHydrophillicDistance signifies the distance between the most hydrophobic and hydrophilic point on the vdW surface
	HydrophillicDistance	HydrophillicDistance signifies the distance between the hydrophilic groups on the vdW surface
	SdssS(sulfate)E-index	SdssS(sulfate)E-index signifies the electropological state indices for the number of sulfate groups connected with two single and two double bonds

The 2D QSAR model to define the interactions with Pgp had eight 2D contributing descriptors. The full description of the 2D descriptors of Model 58 are presented in Table 1. The eight descriptors used for Model 58 descriptors are DipoleMoment, 6chaincount, Chi4, K3alpha, SaaaCcount, SAMostHydrophobic, HydrophillicDistance, and SdssS(sulfate)E-index. These molecular descriptors characterize the specific information about the sulfonylureas that drive the interaction with Pgp.

The 2D equation defining the Pgp and sulfonyleurea activity is presented here:

pPgp Efflux = DipoleMoment (5.1080, 5.9350) 6ChainCount (-0.0390, -0.0280) chi4
(2.0000, 3.0000) k3alpha (8.8890, 9.1500) SaaaCcount (6.4530, 8.1170)
SAMostHydrophobicHydrophilicDistance (0.0000, 0.0000) SddssS(sulfate)E-index
(0.0000, 0.0000)

Molecule	Efflux Ratio	logEfflux Ratio	Predicted logEfflux Ratio	Residual	Molecule	Efflux Ratio	logEfflux Ratio	Predicted logEfflux Ratio	Residual
1	6.39	0.806	0.959	-0.153	41	1.76	0.246	0.076	0.169
2	2.75	0.439	0.792	-0.352	42	2.24	0.35	0.397	-0.047
3	6.21	0.793	0.418	0.375	43	1.52	0.182	0.106	0.076
4	5.51	0.741	0.898	-0.157	44	1.09	0.037	0.04	-0.003
5	2.3	0.362	0.458	-0.096	45	1.34	0.127	0.402	-0.275
6	0.93	-0.032	-0.052	0.02	46	1.54	0.188	0.207	-0.019
7	0.9	-0.046	-0.596	0.55	47	3.57	0.553	0.37	0.183
8	0.99	-0.004	0.017	-0.022	48	12.4	1.093	0.695	0.399
9	0.53	-0.276	-0.13	-0.145	49	3.05	0.484	0.685	-0.201
10	0.82	-0.086	-0.056	-0.031	50	5.89	0.77	0.275	0.495
11	0.76	-0.119	-0.13	0.011	51	2.89	0.461	0.627	-0.166
12	0.7	-0.155	0.138	-0.293	52	4.37	0.64	1.001	-0.36
13	0.65	-0.187	-0.132	-0.055	53	12.5	1.097	0.967	0.129
14	0.74	-0.131	-0.114	-0.016	54	9.38	0.972	0.893	0.08
15	0.55	-0.26	-0.121	-0.139	55	1.36	0.134	0.35	-0.217
16	0.56	-0.252	-0.124	-0.128	56	57.4	1.759	1.082	0.677
17	5.4	0.732	0.698	0.034	57	5.35	0.728	0.922	-0.194
18	10.2	1.009	1.027	-0.018	58	7.64	0.883	1.008	-0.125
19	4.17	0.62	0.68	-0.06	59	6.7	0.826	0.861	-0.035
20	2.99	0.476	0.45	0.025	60	16.5	1.217	1.104	0.113
22	9.3	0.968	0.559	0.41	61	3.62	0.559	0.493	0.066
23	2.43	0.386	0.551	-0.165	62	3.08	0.489	0.361	0.128
24	1.33	0.124	0.11	0.013	63	9.74	0.989	0.883	0.106
25	9.73	0.988	0.72	0.268	64	7.81	0.893	0.941	-0.049
26	8.45	0.927	0.976	-0.049	65	14.3	1.155	0.94	0.215
27	3.83	0.583	0.401	0.182	66	11.7	1.068	0.831	0.238
28	12.8	1.107	1.034	0.073	67	1.72	0.236	0.521	-0.285
29	5.41	0.733	0.941	-0.208	68	28.4	1.453	1.315	0.138
30	2.04	0.31	0.636	-0.327	69	25.5	1.407	0.695	0.711
31	8.52	0.93	0.661	0.269	70	7.45	0.872	0.964	-0.092
32	12.9	1.111	1.144	-0.033	71	18.1	1.258	1.393	-0.135
33	21	1.322	1.199	0.123	72	24.3	1.386	1.472	-0.086
34	15.3	1.185	0.899	0.286	73	1.34	0.127	0.428	-0.301
35	3.37	0.528	0.362	0.165	74	1.06	0.025	0.469	-0.443
36	1.56	0.193	0.115	0.078	75	2.93	0.467	0.5	-0.033
37	5.08	0.706	0.878	-0.172	76	4.29	0.632	0.527	0.106
38	0.44	-0.354	0.243	-0.596	77	0.85	-0.072	0.699	-0.771
39	1.62	0.21	-0.064	0.274	78	12.4	1.093	1.098	-0.005
40	0.68	-0.166	0.314	-0.48	79	6.07	0.783	0.797	-0.014

Table 3 Molecules used in study with experimental, predicted, and residual activity.

To further evaluate the model describing the sulfonylurea and Pgp interaction, the nearest neighbor algorithm was performed at three, six, or nine nearest neighbors for the calculations. Though all the models presented similar results, the kNN models with the increased nearest neighbor values did not outperform the simpler Model 58 with only three nearest neighbor parameters. In fact, as shown in Table 4, Model 58 with the $n = 3$ parameter outperformed the $n = 6$ and $n = 9$ nearest neighbor models with better Predicted r^2 and Ext Val r^2 values, in a head to head comparison. The three most representative kNN models using the 3, 6, and 9 nearest neighbors are presented in Table 4 for comparison.

Statistical Parameter	2D kNN QSAR Model 58	2D kNN QSAR Model 31	2D kNN QSAR Model 50
n	3	6	9
k	54	54	54
deg. of free	46	48	48
q^2	0.7151	0.7306	0.7210
q^2 se	0.2536	0.2606	0.2626
Predicted r^2	0.8150	0.7961	0.6312
Predicted r^2 se	0.2705	0.2120	0.3149
ext val r^2	0.8288	0.7706	0.7880
ext val r^2 se	0.2261	0.2727	0.2472

Table 4. Comparison of the 3-6-9 nearest neighbors Models for Pgp

This was relatively unexpected as usually the more neighbors, the more rigorous the calculations due to the larger fields of interaction, and hence a better model. However, the structural similarity of the sulfonylurea analogs made the selection of a larger nearest neighbor factor an insignificant point. As the longer and more extensive calculations for

increased nearest neighbor parameters did not prove to be a better modeling assumption, further modeling attempts will be performed as simple as possible, increasing the throughput without sacrificing robustness. As you presented in Table 4 above, the nearest neighbor calculations for the $n = 3, 6,$ or 9 values were close but turned out to be not that as predictive as the Model 58 ($n = 3$). Comparing the models, we see that the cross validation was better in the $n = 6$ and 9 models (0.7151 to 0.7306 to 0.7210); however, the $n = 3$ model beat the others in both the $pred_r^2$ (0.8150 compared to 0.7961 and 0.6312), and external validation r^2 (0.8288 compared to 0.7706 and 0.7880).

BCRP 2D QSAR DISCUSSION

The optimum model to describe the sulfonylurea-BCRP interaction within the 2D space was obtained in Model 89, using the MLR methodology, with the sphere exclusion technique.¹⁵⁸ Model 89 parameters are shown in Table 3, proved very robust and an excellent cross validation (q^2), with the predicted r^2 and externally validated r^2 also very close to in value, but not over-predicting, similar to the model for Pgp. The external predictability of Model 89 was determined by the predicted r^2 ($pred_r^2$) value, which was 0.7711 , meaning that the model has a prediction rate of 77.11% .

Statistical Parameter	2D QSAR MLR Model 89
n	38
deg. of freedom	30
r^2	0.8690
q^2	0.8131
F_{test}	28.4199
r^2 se	0.1548
q^2 se	0.1849
Predicted r^2	0.7711
Predicted r^2 se	0.1856
External val r^2	0.9185
Ext val r^2 se	0.1397

Table 5. Statistical results of BCRP 2D QSAR MLR model

As shown in Table 5 above, the MLR Model 89 also proved very robust and demonstrated excellent linearity with low standard error. Model 89 models was very accurate, with excellent cross validation (q^2), with the predicted r^2 and externally validated r^2 very close in value, but as seen in the Pgp model, also not over-predicting. The external predictability of Model 89 was determined by the predicted r^2 ($pred_r^2$) value, which was 0.9185, meaning that Model 89 has an external prediction rate of 91.85%.

Graphing the predicted verse the experimental Pgp activity also demonstrated the linear correlation between the two and is presented in Figure 17.

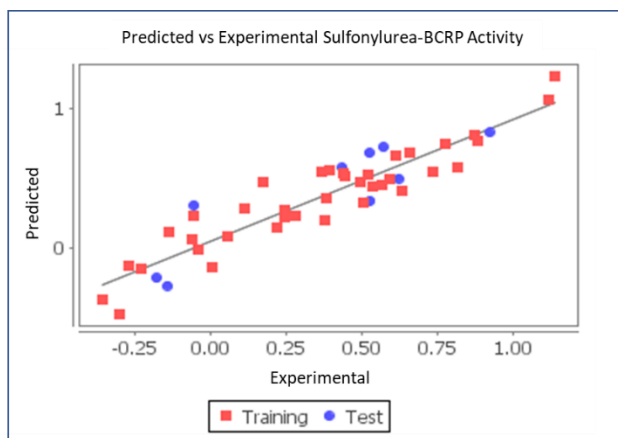


Figure 17. Predicted BCRP activity vs. experimental activity for the training and test sets for model 89.

There were seven 2D contributing descriptors for Model 89. The seven descriptors used in Model 89 are the vdWSurfaceArea, SKMostHydrophobicHydrophilicDistance, SAMostHydrophobicHydrophilicDistance, YcompDipole, SddssS(sulfate)E-index, DipoleMoment, and SsNH2E-index. These molecular descriptors characterize the specific information about the sulfonylureas that drive the interaction with BCRP. The full description of the 2D descriptors of Model 89 are presented in Table 6.

Table 6. Molecular Descriptors used in BCRP 2D QSAR Study

Model	Molecular Descriptor	Description
89	vdWSurfaceArea	This descriptor signifies total van der Waals surface area of the molecule
	SKMostHydrophobicHydrophilicDistance	SKMostHydrophobicHydrophilicDistance signifies the most hydrophobic value on the van der Waals surface (by Kellog Method using Slogp)
	SAMostHydrophobicHydrophilicDistance	SAMostHydrophobicHydrophilicDistance signifies the distance between the most hydrophobic and hydrophilic point on the vdW surface
	YcompDipole	YcompDipole signifies the y component of the dipole moment (external coordinates)
	SdssS(sulfate)E-index	SdssS(sulfate)E-index signifies the electropological state indices for the number of sulfate groups connected with two single and two double bonds
	DipoleMoment	DipoleMoment signifies the dipole moment calculated from the partial charges of the molecule
	SsNH2E-index	SsNH2E-index signifies the electropological state indices for the number of -NH2 groups connected with two single bonds

Another way to assess the 2D molecular descriptors in Model 89 is to understand the weight % contributions of each descriptor. As shown in Figure 18, four of the molecular descriptors had positive contributions on the model: vdWSurfaceArea, SAMostHydrophobicHydrophilicDistance, YcompDipole, and SsNH2E-index contributing approximately 70% to the model overall. Three molecular descriptors had negative contributions on the model: SKMostHydrophobicHydrophilicDistance, SdssS(sulfate)E-index, and DipoleMoment contributing the remaining 30% to the model. The % contribution values of each molecular descriptor are presented in Figure 18.

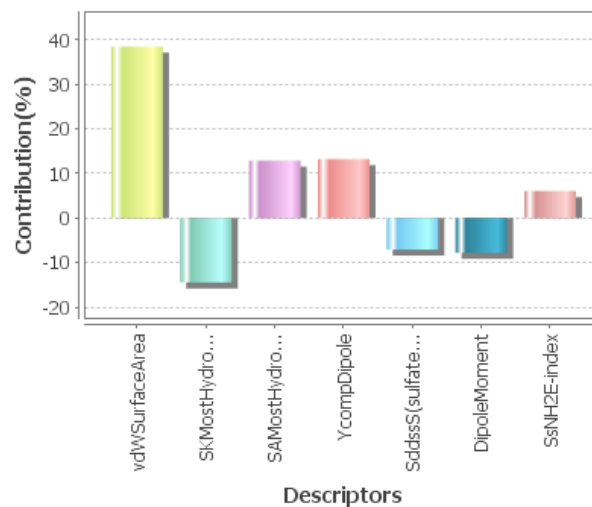


Figure 18. Graph depicting 2D QSAR variables and % contributions.

The 2D equation defining the BCRP and sulfonyleurea activity is presented here:

$$\begin{aligned}
 \text{pBCRPEfflux} = & \text{vdWSurfaceArea } 0.0038(\pm 0.0003) \\
 & \text{SKMostHydrophobicHydrophilicDistance } -0.0315(\pm 0.0072) \\
 & \text{SAMostHydrophobicHydrophilicDistance } 0.0316(\pm 0.0089) \text{ YcompDipole} \\
 & 0.0531(\pm 0.0134) \text{ SddssS(sulfate)E-index } -0.0600(\pm 0.0175) \text{ DipoleMoment } - \\
 & 0.0562(\pm 0.0237) \text{ SsNH2E-index } 0.0445(\pm 0.0207) -1.6761
 \end{aligned}$$

Molecule	Efflux Ratio	logEfflux Ratio	Predicted logEfflux Ratio	Residual	Molecule	Efflux Ratio	logEfflux Ratio	Predicted logEfflux Ratio	Residual
1	2.78	0.444	0.519	-0.075	29	3.34	0.524	0.681	-0.157
2	1.9	0.279	0.225	0.054	30	1.49	0.173	0.473	-0.299
3	3.21	0.507	0.32	0.187	31	3.37	0.528	0.337	0.191
4	3.45	0.538	0.437	0.101	32	4.28	0.631	0.404	0.227
5	1.14	0.057	0.081	-0.024	32	4.28	0.631	0.404	0.227
6	1.01	0.004	-0.138	0.143	33	3.32	0.521	0.528	-0.007
7	0.88	-0.056	-0.343	0.288	34	7.67	0.885	0.765	0.119
8	0.87	-0.06	0.057	-0.118	35	3.9	0.591	0.497	0.094
9	0.67	-0.174	-0.219	0.045	36	1.87	0.272	0.242	0.03
10	0.54	-0.268	-0.133	-0.134	37	2.75	0.439	0.539	-0.1
11	0.55	-0.26	-0.254	-0.006	38	0.877	-0.057	0.231	-0.288
12	0.59	-0.229	-0.148	-0.081	39	1.76	0.246	0.223	0.023
13	0.72	-0.143	-0.273	0.13	40	0.881	-0.055	0.306	-0.361
14	0.91	-0.041	-0.018	-0.023	41	13.1	1.117	1.06	0.057
15	0.44	-0.357	-0.371	0.014	42	3.7	0.568	0.686	-0.118
16	0.5	-0.301	-0.474	0.173	43	8.33	0.921	0.829	0.091
17	2.32	0.365	0.545	-0.179	44	1.3	0.114	0.284	-0.17
8	3.72	0.571	0.721	-0.151	45	13.4	1.127	1.237	-0.11
19	2.41	0.382	0.358	0.024	46	6	0.778	0.747	0.031
20	1.76	0.246	0.277	-0.031	47	4.54	0.657	0.679	-0.022
22	2.4	0.38	0.194	0.186	48	7.45	0.872	0.808	0.064
23	6.54	0.816	0.583	0.233	49	12.4	1.093	1.102	-0.008
24	1.65	0.217	0.14	0.077	50	2.3	0.362	0.561	-0.199
25	4.18	0.621	0.497	0.124	51	3.13	0.496	0.474	0.022
26	3.67	0.565	0.455	0.11	52	0.73	-0.137	0.114	-0.25
27	2.72	0.435	0.575	-0.14	53	4.11	0.614	0.664	-0.05
28	5.43	0.735	0.548	0.187	54	3.88	0.589	0.599	-0.01

Table 7. Molecules used in the BCRP study with experimental, predicted and residual activity values.

The sulfonylurea interactions with Pgp and BCRP were well characterized in the respective 2D QSAR models. Both 2D QSAR models were comprised 7 and 8 molecular

descriptors defining the activity in BCRP and Pgp, respectively. Most of the descriptors defining the activity for either Pgp or BCRP were unique, however there were 3 descriptors that were shared in the 2D models. The *max hydrophobic-hydrophilic distance* (positive coefficient for both), the *sulfate index* (negative coefficient for BCRP, positive for Pgp) and the *dipole moment* (negative coefficient for BCRP and positive for Pgp) were shared in both models and are therefore important features to describe the sulfonyleurea interactions with the ABC transporter proteins in general. Examining the values individual values for each descriptor demonstrate the impact on each model and help us understand the importance of each on the respective models. It is difficult to compare the importance of the descriptors in each model directly due to the nature of the statistical analysis (kNN vs MLR), however the similarity in the structure and function of the molecules cannot be overlooked when dealing with the ABC transporters. The shared descriptors and the definitions are presented in Table 8.

Table 8. Descriptors shared by both Pgp and BCRP 2D QSAR Models

Molecular Descriptor	Description
SAMostHydrophobicHydrophilicDistance	SAMostHydrophobicHydrophilicDistance signifies the distance between the most hydrophobic and hydrophilic point on the vdW surface
SdssS(sulfate)E-index	SdssS(sulfate)E-index signifies the electropological state indices for the number of sulfate groups connected with two single and two double bonds
DipoleMoment	DipoleMoment signifies the dipole moment calculated from the partial charges of the molecule

Pgp 3D QSAR DISCUSSION

The optimum model to describe the sulfonylurea-Pgp interaction with the 3D space was obtained in Model 10, using the MLR methodology, also using the sphere exclusion technique, and with the added Del Re energy minimization calculations for the 3-dimensional space.¹⁵⁹ Del Re energy minimizations are based on the dissociation energies of the bonds, accounting for the overlap of the dipole moments and often used in QSAR modeling parameterization.¹⁶⁰ Model 10 parameters are presented in Table 4 and proved very robust and demonstrated excellent linearity with an r^2 value of 0.8304, a cross validation value of 0.7501, and a predicted r^2 value of 0.7349, also not overpredicting against the external validation r^2 of 0.8806. The external predictability of Model 11 was determined by the predicted r^2 ($pred_r^2$) value, which was 0.8806, meaning that the model has a prediction rate of 88.06%. The 3D model was better than the 2D QSAR model in the cross validation (q^2 of 0.7501 vs 0.7151) and external validation r^2 (0.8806 vs 0.8266); however, the predicted r^2 capability was better in the 2D model (0.8150 vs 0.7349).

The 3D QSAR model statistical parameters and values are presented in table 9.

Table 9. The Pgp 3D QSAR Model Statistical Parameters and Values.

Statistical Parameter	3D QSAR MLR Model 10
n	58
deg. of freedom	44
r^2	0.8304
q^2	0.7501
F_{test}	19.5892
r^2 se	0.2128
q^2 se	0.2584
Predicted r^2	0.7349
Predicted r^2 se	0.6234
External val r^2	0.8806
Ext val r^2 se	0.1683

Plotting the predicted Pgp activity against the experimental activity also provides an assessment of the model. As shown in Figure 19, the predicted vs experimental Pgp activity for the training and test sets showed excellent linearity. There was one outlier in the test set (molecule 77) that had a very high Papp value (12.4) but was predicted to be low due to the 2-methyltetrahydrofuran ligand attached to the benzamido group.

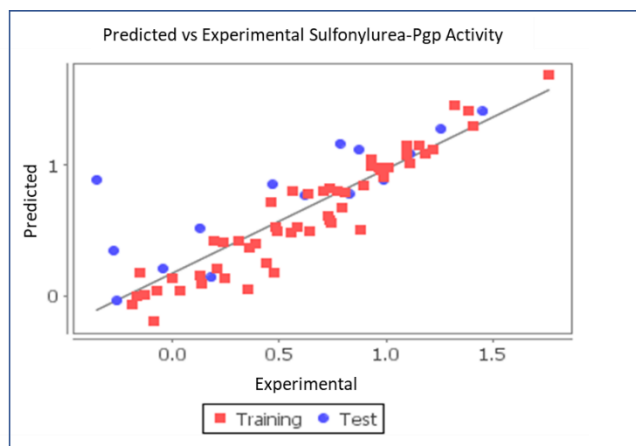


Figure 19. Graphical representation of predicted Pgp activity vs. actual activity for the training and test sets for MLR Model 10.

There were eleven 3D descriptors for Model 10 representing the steric and electrostatic space contributing to the activity model, as presented in Figure 19. The descriptors are denoted as electrostatic (E) or steric (S), and the corresponding number is the location of the grid surrounding the molecule. The steric descriptors represented the largest positive contributors to the QSAR model with S_1446, S_1970, S_3790, S_2316, S_1715, S_834, S_2320, and S_3219 positively contributing to the model, and accounting for approximately 75% of the weighted activity overall. One steric descriptor (S_1060) and the two remaining electrostatic descriptors (E_3205 and E_714) negatively contributed to the interaction.

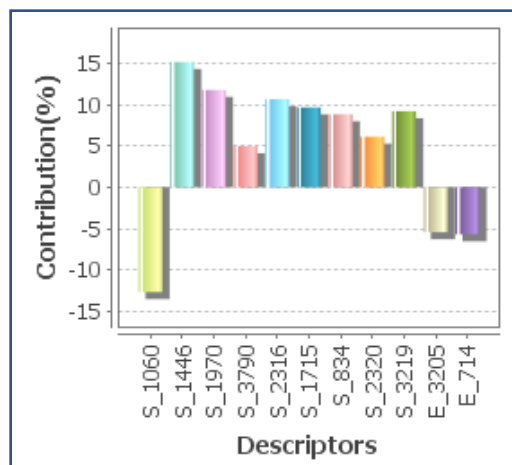


Figure 20. Steric and Electrostatic descriptors contributions for the 3D QSAR modeling of Pgp activity for 3D QSAR del re energy minimization.

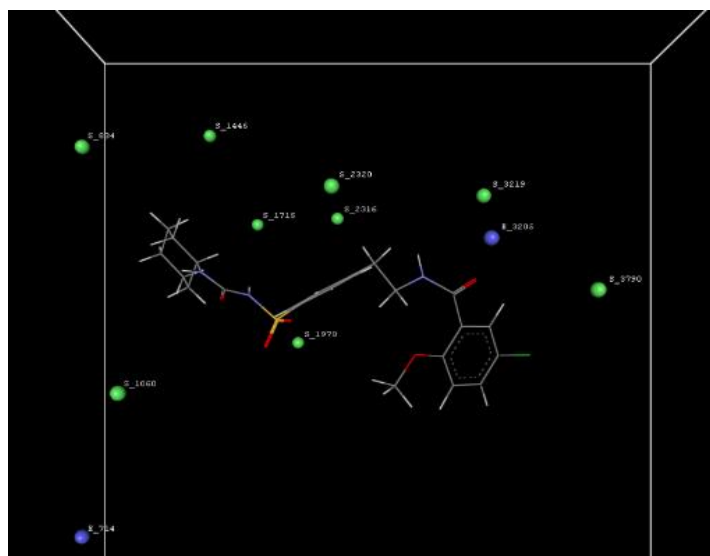


Figure 21. Glyburide molecule showing the points of Pgp 3D model.

The plots in Figure 21, show the steric and electrostatic field points indicating the region of local fields round the aligned molecule Glyburide. The colored spheres (blue and green) represent the fields, steric and electrostatic, respectively. In the 3D QAR model,

the steric descriptors with positive values represent areas with high steric tolerances, meaning bulky groups would be favored; and steric descriptors with negative values indicate areas with low tolerance, meaning smaller groups would be favored. The electrostatic descriptors with positive values represent areas where electron-donating groups are favored; and the negative values represent areas where the electron-withdrawing groups are favored.

The equation governing the sulfonylurea-Pgp 3D QSAR model is:

$$\text{pPgp Efflux}_{\text{gas mars}} = -0.0152(\pm 0.0024) (S_{1060}) + 0.0236(\pm 0.0030) (S_{1446}) + 0.0163(\pm 0.0026) (S_{1970}) + 0.0134(\pm 0.0058) (S_{3790}) + 0.0167(\pm 0.0032) (S_{2316}) + 0.0170(\pm 0.0036) (S_{1715}) + 0.0149(\pm 0.0032) (S_{834}) + 0.0085(\pm 0.0028) (S_{2320}) + 0.0177(\pm 0.0039) (S_{3219}) - 0.0357(\pm 0.0126) (E_{3205}) - 0.0493(\pm 0.0176) (E_{714}) + 0.2696$$

The equation above shows the contributions for the various descriptors contributing to the explanation of the Pgp activity. Those descriptors having a positive value shows that an increase is needed for Pgp activity. Conversely, there were three descriptors that show an inversely proportional relationship in that decreasing the value of that descriptor will increase the Pgp activity. From the model it is observed that the electrostatic fields E_714 and E_3205 have negative coefficients on both the cyclohexyl moiety and on the carbonyl of the amide, respectively. Also, the negative coefficient on steric descriptor S_1060 shows that the cyclohexyl ring needs smaller group at that position to increase the Pgp activity. The remaining steric field descriptors have positive coefficients, and therefore would require bulkier groups to increase the Pgp activity. The S_1446, S_1715, S_1970, S_2316, S_2320, S_3129, and S_3790 steric descriptors show an increase in Pgp

activity with the increased bulky groups at the cyclohexyl ring, urea, sulfonyl, central aryl ring, benzamido, and the halogen substitution of the benzamido group, respectively.

Molecule	Efflux Ratio	logER Ratio	Pred logER	Residual	Molecule	Efflux Ratio	logER Ratio	Pred logER	Residual
1	6.39	0.806	0.635	0.17	41	1.76	0.246	0.226	0.019
2	2.75	0.439	0.246	0.194	42	2.24	0.35	0.197	0.153
3	6.21	0.793	0.384	0.409	43	1.52	0.182	0.209	-0.027
4	5.51	0.741	0.557	0.184	44	1.09	0.037	-0.012	0.05
5	2.3	0.362	0.394	-0.033	45	1.34	0.127	0.125	0.002
6	0.93	-0.032	0.16	-0.191	46	1.54	0.188	0.146	0.041
7	0.9	-0.046	0.151	-0.197	47	3.57	0.553	0.661	-0.108
8	0.99	-0.004	0.288	-0.292	48	12.4	1.093	1.31	-0.217
9	0.53	-0.276	-0.141	-0.135	49	3.05	0.484	0.922	-0.438
10	0.82	-0.086	0.354	-0.441	50	5.89	0.77	0.177	0.593
11	0.76	-0.119	-0.236	0.117	51	2.89	0.461	0.286	0.175
12	0.7	-0.155	0.38	-0.535	52	4.37	0.64	0.754	-0.113
13	0.65	-0.187	0.267	-0.454	53	12.5	1.097	0.99	0.107
14	0.74	-0.131	0.175	-0.306	54	9.38	0.972	1.16	-0.188
15	0.55	-0.26	-0.264	0.004	55	1.36	0.134	0.015	0.118
16	0.56	-0.252	-0.277	0.025	56	57.4	1.759	0.616	1.143
17	5.4	0.732	0.717	0.016	57	5.35	0.728	0.187	0.541
18	10.2	1.009	0.924	0.085	58	7.64	0.883	0.851	0.032
19	4.17	0.62	0.746	-0.126	59	6.7	0.826	0.687	0.139
20	2.99	0.476	0.122	0.354	60	16.5	1.217	1.433	-0.216
22	9.3	0.968	0.793	0.176	61	3.62	0.559	0.735	-0.176
23	2.43	0.386	0.467	-0.081	62	3.08	0.489	0.466	0.022
24	1.33	0.124	0.068	0.056	63	9.74	0.989	1.062	-0.073
25	9.73	0.988	0.606	0.382	64	7.81	0.893	0.753	0.139
26	8.45	0.927	0.727	0.2	65	14.3	1.155	1.162	-0.007
27	3.83	0.583	0.452	0.132	66	11.7	1.068	0.934	0.134
28	12.8	1.107	1.107	0	67	1.72	0.236	0.24	-0.004
29	5.41	0.733	0.632	0.101	68	28.4	1.453	1.309	0.145
30	2.04	0.31	0.259	0.05	69	25.5	1.407	1.477	-0.07
31	8.52	0.93	0.02	0.91	70	7.45	0.872	0.991	-0.119
32	12.9	1.111	1.034	0.077	71	18.1	1.258	0.828	0.43
33	21	1.322	0.633	0.69	72	24.3	1.386	1.375	0.01
34	15.3	1.185	1.271	-0.086	73	1.34	0.127	0.077	0.051
35	3.37	0.528	0.562	-0.035	74	1.06	0.025	-0.104	0.13
36	1.56	0.193	0.096	0.097	75	2.93	0.467	0.574	-0.107
37	5.08	0.706	0.825	-0.119	76	4.29	0.632	0.517	0.115
38	0.44	-0.354	0.147	-0.5	77	0.85	-0.072	0.945	-1.017
39	1.62	0.21	0.122	0.088	78	12.4	1.093	0.908	0.185
40	0.68	-0.166	0.224	-0.39	79	6.07	0.783	0.661	0.123

Table 10. Molecules used in the Pgp study with experimental, predicted and residual activity values.

BCRP 3D QSAR DISCUSSION

The optimum model to describe the sulfonylurea-BCRP interaction with the 3D space was obtained in Model 65, using the MLR methodology, also using the sphere exclusion technique, and with Gasteiger Marsili energy minimization calculations.¹⁶¹ Gasteiger Marsili energy calculation for the 3D space is a method of calculating the energies of the atomic charges in the sigma and pi systems and is also used routinely as an energy calculation tool for QSAR modeling.¹⁶² Model 65 also proved very robust and demonstrated excellent linearity with an r^2 value of 0.9063%, a cross validation value of 0.7789 and a predicted r^2 value of 0.8687. The predictive ability of all the 3D QSAR models was further confirmed by the predicted r^2 and the external validation test data set, both of which demonstrated excellent acceptance criteria with only a slight overprediction when comparing the predicted r^2 to the external validation r^2 values.

The BCRP 3D QSAR model statistical parameters and values are presented in table 11.

Statistical Parameter	3D QSAR MLR Model 65
n	58
deg. of freedom	32
r^2	0.9063
q^2	0.7789
F_{test}	38.7034
r^2 se	0.1290
q^2 se	0.1981
Predicted r^2	0.8687
Predicted r^2 se	0.2092
External val r^2	0.8121
Ext val r^2 se	0.3436

Plotting the predicted BCRP activity against the actual experimental activity also provides an assessment of the model. As shown in Figure 22 the predicted vs actual BCRP activity for the training and test sets showed excellent linearity.

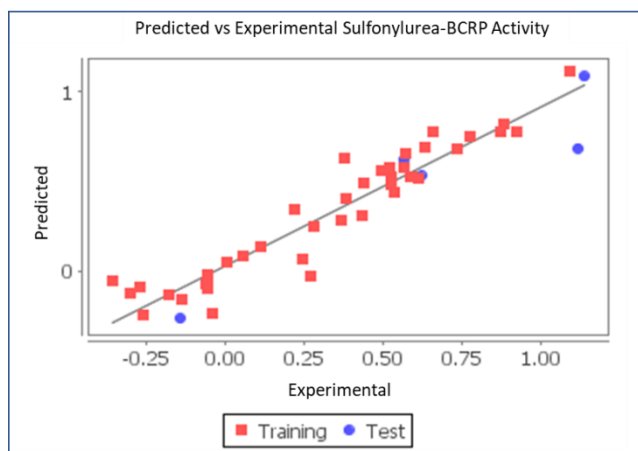


Figure 22. Graphical representation of predicted BCRP activity vs. actual activity for the training and test sets for MLR Model 65.

There were eight 3D contributing descriptors for Model 65 representing the steric and electrostatic space surrounding the molecules. For reference, the descriptors are denoted

as electrostatic (E) or steric (S), and the corresponding number is the location of the grid surrounding the molecules. The steric descriptors were the largest positive contributors to the QSAR model with the S_1940, S_1950, and S_1292 descriptors contributing approximately 58% to the overall model. The steric descriptor S_1926 and S_2156, and the electrostatic descriptors E_1375, E_1458, and E_2086 contributed negatively to the interactions. contribution plot in Figure 23 accounts for the individual descriptors contributions toward the biological activity.

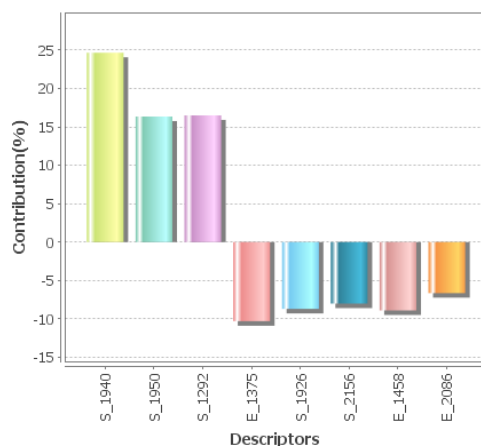


Figure 23. Steric and Electrostatic descriptors contribution plots for the 3D QSAR modeling of BCRP activity for 3D QSAR Model 65 Gasteiger-Marsili energy minimization.

The equation governing the 3D QSAR model is:

$$\text{pBCRP Efflux} = 0.0205(\pm 0.0015) (S_{1940}) + 0.0164(\pm 0.0018) (S_{1950}) + 0.0209(\pm 0.0023) (S_{1292}) - 0.0652(\pm 0.0107) (E_{1375}) - 0.0134(\pm 0.0027) (S_{1926}) - 0.0203(\pm 0.0048) (S_{2156}) + 0.0149(\pm 0.0032) (S_{834}) - 0.0134(\pm 0.0027) (S_{2156}) - 0.0203(\pm 0.0048) (E_{1458}) - 0.0225(\pm 0.0041) (E_{1458}) - 0.0370(\pm 0.0099) (E_{2086}) - 0.0011$$

The equation above shows the contributions for the various descriptors contributing to the explanation of the BCRP activity. Those descriptors having a positive value shows that an increase in that descriptor increases the BCRP activity. Conversely, there were three descriptors that shown an inversely proportional relationship in that decreasing the value of that descriptor will increase the BCRP activity. From the model it is observed that the electrostatic fields E_714 and E_3205 need more negative ligands to increase activity, with a negative coefficient on both the cyclohexyl moiety and on the carbonyl of the amide, respectively. Also, the steric descriptor S_1060 shows that the cyclohexyl ring needs smaller group at that position. The field points model is shown in Figure 24.

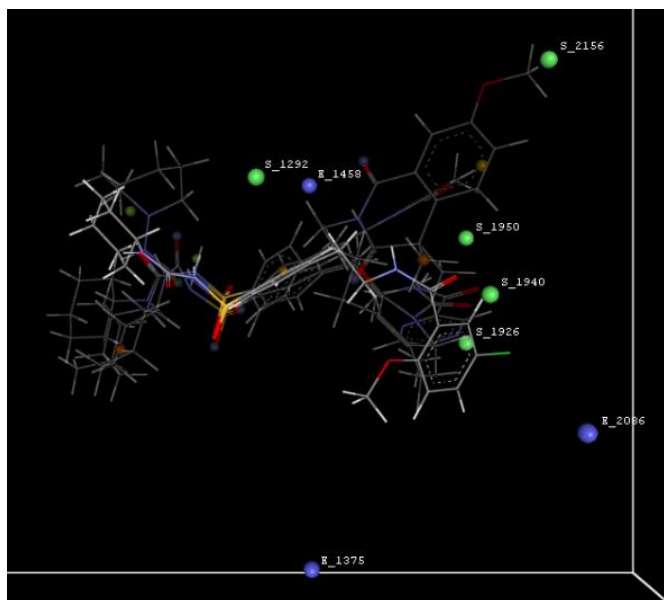


Figure 24. Field point model detailing steric and electrostatic descriptors for the 3D QSAR Modeling.

The plot of steric and electrostatic field points indicates the region of local fields around the aligned molecules.¹⁶³ The colored spheres (blue and green) represent the fields, steric

and electrostatic, respectively. In the 3D QAR model, the steric descriptors with positive values represent areas with high steric tolerances, meaning bulky groups would be favored; and steric descriptors with negative values indicate areas with low tolerances, meaning smaller groups would be favored. The electrostatic descriptors with positive values represent areas where electron-donating groups are favored; and the negative values represent areas where the electron-withdrawing groups are favored.

From the model it is observed that the steric fields S_1940, S_1950, and S_1292 have positive coefficients, meaning that an increase in bulky groups on the benzamido and sulfonylurea ligands, respectively, will increase the BCRP activity. Similarly, the steric and electrostatic descriptors with negative coefficients require smaller or more negative ligands to increase activity. The steric descriptors S_1926 and S_2156 negative coefficients mean that smaller ligands at the far side of the substituted benzyl ring will increase activity. The electrostatic descriptors E_1375, E_2086 and E_1458 have negative coefficients that dictate more negative ligands need to be present on the benzamido and central ring to increase activity.

Molecule	Efflux Ratio	logEfflux Ratio	Predicted logEfflux Ratio	Residual	Molecule	Efflux Ratio	logEfflux Ratio	Predicted logEfflux Ratio	Residual
1	2.78	0.444	0.201	0.243	29	3.34	0.524	0.596	-0.073
2	1.9	0.279	0.2	0.079	30	1.49	0.173	0.623	-0.45
3	3.21	0.507	0.734	-0.228	31	3.37	0.528	0.653	-0.126
4	3.45	0.538	0.385	0.153	32	4.28	0.631	0.573	0.058
5	1.14	0.057	0.057	0	32	4.28	0.631	0.831	-0.199
6	1.01	0.004	0.212	-0.207	33	3.32	0.521	0.669	-0.148
7	0.88	-0.056	0.106	-0.161	34	7.67	0.885	0.766	0.119
8	0.87	-0.06	-0.025	-0.035	35	3.9	0.591	0.573	0.018
9	0.67	-0.174	-0.19	0.016	36	1.87	0.272	-0.037	0.309
10	0.54	-0.268	0.008	-0.276	37	2.75	0.439	0.493	-0.054
11	0.55	-0.26	-0.268	0.008	38	0.877	-0.057	0.055	-0.112
12	0.59	-0.229	0.05	-0.279	39	1.76	0.246	0.239	0.007
13	0.72	-0.143	-0.263	0.12	40	0.881	-0.055	0.073	-0.128
14	0.91	-0.041	-0.275	0.235	41	13.1	1.117	0.84	0.277
15	0.44	-0.357	-0.049	-0.308	42	3.7	0.568	0.38	0.189
16	0.5	-0.301	-0.171	-0.13	43	8.33	0.921	0.766	0.154
17	2.32	0.365	0.505	-0.14	44	1.3	0.114	0.05	0.064
18	3.72	0.571	0.624	-0.054	45	13.4	1.127	1.179	-0.052
19	2.41	0.382	0.258	0.124	46	6	0.778	0.621	0.157
20	1.76	0.246	0.661	-0.415	47	4.54	0.657	0.747	-0.089
22	2.4	0.38	0.73	-0.35	48	7.45	0.872	0.631	0.241
23	6.54	0.816	1.083	-0.267	49	12.4	1.093	1.178	-0.085
24	1.65	0.217	0.444	-0.227	50	2.3	0.362	0.583	-0.222
25	4.18	0.621	0.654	-0.032	51	3.13	0.496	0.628	-0.132
26	3.67	0.565	0.631	-0.067	52	0.73	-0.137	-0.234	0.098
27	2.72	0.435	0.37	0.065	53	4.11	0.614	0.614	0
28	5.43	0.735	0.665	0.069	54	3.88	0.589	0.55	0.039

Table 12. Molecules used in the BCRP study with experimental, predicted and residual activity values.

PHARMACOPHORE MODELING DISCUSSION

A pharmacophore model is a 3D representation of the steric and electrostatic features needed to ensure the optimal molecular interactions with the desired biological activity.

¹⁶⁴ Pharmacophore identification studies were performed using the MolSign module of the VLifeMDS® v4.6 software package. In general, the pharmacophore models consist of Hydrogen bond donors, Hydrogen bond acceptors, aromatic/hydrophobic groups, and positive or negative ionizable groups. The features of the pharmacophore are color coded as Hydrogen bond donors (Green), Hydrogen bond acceptors (Blue), hydrophobic (Orange), Aliphatic (Buff), Negative (Dark Red), and Positive (Dark Green). For visual reference, the software designates the smaller colored spheres to represent the key features of Glyburide, with the larger spheres representing the more common key features across the series of sulfonylurea analogs (larger spheres are shown in Pharmacophore models). In the case of Glyburide, there were 12 key pharmacophore points identified in the molecule, as shown in Figure 25.

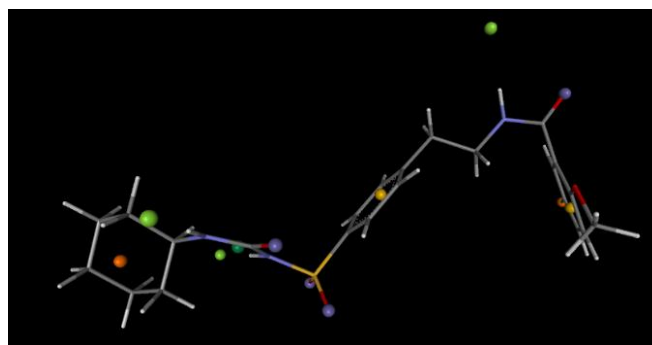


Figure 25. Glyburide Pharmacophore features.

Like the QSAR modeling efforts, the first and second-generation sulfonylureas were analyzed against the low energy conformer Glyburide as the template. As expected, only 5 of the sulfonylureas overlaid precisely to the core conformer structure. The first-

generation sulfonylureas are lacking the benzamido ligand of the scaffold and therefore only partially fit the conformer; with Glimepiride, Glisoxepide, Gliquidone, Glipizide, and Gliclazide, all fit the scaffold overlay.

For the pharmacophore evaluation, the 45 sulfonylurea analogs demonstrating Pgp activity, and the 25 sulfonylureas demonstrating BCRP activity were used to build the respective models. In the VLifeMDS® MolSign software module, Glyburide was loaded as the reference molecule. There are three parameters to optimize that influence the pharmacophore generation: primary feature count, tolerance limit and maximum distance allowed. Briefly, the primary feature count is the number of features in the pharmacophore; the tolerance limit is set to between 10-30% and accounts for variability in the pharmacophore features; and the max distance allowed determines how far apart a feature can be from another (max distance is 15Å). For the pharmacophore generation, the parameters were optimized to capture the best feature coverage of the molecules in the study. For both the reported Glyburide pharmacophores, the feature count was set to 5, the tolerance limit was set to 10%, and the max distance was set to 10Å.

These parameters were optimized to maximize the pharmacophore model activity to capture as many molecular features as possible without dampening the sensitivity. Too few or too many features will not allow for a robust model by including too many or too few molecules in the model. Meaning, allowing for too wide criteria on the tolerance may include features that are not shared across the entire molecule set; on the feature count, limiting the feature count to a reasonable value (i.e., 5) forces the algorithm to pick the best features to define the activity without selecting the entire molecule; and limiting the distance allows for feature resolution across the entire molecule. The impact of these

assumptions is that we are building a local model maximizing the activity of the sulfonyleureas against Glyburide, to best explain the transport behavior of Glyburide in the ABC transporters Pgp and BCRP.

From the pharmacophore generation, the sulfonyleurea-Pgp and sulfonyleurea-BCRP pharmacophores each contained 5 key features describing the steric and electrostatics of the protein-sulfonyleurea activity. The key pharmacophore features were aromatic rings, hydrogen donors, and hydrogen acceptors. Though these features were similar across both ABC transporter models, there were important differences concerning the activities and therefore the pharmacophore models will be discussed separately.

SULFONYLUREA-Pgp PHARMACOPHORE

The sulfonyleurea-Pgp pharmacophore contained 5 features, 2 aromatic rings, 1 Hydrogen donor, and 2 Hydrogen acceptors, as pictured in Figure 26. The H donor feature was assigned to the amide of the sulfonyleurea, with the H acceptors being the carbonyl of the sulfonyleurea and benzamido moieties. The benzamido and aryl ring accounted for the two aromatic rings. The 5-point pharmacophore was supported by 39 of the 45 molecules, sharing all five of the key features. This was the maximum number of sulfonyleurea analogs included with the 5-feature pharmacophore. The inclusion rate was higher with less features of the pharmacophore, but the pharmacophore was not as strong at explaining the features responsible for the activity. This is an important step in pharmacophore generation, the pharmacophore model should represent the activity of the molecules studied as closely as possible.

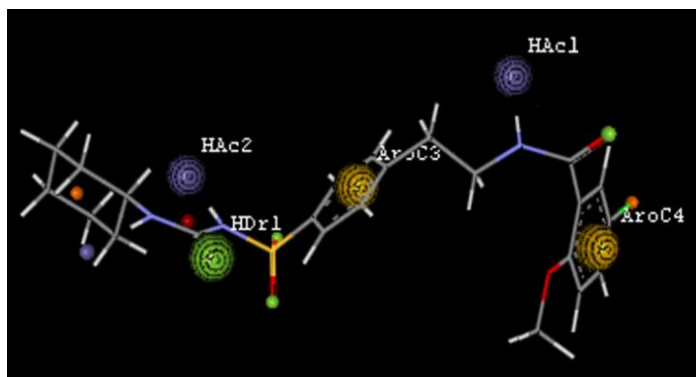


Figure 26. Glyburide Pharmacophore detailing the 5 points of interest.

As expected, the 5 second generation sulfonylureas fit the pharmacophore template well, being similar in size and structure to Glyburide. The first-generation sulfonylureas however are much smaller in size and do not contain the ligands attached at the para position of the arylsulfonylurea core structure. For reference, the core sulfonylurea structure is presented in Figure 26, with the para position of the arylsulfonylurea ring denoted as R₁ circled in blue.

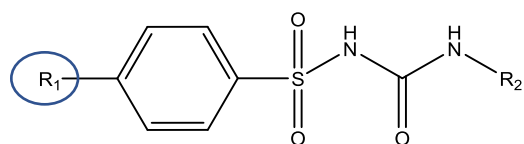


Figure 26. Sulfonylurea-BCRP Pharmacophore denoting the para position of the arylsulfonylurea ring.

SUFONYLUREA-BCRP PHARMACOPHORE

Similar to the Pgp pharmacophore, the sulfonylurea-BCRP pharmacophore contained 5 features, but differed in the types and location of the features. The 2 aromatic rings, 1 Hydrogen donor, 1 Hydrogen acceptors, and 1 hydrophobic as pictured in Figure 27. The H donor feature was assigned to the amide of the sulfonylurea, with the H acceptor assigned to the carbonyl of the benzamido moiety. As expected, the benzamido and aryl rings accounted for the two aromatic rings. The hydrophobic feature was assigned to the substituted benzamido ring, near the Chlorine. The 5-point BCRP pharmacophore was supported by 21 of the 25, sharing all five of the key features to represent the broadest group of the molecule set. Again, this was the highest number of sulfonylureas included in the 5-point pharmacophore. The inclusion rate was higher for lower feature count pharmacophores but did not represent all of the key features properly. The pharmacophore model is presented in Figure 28.

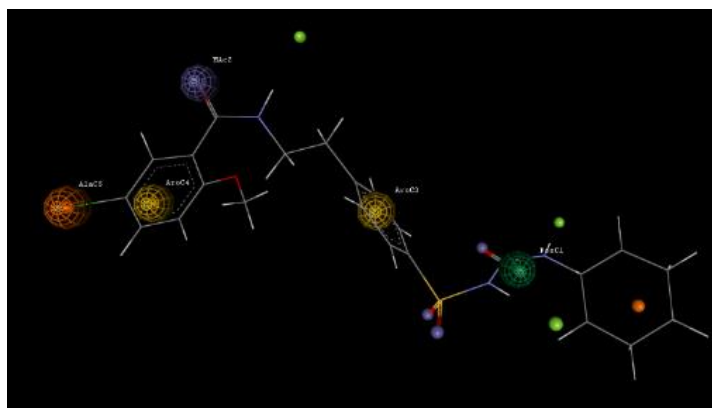


Figure 28. Glyburide-BCRP Pharmacophore detailing the 5 points of interest.

PHARMACOPHORE MODELING DISCUSSION

The value of the pharmacophore model is the highlight of the ligands at certain points on the molecule structure that drive the structure activity relationship. This is possible to accomplish as all of the molecules in the study have been normalized to the most active molecule (Glyburide), providing the means to identify the structural changes that are believed to be implicated in the observed pharmacological activity.

The two pharmacophore models generated showed many similarities and some interesting differences. Both models shared the two aromatic rings, but differed in the hydrogen donor, hydrogen acceptor and hydrophobic features. For the Pgp pharmacophore, the H donor feature represented the amide of the sulfonyleurea, with the H acceptors being the carbonyls of the sulfonyleurea and benzamido moieties. The Pgp pharmacophore represented a uniform feature distribution across the molecule driving the activity. The BCRP pharmacophore however, highlighted the importance of the substituted benzamido ligand for BCRP activity, with the H donor feature representing the amide of the sulfonyleurea, the H acceptor representing the carbonyl of the benzamido moiety, and the hydrophobic feature was assigned to the substituted benzamido ring, near the Chlorine. This hydrophobic character is the main difference between the Pgp and BCRP activity models.

This combination of hydrophilic and hydrophobic character matches well with the understanding that these ABC proteins rely on these broad moieties instead of very specific chemical structures.¹⁶⁵ Clearly from both models, the activity in both the Pgp and BCRP models was driven by the arylsulfonyleurea and the substituted benzamido

ring. The non-substrates of both proteins were lacking at least the benzamido ligand and the steric and electrostatic character that it brings.

As expected, a large set of the sulfonylurea analogs that do not have Pgp or BCRP activity, also contain some or all of these features. However, for those molecules that do not have all the key feature points for either pharmacophore, the activity is obviously lacking. For those molecules that share the key features, but still lack activity, there were a few noticeable differences. These molecules also had other substituents that interfered with the activity, bulky groups, or electron withdrawing/adding.

As there is no crystal structure of Pgp or BCRP currently available, the pharmacophore model allows for a mapping of the key features on the molecule that relate to an increase in activity. The specificity of the pharmacophore model will be lacking as a true binding pocket definition of size and electrostatics for either protein is not known. However, the pharmacophore models for both Pgp and BCRP represent the key molecular features (steric/electrostatic character) of the ligands on the molecule Glyburide that explain the ABC transporter activity.

GENERAL DISCUSSION

The oral hypoglycemic sulfonylurea molecule Glyburide has been shown to be actively transported from various biological tissues through a pronounced interaction with the ATP binding cassette (ABC) active transporter proteins. In our research, the interactions of a series of sulfonylureas and two of the ABC transporter proteins (Pgp and BCRP) were studied in two MDCK cell monolayer transport assays, MDCK-MDR and MDCK-BCRP.

The cell lines are rigorously characterized and shown to have no other transporter proteins present, so the transport activity is regarded as a direct effect of the molecule and the specific protein.

In total, 78 sulfonylurea analogs were used in the Pgp assays, and 54 were used in the BCRP assay. A subset of these sulfonylurea analogs exhibited either Pgp or BCRP activity with 45 demonstrating Pgp substrate activity, and 25 demonstrating BCRP activity. Substrate activity was determined based on the Efflux Ratios (ER), which is the ratio of the transport in the basolateral to apical direction divided by the transport in the apical to basolateral direction. The integrity of the cell monolayers was checked by trans-epithelial resistance measurements, and the ER benchmarked with positive and negative controls, showing the cell monolayers are performing as expected. The negative control for both assays was antipyrine, which demonstrated equivalent transport in both directions; and compounds were chosen for the positive controls that are known substrates for each protein. Specifically, the positive controls were topotecan for the MDCK-BCRP cells, and vinblastine for the MDCK-MDR cells. The molecules whose ER in the Pgp and BCRP transport assays were ≥ 2.5 (2.5 times greater transport in one direction) were considered substrates. The second-generation sulfonylureas and analogs demonstrated considerable Pgp and BCRP activity, further confirming the ability of the sulfonylurea analogs to be substrates of both ABC transporter proteins.

Care was taken to select the experimental concentrations that resulted in relevant and comparable results between the two studies. Of special note are the three sulfonylureas Glimpiride, Glisoxepide and Gliquidone, that were identified as substrates of Pgp and

BCRP and have not been previously reported. Our results also confirm Glyburide as a substrate of Pgp and BCRP, as previously reported.¹⁶⁶

The first reported carrier mediated transport of Glyburide was carried out by Goldstein *et al* demonstrating that Glyburide was a substrate of Pgp.¹⁶⁷ As discussed earlier, subsequent studies have repeatedly demonstrated that Glyburide is actively transported by other ABC transporters, mainly BCRP and MRPs. As there are many studies with BCRP and Glyburide, we chose to revisit the earlier Pgp transport of Glyburide, to understand the substrate potential of the sulfonylurea class. The first part of our research was to test the concentration dependence transport activity of Pgp using the MDCK-MDR cell line. Glyburide, Glipizide, Glimepiride, Gliquidone, and Glisoxepide were run in the transport assay, with concentrations varying from 2-100 μ M, and the apparent permeability and subsequent ER were calculated at each concentration.

The four sulfonylureas showed carrier mediated transport activity as the rates of efflux from the Pgp assay exceeded the rates of absorption for each Glyburide, Glimepiride, Gliquidone, and Glisoxepide. These four analogs showed linear response in uptake and efflux until the highest concentrations. At such high concentrations, the sulfonylureas were acting as inhibitors and blocking their own up transport. This was expected as Glyburide, Glipizide and Gliclazide have been reported as a Pgp inhibitor at high concentrations.¹⁶⁸ Glipizide and Gliclazide, though structurally similar to the second-generation sulfonylureas, demonstrated no/slight Pgp activity and no BCRP activity in our studies, with the rate of transport similar in both directions. It has also been reported that both Glipizide and Gliclazide are Pgp substrates at high concentrations (100 μ M and

500 μ M, respectively), but at the lower concentrations in our study, neither compound was shown to have any Pgp or BCRP activity.¹⁶⁹

The second part of our research looked at the transport mediated activity of the series of sulfonylurea analogs at a standard concentration of 2 μ M. The concentration was held constant so as to identify the structure activity relationship and build three-dimensional pharmacophore and QSAR models to explain the nature and character of the Pgp- and BCRP-sulfonylurea interactions. The cell assays were performed for all available sulfonylurea analogs, and the apparent permeability and subsequent ER were calculated. The ER were then converted to log(ER) to use as the biological activity in the two and three-dimensional QSAR models. The 45 compounds that showed Pgp activity and the 25 compounds that showed BCRP activity were used to build the respective pharmacophore and QSAR models detailing the molecular attributes of the interaction.

The pharmacophore models demonstrated that the two main sections of the molecule, the benzamido and aryl-sulfonylurea moieties, are key to explaining the interaction with both Pgp and BCRP. In fact, in our study the molecules that lacked either substituent showed no Pgp/BCRP activity. The pharmacophore model for each protein detailed 5 features responsible for activity, with the models consisting of aromatics, 2 hydrogen acceptors, 1 hydrogen donor, and 1 hydrophobic group. The five-feature count was determined to be the most appropriate value to use based on trial and error with the software program.

There was a balance of too few/too many features in the pharmacophore and still have a model that represents the key points across the entirety of the molecule. The Pgp pharmacophore consisted of two aromatic rings, two hydrogen acceptors and one hydrogen donor. Meanwhile, the BCRP pharmacophore shared the aromatic and one

hydrogen acceptor but differed in that there was only one hydrogen donor, with the added feature of hydrophobic character on the benzamido ligand. The Pgp and BCRP pharmacophore models are presented in Figure 29 as simple diagrams.

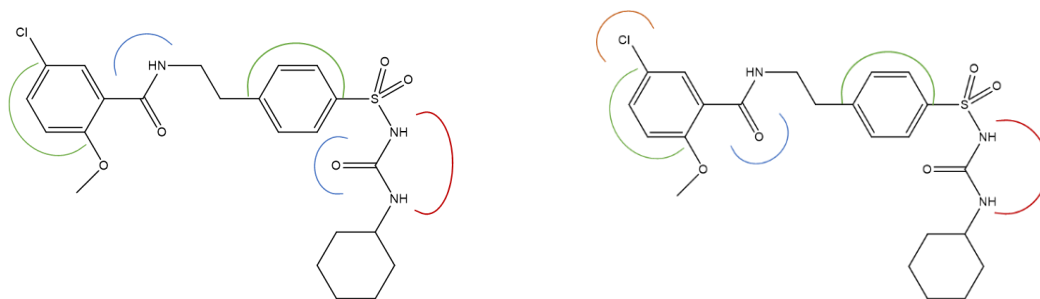


Figure 29. Simple diagrams of key pharmacophore features of the Pgp (left) and BCRP (right) models, superimposed on the molecule Glyburide. *Key: green aromatic, blue hydrogen acceptor, red hydrogen donor, and orange hydrophobic.*

Further evaluation of the sulfonamide activities to the molecular structure through the 3D QSAR models detailed the individual molecular features that add or subtract from the observed Pgp or BCRP activity. Based on the sulfonamide analog structures tested in our work, the ligands attached at the far end of the aryl-sulfonamide section of the molecule appear to be less influential, as the structures can range from a simple alkane to complex with multiple aromatic rings. Meanwhile, the ligands attached to the para position of the arylsulfonamide drive the activity of both Pgp and BCRP. Specifically, the benzamide is needed for either activity; with the ligands attached to the ring also influencing the activities. From our work, the ligands that increase the electron cloud are too hydrophilic and decrease the activities. Conversely, the ligands that increase hydrophobic character or maintain the electronics of the benzyl ring, maintain or increase the activities. A

schematic representation of the core arylsulfonylurea attached to the benzamido ligand is presented in Figure 30 with some example ligands that increase or decrease activity based on our work.

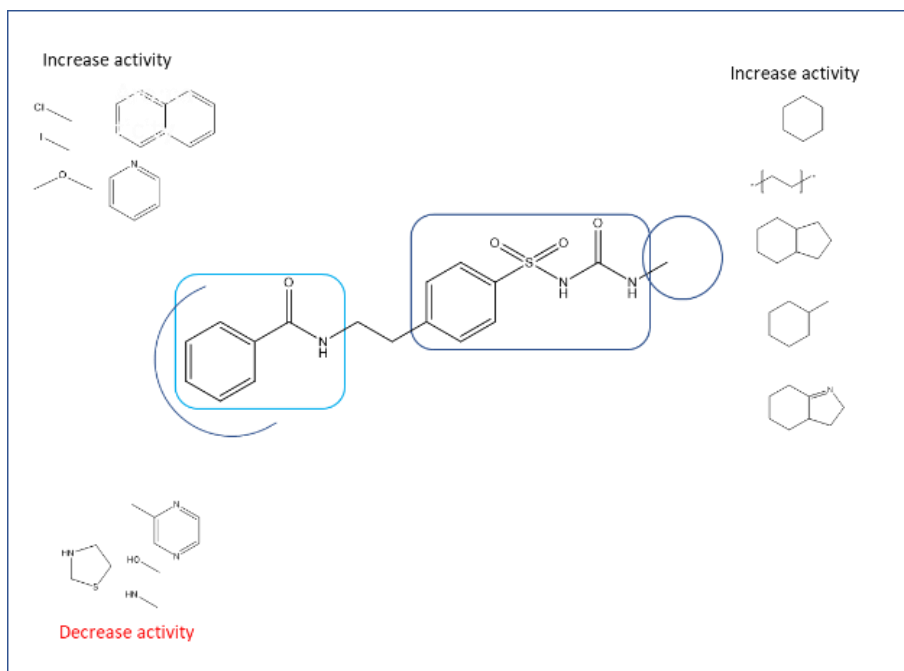


Figure 30. Core structure of sulfonylurea with the potential ligands that can increase or decrease the activity for both Pgp and BCRP. Note: light blue highlights benzamido ligand; dark blue highlights arylsulfonylurea; blue circle denotes where bonding occurs for ligands; and blue semi-circle denotes where bonding occurs for ligands.

The SAR of the sulfonylureas with the SUR1 receptor was first reported by Meyer *et al* in 1999 and described the ligands on Glyburide that are required for SUR1 activity. Meyer reported that removing the cyclohexyl or benzamido ligand marketed reduced SUR1 activity. In fact, swapping the larger ring structures for smaller, less bulky groups (i.e., methyl group) had the same effect.¹⁷⁰ This was also witnessed in our work, the sulfonylureas that more closely resembled the Glyburide structure, containing the

benzamido and aryl-sulfonylurea portions, were more likely to be substrates of Pgp and BCRP. Similarly, if the sulfonylurea or analogs were missing one or the other benzamido of aryl-sulfonylurea portion, then they were not recognized as Pgp or BCRP substrates. Further, as demonstrated in the pharmacophore models, strategic placement of the hydrogen donating/accepting, aromatics, hydrophobic, or bulky groups increased the Pgp and BCRP activity.

Knowing that the sulfonylureas work through binding to the SUR1 protein (ABCC8), which is also an ABC transporter protein like Pgp and BCRP, we looked to what is known of the sulfonylurea and the target protein in the treatment of diabetes. The sulfonylureas are designed to act on the SUR1 receptor, and therefore it would not be controversial to propose that the same elements responsible for binding to the SUR1 receptor would also positively affect the interaction with Pgp or BCRP. This is exactly what was determined by Bessadock *et al.* In fact, Bessadock performed a phylogenic protein search of the ABC transporter proteins demonstrating that Pgp and SUR1 are from the same protein cluster. Similarly, Vila-Carriles *et al* proposed that the SAR driving the 2nd generation sulfonylureas has been to increase the binding affinity with the sulfonylurea receptor, interacting with both the proposed A and B sites of the SUR receptor, as shown in Figure 31.¹⁷¹

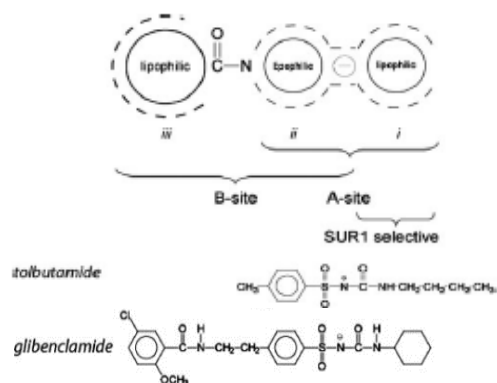


Figure 31. Representative binding sites on SUR1, tolbutamide and glyburide presented as examples, reproduced from Vila-Carriles.

The second-generation sulfonylureas were designed to interact with both binding pockets of the SUR1 protein, and in doing so were considerably more potent than the preceding generation. This increased potency across the generations is the same impact as seen in our work, in fact it mimics it very closely. Simply, those analogs that did not have both the arylsulfonylurea and benzamido ligands did not exhibit Pgp or BCRP activity.

Building on the similarity of the SUR1 and Pgp transporter proteins theory, Bessadock *et al* have reported the Glyburide pharmacophore based on the 3-dimensional alignment of Glyburide with vinblastine, a known Pgp inhibitor. Their pharmacophore models called out five key features: the two aromatic rings, two hydrogen donor groups (NH and NH proximal to S), and one electron donor group (C=O) and is presented in Figure 30. Our work is very much in line with these findings and confirms the Bessadock model. Also, this model is representative of the hypothesized molecule features of the SUR1, which

was expected based on the proximity on the ABC membrane transporter phylogenetic tree.

172

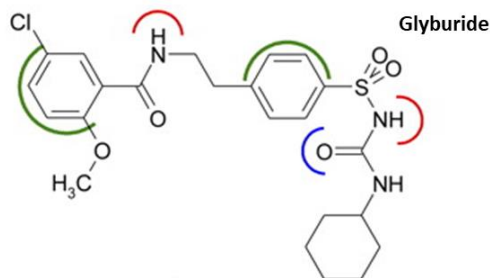


Figure 32. Key features in Glyburide-Pgp interaction, reproduced from Bessadock. Key: green is aromatic red is hydrogen donating, blue is hydrogen accepting groups.

We have found that pharmacophore model presented in Figure 31 accounts for many of the same molecular features as reported in our research. We confirm the necessity of the two aromatic rings, the two hydrogen donors, and the hydrogen acceptor. These features are confirmed by the Pgp substrate activity of the 45 sulfonylurea molecules used to build the pharmacophore.

CONCLUSION

Pgp and BCRP are the most studied ABC transporter proteins and have been found to be largely responsible for the multidrug resistance phenomenon in cancer therapies, but characterization of either has been difficult due to the lack of the membrane crystal structure and general substrate promiscuity. Numerous groups are working towards generating the crystal structure of the ABC transporters, but that work is still years to come.^{173, 174} The lack of a defined substrate binding pocket for either Pgp or BCRP

proteins has made it difficult to develop one single QSAR or pharmacophore model describing the spatial and structural features responsible for activity.¹⁷⁵ However, as demonstrated here, modeling transporter activity can aid in the understanding and general knowledge of the drug-transporter interactions.

By using a large data set of sulfonylurea analogs representing the space of the oral hypoglycemic compounds, we evaluated the substrate activity against to the ABC transporter proteins Pgp and BCRP. This resulted in confirming the substrate activity for 41 analogs in the Pgp assay, and 25 analogs for the BCRP assay. Also, we have demonstrated that Glimepiride, Glisoxepide, and Gliquidone are substrates of Pgp and BCRP, all of which are previously unreported.

Our work has also confirmed the pharmacophore model previously presented in literature, demonstrating that the sulfonylureas need certain 3-dimensional molecular features to be substrates of Pgp and BCRP. Specifically, the benzamido and arylsulfonylurea ligands are needed for both Pgp and BCRP activity. Furthering this understanding, is the need for hydrogen donators/acceptors for Pgp activity, and the need of hydrogen donators/acceptors and hydrophobic groups for BCRP activity. We also found that the substituted benzamido ligand is important for both Pgp and BCRP activity, with the ligand attached to the arylsulfonylurea not influencing the activities.

Computational QSAR models describing the Pgp and BCRP activity for a series of sulfonylurea analogs were derived with statistical significance and predictive capabilities by using the 2-dimensional and 3-dimensional molecular descriptors presented in the VLifeMDS® suite. The predicative ability of these models observed for the training, test, and validation sets of molecules make these models useful for designing new compounds

to help explain sulfonylurea-Pgp and sulfonylurea-BCRP activity. Further, this is the first set of QSAR studies performed to explain the ABC protein interactions of the hypoglycemic sulfonylureas.

CHAPTER 3
COMPARISON OF PGP AND BCRP ACTIVITY FOR A SERIES OF
SULFONYLUREAS BY ACTIVITY CLIFF ANALYSIS

by

Samuel D Bell⁷ ; Brian Bronk⁸ ; William Euler⁹

is submitted to Molecular Pharmaceutics

⁷ PhD Candidate, Department of Chemistry, The University of Rhode Island, Kingston, RI 02881. Email: sbell@chm.uri.edu

⁸ Adjunct Professor, Department of Chemistry, The University of Rhode Island, Kingston, RI, 02881. Email: brian.bronk@sanofi.com

⁹ Professor, Department of Chemistry, The University of Rhode Island, Kingston, RI, 02881. Email: weuler@chm.uri.edu

COMPARISON OF PGP AND BCRP ACTIVITY FOR A SERIES OF SULFONYLUREAS BY ACTIVITY CLIFF ANALYSIS

ABSTRACT

Activity Atlas software was used to describe the protein activity between a series of sulfonylureas and two of the ATP Binding Cassette (ABC) transporter proteins found to be largely responsible for the active transport of Glyburide, Pgp and BCRP. The Activity Cliff Analysis has provided a platform to understand the interactions that are important to the guide the drug-protein interaction, with the potential to better design medications for targeted delivery, for instance in pregnant women. The Activity Cliff Analysis is based on the key features of average shape, hydrophobic region, and electrostatic patterns of the active compound, and were mined and mapped to detail the differences in molecular features driving the ABC protein activity to either Pgp or BCRP, specifically.

As described in our previous work, Activity Atlas was used on a large series of sulfonylurea analogs, with the objective of investigating and understanding the molecular features that underlie the ABC protein activity in the hopes of better design of pregnancy centered medications. As expected there were many similarities in the molecular features driving the protein-sulfonylurea activity; but there were also many appreciable differences as demonstrated by the analysis of the hydrophobic, electrostatic and shape molecular descriptors. When coupled to the 3D QSAR data, the Activity Atlas method is particularly useful to visualize and decipher structure activity relationships.

INTRODUCTION

Glyburide is a second-generation sulfonylurea used in the treatment of Type II Diabetes and has been shown to be especially effective in patients that retain some level of insulin production from the pancreatic beta cells. As outlined in the Chapter 1 Introduction section, researchers began looking to Glyburide as a treatment option for gestational diabetes mellitus (GDM). The similarities in the pathophysiology of type II and GDM make the oral hypoglycemic agents a smart choice, as compared to insulin. In fact, researchers have run numerous clinical studies demonstrating that Glyburide is as safe and efficacious in pregnant women as insulin, without many of the insulin related difficulties.

It is in these studies of Glyburide with GDM that researchers have determined a unique placental transport activity. Specifically, Glyburide has been demonstrated to not cross the placental barrier to any appreciable effect; and, Glyburide will leave the fetal compartment against the concentration gradient.^{176, 177} Numerous studies have been performed to understand the mechanism responsible, and it has been found that Glyburide is actively transported by the ATP binding cassette (ABC) transporter proteins, specifically Pgp, BCRP and the MRPs.^{178, 179, 180, 181, 182, 183} The ABC proteins are responsible for the active transport of endogenous and exogenous molecules at the barrier membranes throughout the body and have been shown to be important players in the pharmacokinetic profiles and disposition of many drugs. The documented interactions of Glyburide with the ABC transporter proteins have prompted numerous studies evaluating Glyburide, Glipizide, and Gliclazide, with similar results.¹⁸⁴ In these studies Glyburide, Glipizide, and Gliclazide have been

shown to act as substrates or inhibitors of the ATP transporter proteins, depending on the concentration dosed.^{185, 186, 187} Figure 32 shows the molecular structure of the three sulfonylureas most studied with the ABC transporters.

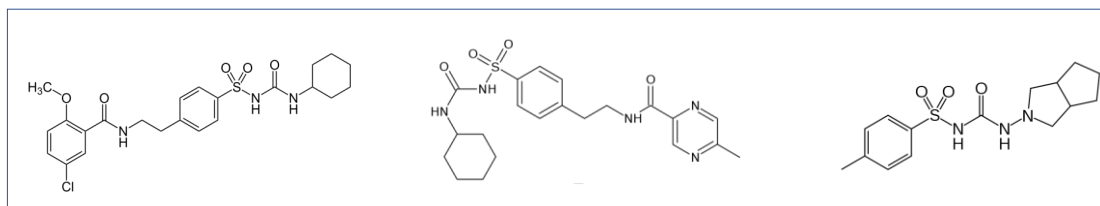


Figure 33. Glyburide, Glipizide, and Gliclazide structures.

Many studies have been also performed to understand the placental transport, pharmacokinetics/pharmacodynamics, or even to determine the proteins responsible for the transport of Glyburide. Our research is the first investigation to study the interaction of the sulfonylurea hypoglycemic agents and the ABC transporter proteins. In this investigation, a series of sulfonylurea analogs were studied for activity against Pgp and BCRP in cell-based transport assays. From the transport assay data, we used Cressets Activity Atlas modeling capabilities to identify and describe the key molecular features of the sulfonylurea analogs driving the interaction with either the Pgp or BCRP. Understanding the differences in the molecular targets could have a profound impact on tailored drug delivery and the future of medicine. Specifically, these studies may contribute to the design of medications for pregnant women that are safe and efficacious, without presenting any harm to the fetus.

DATA SET

A total of 78 sulfonylurea analogs were available to be evaluated in the Pgp and BCRP cell-based transport assays. For the Pgp assay, all 78 compounds were tested, with a subset of 53 compounds tested in the BCRP assays. The transport assays were performed in Madin-Darby Canine Kidney cells that were transfected with overexpressing Pgp or BCRP genes. The transport assays were validated with positive and negative transport control compounds, and the cell-monolayers determined acceptable for use by measuring the trans-epithelial resistance, as discussed in the preceding chapters. As our research and published articles have shown, Glyburide has been reported as a substrate for both Pgp and BCRP, and as a substrate and/or inhibitor for other ABC transporters and was therefore used as the reference molecule in the studies. As a crystal structure of the sulfonylureas with either protein has not been reported, the lowest energy conformation was used in these studies as described by Lins et al.¹⁸⁸ The lowest energy conformations were determined with by Chemaxon® and ChemDraw® software using the MMFF94 energy minimization calculation algorithms.^{189, 190}

The sulfonylurea analogs were tested at a constant concentration (2µM) as per internal procedure, with each measurement performed in at least triplicate to assure adequate statistical control. The data generated from each cell-based assay was then used to build 2D and 3D quantitative structure activity models (QSAR) and a pharmacophore model with the molecule design software suite from VLifeMDS. The 2D and 3D QSAR models demonstrated excellent predictability, but for the work presented here, we will focus on the 3D data set and modeling. For both cell-based assays, the 3D

protein models demonstrated excellent predictability with the Pgp model demonstrating a linearity value of $r^2 = 0.8304$ and cross-validation of $q^2 = 0.7501$; and the BCRP model demonstrating a linearity value of $r^2 = 0.9083$, with a cross-validation value of $q^2 = 0.7789$.

CONFORMATION HUNT AND ALIGNMENT OF MOLECULES

The first step of the modeling efforts was to generate the most stable conformations and to overlay the molecules to a template. As Glyburide is well characterized and known to interact with Pgp and BCRP, we used Glyburide as the template molecule for conformer hunting and molecular alignments. The conformation hunt was carried out with Cresset Forge® software package using the MMFF94 energy minimized structure of Glyburide, as we have previously reported.¹⁹¹ The remaining sulfonylurea analogs were aligned by the maximum common substructure, using the “very accurate but slow” configuration setting to maximize success. The details of the conformation hunt parameters are:

Max Number of conformations 1000

RMS cutoff for duplicate conformers: 0.5

Gradient cutoff for conformer minimization: 0.1kcal/mol

Energy window: 3kcal/mol

As with all 3D model generation, the molecular alignment is the most critical first step and if not performed correctly can lead to incorrect modeling practices. After

completion of the alignment process, visual inspection of the all the molecular alignments was performed to make sure there were no disparities between molecules. The molecules were evaluated for maximal alignment scores against Glyburide and the molecules that were suboptimal, were adjusted and rescored. For example, manipulating the phenyl ring of the benzamido substructure proved to be the most common fix, and maximized the substructure similarity scores to Glyburide.

ACTIVITY ATLAS MODELING

The Activity Atlas modeling is part of the Cresset Forge® molecular dynamics software package and is routinely used for the design and discovery of new molecules. The Activity Atlas modeling suite performs three types of analyses that are key to the understanding the activity for the molecules against a specific target, and are defined as the Average of the Actives, Activity Cliff Summary, and the Regions Explored Analysis.¹⁹² For our research, the Regions Explored analysis was not performed as it is an assessment of what regions have been explored on the molecule, disregarding the biological activity. For the research performed here, we will discuss the Average of Actives and Activity Cliff Analysis, as they will have more insight on the activity of the sulfonylureas.

ACTIVITY CLIFF MODELING

As described in the literature references, Activity Analysis modeling can pinpoint the critical region of the structure activity relationships (SAR), providing a visual summary of the activity cliff for each of the data sets.¹⁹³ An Activity Cliff is defined as a pair or series of structurally similar compounds that have a large difference in potency or activity.¹⁹⁴ This is especially pertinent for sets of molecules run in different assays, allowing the data to be combined and compared to further characterize the molecules, the associated biological activity and critical differences in SAR.

As discussed by Cheesewright *et al.*, describing how the molecule fits into a binding pocket requires the ability to define the properties near the molecular surface, and not simply as a collection of atoms.¹⁹⁵ Normally, this modeling effort would be too calculation-intensive with long computer run times. The benefit of the Cresset software to simplify and this process and condense the complex three-dimensional fields (for example, electrostatic and van der Waals) down to local extrema, called field points. These field points are defined for key molecular features, such as H⁺ donor, H⁺ acceptor, positive/negative ionic character, hydrophobic character, etc. The field points are then grouped into field patterns, with these field patterns able to compare molecules directly, representing a summary of the 3D properties of each molecule.

In order to evaluate the molecular features against a given biological activity, a 3D lattice of grid points is created covering the entire volume surrounding the molecule. For each point or each pair of points, a coefficient is then created to define the space. The calculation for each coefficient is calculated by:

$$C_{\text{eff}} = (\text{disparity} - \text{minDisparity}) * \Delta\text{Field}_{\text{xyz}} * \text{weight}$$

Where C_{eff} is the grid point

Disparity is the value between two molecules

MinDisparity is a minimum threshold value

$\Delta\text{Field}_{\text{xyz}}$ is the field difference at this point described for this molecular pair

Weight is the product of the molecule and alignment weights

The calculation for the coefficient represented in the above equation helps pinpoint the critical regions of the structure activity relationship by looking at each grid point in relation to the others.

AVERAGE OF ACTIVES MODELING

The Average of Actives Analysis Model describes the common attributes that the active molecules in the data set have in common. This calculation is performed for all field points and at each grid point surrounding the molecules. Building on the Activity Cliff modeling, the Average of Actives is a summary of the Activity Cliff modeling and also creates a 3D lattice of grid points of the lattice surrounding the aligned molecules and calculates a coefficient. The coefficient for the Average of Actives modeling is calculated according to the equation ¹⁹⁶:

$$\text{Coeff} = \text{Field}_{\text{xyz}} * \text{Weight}$$

Where Co_{eff} is the coefficient for the grid point

$\text{Field}_{\text{xyz}}$ is the field at the grid point for the active molecule

Weight is the product of the molecule and alignment weights

RESULTS

The results of the Activity Cliff Analysis show distinct difference between the sulfonylurea analogs interactions with ABC transporters, Pgp and BCRP. To ensure robust calculations, the molecules were energy minimized using the MMFF94 energy field, and then conformer generation was performed to ensure the molecular structure disparity was minimized to eliminate variability and allow for the modeling to be governed only by the biological activity of the aligned structures.

In performing the comparative analysis differentiating the model systems, we compared the BCRP activity data against the Pgp activity data (Figure 2). As shown in the Figure, there is good correlation between the Pgp and BCRP activity, with a linearity score of 0.84. This correlation shows that the nature of transport for the two proteins is similar, with more sulfonylurea analogs substrate of Pgp than that of BCRP, as shown by the activity. This proved a very interesting point as the understanding was that Glyburide (and by assumption, the sulfonylurea class) would show more substrate activity with BCRP, as is reported in literature.¹⁻⁸ The activity map detailing the Pgp activity to that of BCRP is shown in Figure 34.

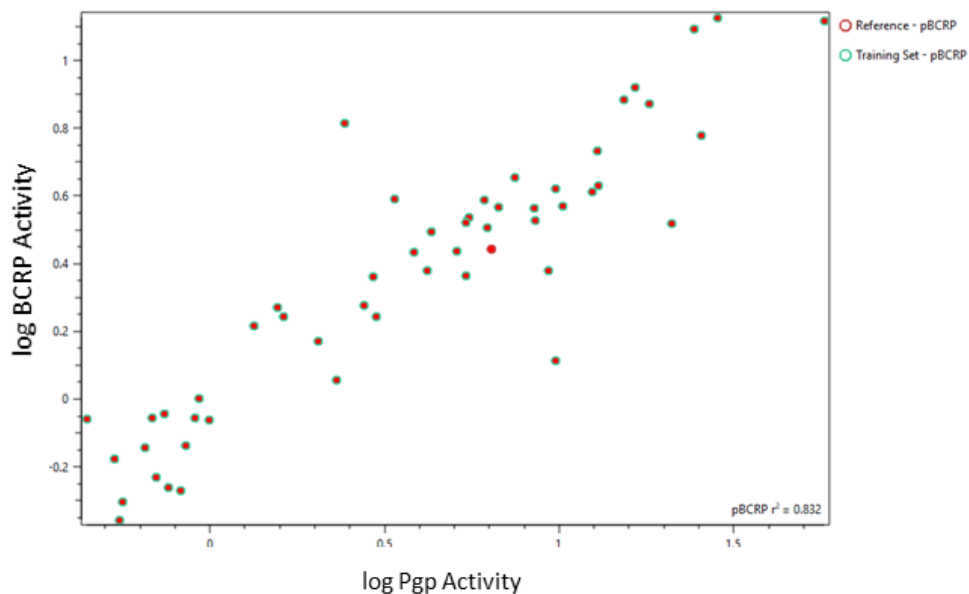


Figure 34. Activity map of the sulfonylurea analogs tested in the Pgp and BCRP efflux assays.

Also shown in the Pgp and BCRP activity map in Figure 33 there are three regions that describe the activity of the sulfonylurea analogs and the Pgp and BCRP transporter proteins. For reference, Glyburide is the red dot in the center of the graph (data points 0.45 BCRP and 0.8 Pgp) and splits the activity data into three distinct categories: Pgp/BCRP activity less than Glyburide, Pgp/BCRP activity similar to Glyburide, and Pgp/BCRP activity greater than Glyburide. The molecules with Pgp and BCRP activity less than Glyburide are straightforward to explain as the molecules in this group are smaller in molecular weight and, in the preponderance of cases, lack the large, lipophilic benzamido ligand. This point is important as it has been shown that the first-generation sulfonylureas that are smaller, and less hydrophobic do not interact with the ABC transporter proteins as the second generations sulfonylureas have been shown to do.¹⁹⁷ The analogs that have Pgp/BCRP activity similar to

Glyburide are similar in structure, molecular weight, and ligand placement, and therefore will behave in a like manner, as expected. The third region is those molecules that have increased Pgp/BCRP activity as compared to Glyburide, which can be due to change in the physical-chemical properties of the molecules, such as molecular weight, lipophilicity, etc.

As previously reported by our lab, the pharmacophore of the sulfonylurea-Pgp and the sulfonylurea-BCRP systems demonstrated different feature points, as shown in Figure 3. A simple definition of the pharmacophore model is a representation of the steric and electronic features that are necessary for the interaction with a protein or a biological response. For both of the pharmacophores, the feature points were spread throughout the entire molecule, outlining the areas of interest. As shown in Figure 3, there are four feature points that are similar in both pharmacophores, with two distinct differences. The differences in the Pgp and BCRP pharmacophore models were found to be at the amide and benzamido ring moieties, respectively. For reference, the five-point pharmacophores describing the Pgp and BCRP protein interactions with the sulfonylureas are presented in Figure 35.

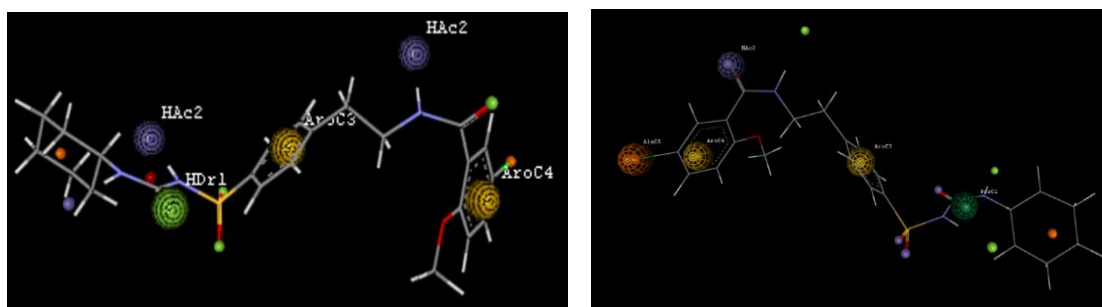


Figure 35. Pharmacophore Models detailing Pgp (left) and BCRP (right) features.

The 3D QSAR modeling of drug-protein interactions is also very important to help understand the similarities and differences of the two protein models. As we have previously demonstrated, the 3D QSAR models identify the molecular features responsible for the activity in the space surrounding the molecules. As shown in Figure 4, the electrostatic and steric field points (blue and green spheres, respectively) of each model are shown overlaid on the most active commercial sulfonylureas (Glyburide, Glimepiride, Glisoxepide, Gliquidone, and Glipizide). As discussed in the previous chapters, these field points and their corresponding charges aid in the understanding of key molecular features but are limited in explaining the activity in the 3D space.

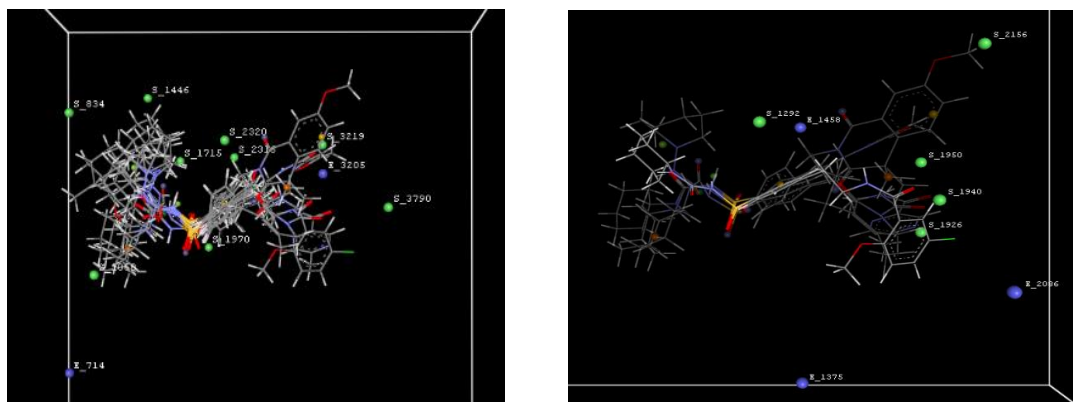


Figure 36. 3D field points describing model space for Pgp (left) and BCRP (right) Pharmacophores.

The Activity Cliff analysis presented in the Cresset Forge® software module provide 3D visualizations of a molecule set giving clear indications about the electrostatic, hydrophobic, and shape features. Taking into account bot pharmacophore and 3D QSAR models, the Activity Cliff Analysis was performed to further characterize the

sulfonylurea and Pgp/BCRP affinity. This comparison gives insight into the molecular attributes influencing the Pgp or BCRP substrate-interaction selectivity. The 3D molecular maps of the Activity Cliff Summary describing the activity for the sulfonylurea analogs are shown in Figure 37.

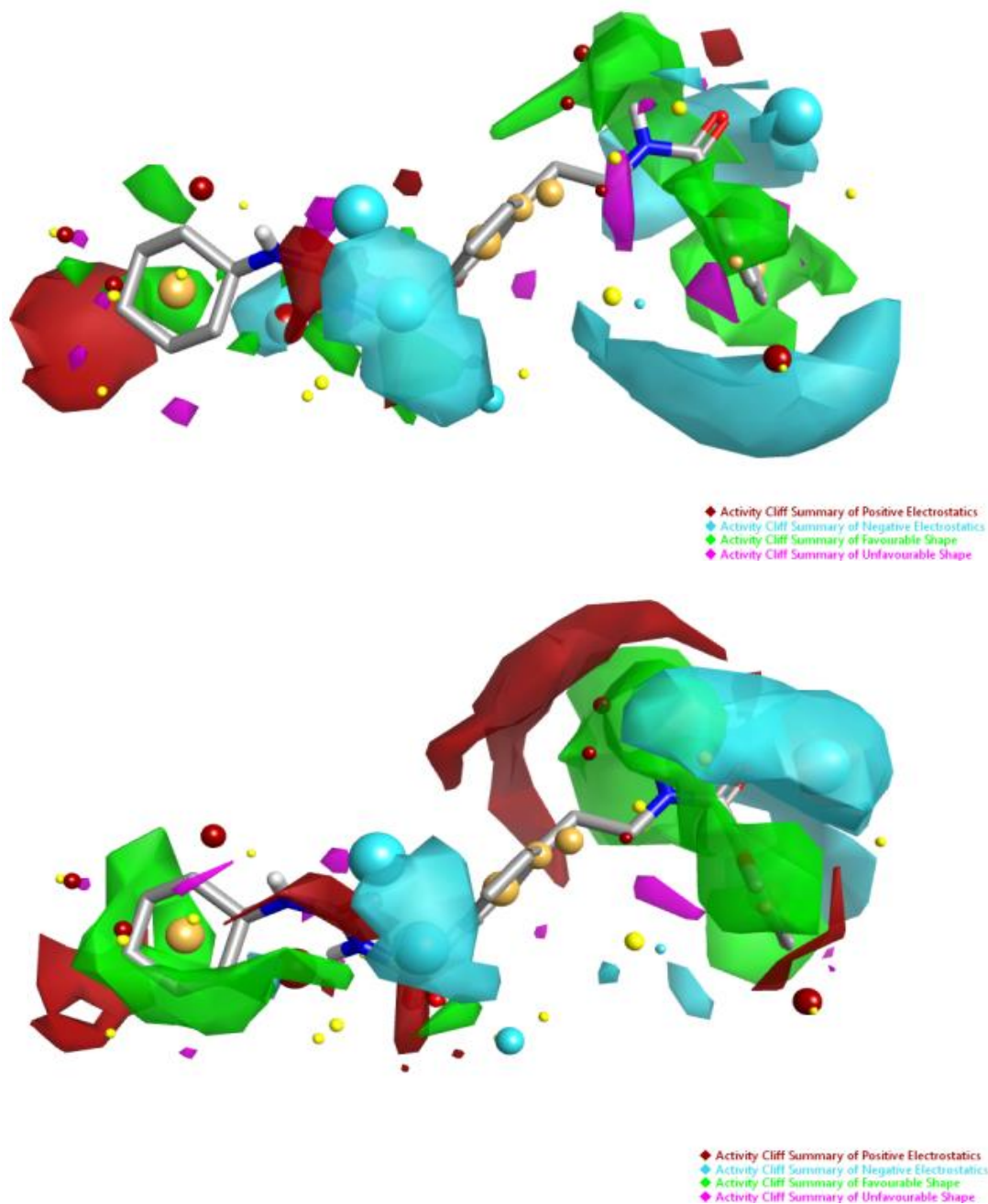


Figure 37. Activity cliff summary maps describing the sulfonylurea-Pgp (top) and sulfonylurea-BCRP (bottom) activity.

Starting with the Activity Cliff Summary maps, we will describe the molecular features needed for each interaction to improve the selectivity of the sulfonylurea

analogs for Pgp or BCRP. As shown in the activity summary maps in Figure 5, there is a good deal of overlap in the electrostatic, hydrophobic, and shape molecular descriptors. However, there is also differences specific to each Pgp and BCRP model that can explain the subsequent interaction. For both sets of sulfonylurea-protein interactions, there are specific parts of the molecule that play an important role regardless of the model. The benzamido, cyclohexyl, and aryl sulfonylurea ligands play an important role for the Pgp and BCRP activity. For further clarity, each of the modeling summary maps will be individually explained, along with the individual summary maps presented in the following sections, and in Figures 38, 39 and 40.

ELECTROSTATICS AVERAGE SUMMARY

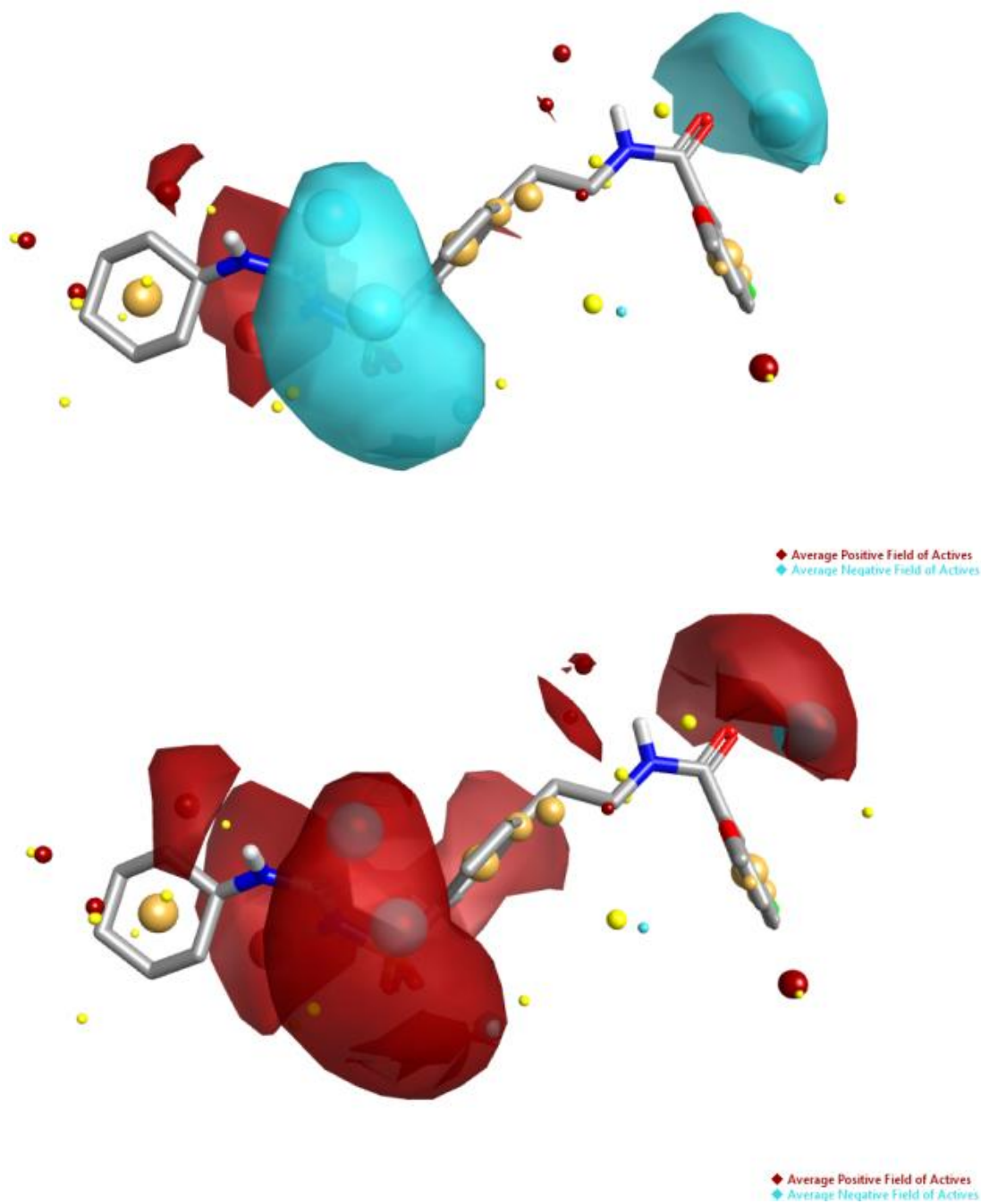


Figure 38. Summary of electrostatics activity for sulfonyleurea interaction with Pgp (top) and BCRP (bottom).

The electrostatics average summary explains where an increase in negative (red) or positive charge (blue) will increase activity. As presented in Figure 6, the electrostatics summary details the differences in the sulfonyleurea interactions needed for the Pgp and BCRP proteins. As shown in Figure 37, there are some pronounced differences in the results for the negative and positive electrostatic effects of the protein-molecule interaction. For the sulfonyleurea-Pgp interaction, there is a mix of positive and negative charges that influence the activity, encompassing the top portion of the sulfonyleurea moiety, and surrounding the carbonyl and methoxy groups on the benzamido moiety. There is also a slight positive effect needed around the two amides of the sulfonyleurea moiety. This is different for the sulfonyleurea-BCRP interaction has an overwhelming positive charge that governs the ligand-protein interaction. This positive charge needed for an increase in activity covers the cyclohexyl ring, across the sulfonyleurea to the central phenyl ring all the way surrounding the carbonyl and methoxy groups of the benzamido moiety.

HYDROPHOBICS AVERAGE SUMMARY

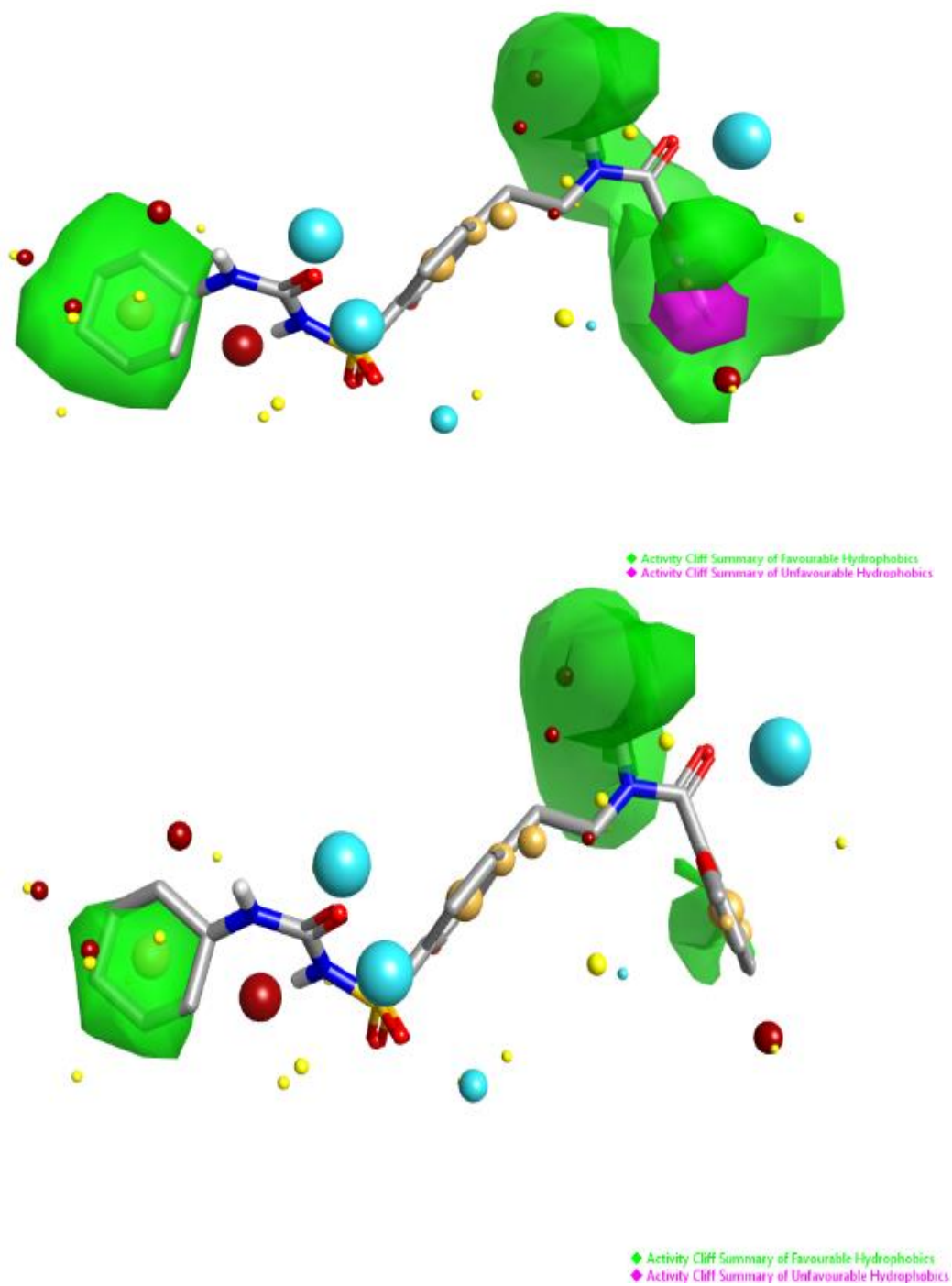


Figure 39. Summary of hydrophobics activity for sulfonyleurea interaction with Pgp (top) and BCRP (bottom).

The hydrophobics average summary explains where an increase in hydrophobic character will increase or decrease the activity and is described as favorable (green) or unfavorable (purple) hydrophobics. As shown in Figure 39, there is some overlap of the hydrophobic character between the two models. For the Pgp model, there is favorable hydrophobic activity surrounding the entire cyclohexyl ring, the amine, chloro, methoxy, and phenyl ring of the benzamido moiety. However, there is a small unfavorable hydrophobic activity around the two carbons of the phenyl ring between the methoxy and chloro moieties. For the BCRP model, there is favorable hydrophobic activity on the farthest carbon atoms of the cyclohexyl ring, surrounding the amide group and the chloro group of the benzamido moiety.

SHAPE SUMMARY

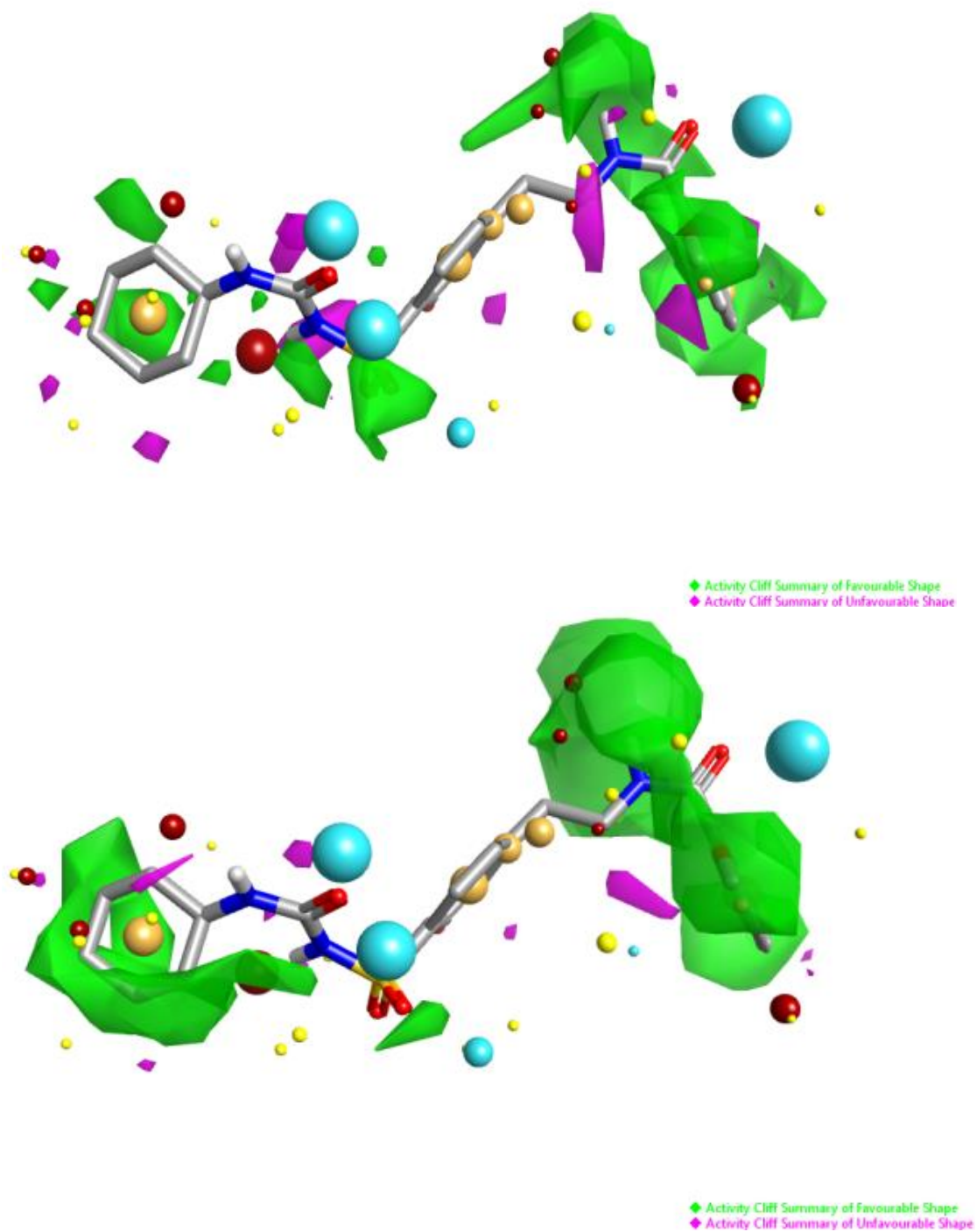


Figure 40. Summary of shape activity for sulfonyleurea interaction with Pgp (top) and BCRP (bottom).

The shape summary explains where bulky groups are needed to increase the activity and is described as favorable (green) or unfavorable (purple) shape. As shown above in Figure 40, the shape summary details the differences in the sulfonylurea interactions of the Pgp and BCRP proteins. For the Pgp model, there are mostly favorable shape descriptors, with two main areas demonstrating unfavorable shape. The favorable shape surrounds the cyclohexyl ring, the sulfonyl and carbonyl moieties, and the larger feature of the amide, methoxy and chloro of the benzamido ligand. The unfavorable shape occurs between the amides and carbonyl of the sulfonylurea moiety. For the sulfonylurea- BCRP interaction, there are mostly favorable shapes, encompassing the outer ring moieties. Moving from left to right in the depiction above, there are two large areas of favorable shape on the bottom half of the cyclohexyl ring through the carbonyl of the sulfonylurea, and on the top half of the molecule, surrounding the amide, methoxy and chloro moieties of the benzamido ligand of the molecule.

DISCUSSION

The ABC transporter proteins are responsible for the active transport of substrates into and out of cells. Specifically, ABC transporter proteins have gained much notoriety for being responsible for the multidrug resistance (MDR) phenomenon in various cancer treatments.¹⁹⁸ Much work has been done over the years to identify the features of a molecules that are responsible for inducing interactions with the ABC efflux transporters.¹⁹⁹ Expanding on that research, many groups have looked to develop global models that will identify the universal features of molecules that are substrates or inhibitors.²⁰⁰ However, this has proven very elusive as the broad substrate

specificity of each of the transporters proteins allows for much overlap for the substrate recognition. From a biological standpoint, the overlap of substrate recognition is needed and very much an inherent part of the body's redundant system of protection.^{201 202}

With this in mind, we endeavored to describe the interaction of a single class of compounds, the sulfonylureas, with two prominent ABC transporters, Pgp and BCRP. In order to decipher the underlying structure activity relationship of the sulfonylurea and ABC transporter proteins, the molecules' transporter activity was examined by the Activity Analysis Cliffs for the electrostatic, hydrophobic, and shape descriptors. The first step in this process was to generate the lowest energy conformers, and then overlay the molecules on the template molecule, Glyburide. This allowed for the activity to be solely a function of the molecular structure, and for the generation of field points surrounding the molecules. These field points were then used for the visualization and calculation of the Activity Cliff data describing each sulfonylurea-protein interaction.

Results of the Activity Cliff analysis study detail many similarities governing the activity and interaction between the sulfonylureas and the ABC transporters, Pgp and BCRP. To start, the central aryl ring serves as a linker to the benzamido and sulfonylurea ligands and does not contribute to the transporter activity calculation. There is electrostatic activity in both models surrounding the sulfonylurea and carbonyl group. Also, there is a good deal of overlap between the models on the favorable shape on activity surrounding the cyclohexyl and benzamido ligands. The

hydrophobic summary also details very similar activity surrounding the cyclohexyl and benzamido ligands of both models.

Though the sulfonylurea-protein models are very similar in many of the electrostatics, hydrophobics and shape character, there are still some obvious differences. The electrostatics Activity Cliff Analysis surrounding the sulfonylurea and carbonyl ligands present differently in each model. The BCRP model requires more positive charges surrounding the entire molecule, at the sulfonylurea in its entirety, around the far side of the central aryl ring, and on the carbonyl of the benzamido ligand. This contrasts with the Pgp model which has a mix of negative and positive charges governing activity; negative charge around the sulfonylurea and benzamido carbonyl, and positive charge surrounding the amides of the sulfonylurea. To describe the structure activity relationship for electrostatics descriptor, having more negative groups at these locations on the molecule will increase Pgp activity and decrease the BCRP activity.

For the shape activity analysis model there are some considerable differences governing the activity for each model. There is a much larger area surrounding the molecule in the BCRP model that requires an increase in bulky groups as compared to the Pgp model. The BCRP model has favorable bulky groups covering the entire cyclohexyl and benzamido ligands. In contrast, the Pgp model has scattered favorable bulky groups on the cyclohexyl and sulfonylurea ligands, with a similar though slightly smaller favored bulky group surrounding the amide and back side of the substituted phenyl ring. To describe the structure activity relationship for the shape

descriptor, having bulky groups on the cyclohexyl favors the BCRP activity, whereas having bulky groups on the benzamido ligand would benefit both models' activity. For the hydrophobic Activity Analysis model there is a great deal of similarity, with only a few small discrepancies governing the activity. The BCRP model has favorable hydrophobic character on the far side of the cyclohexyl ring, and above the amide ligand. In contrast, the Pgp model has favorable hydrophobic character surrounding the whole cyclohexyl group, and surrounding the entire benzamido ligand, wrapping the upper section of the molecule. To describe the structure activity relationship for the hydrophobics descriptor, increasing the hydrophobic character surrounding the benzamido ring would benefit the Pgp activity, whereas increased hydrophobic character on the amide and cyclohexyl ring would benefit both Pgp and BCRP activity. A summary of the learnings from the electrostatic, hydrophobic, and shape activity atlas analysis are presented in Figure 41.

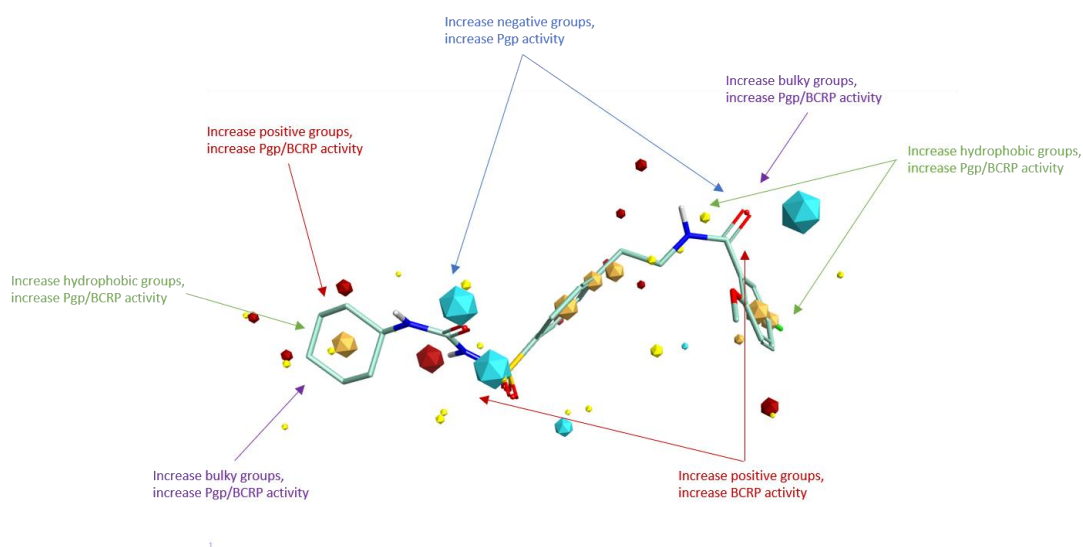


Figure 41. Summary of Activity Atlas modeling for the Pgp and BCRP models on Glyburide.

The Activity Atlas Modeling has proven to be a valuable tool for deciphering the structure activity relationships defining the interactions of sulfonylurea analogs with Pgp and BCRP transporter proteins. Using the Activity Atlas modeling we were able to leverage the three-dimensional insight for a series of sulfonylureas and the associated Pgp/BCRP activity, based on electrostatic, hydrophobic, and shape descriptors. This led to identifying key molecular features that were missed in our previous modeling attempts. The Activity Atlas modeling specifies the need for bulky steric groups, an increase in hydrophobic character, and more positively charged groups on/near the cyclohexyl ring. Also, the Activity Atlas model specifies the need for increased hydrophobic character and bulky steric groups on the benzamido moiety. Finally, and representing the difference in activity between the two proteins, the space immediately surrounding the sulfonylurea and amide groups require different charges to drive the activity, with an increase in negative charge increasing the Pgp activity, and an increase in positive charge increasing the BCRP activity.

CONCLUSION

This is the first summary and comparison of a large series of sulfonylurea analogs activity with the ABC transporter proteins, Pgp and BCRP. Based on the work previously reported on Glyburide and its unique placental transport activity, we sought to define the molecular properties responsible for interaction with the ABC transporters in the hopes of learning how to use this information to better design pregnancy centered medications. The sulfonylurea analogs tested in our work show a higher propensity for Pgp activity as compared to that of BCRP. This means that in

our cell-based transport assays, the same molecule had higher activity in the Pgp model than in the BCRP model. As the cell-based assays are very sensitive to drug concentration effects, we maintained drug concentrations to that were carefully selected to not elicit a false positive or negative response.

Applying the understanding from the activity cliff analysis, the 3D QSAR models generated were condensed down to a simple map of the critical points driving the structure activity relationship for three descriptors: electrostatics, hydrophobics and shape. The Activity Cliff Analysis detailed key similarities and differences governing the molecular features driving activity in the Pgp and BCRP protein models. Though the electrostatic, hydrophobic, and shape activity cliffs were shared across molecules in both models, there are important differences in that could be used to drive the sulfonylurea interaction to Pgp or BCRP. In this regard, the Activity Atlas modeling proved to be a valuable tool as previously undiscovered features were characterized and shown to be of key importance to define the sulfonylurea-Pgp/BCRP activity.

CHAPTER 4

**COMPARISON OF PGP AND BCRP ACTIVITY FOR A SERIES OF
SULFONYLUREAS BY ACTIVITY CLIFF ANALYSIS**

by

Samuel D Bell¹⁰ ; Brian Bronk¹¹ ; William Euler¹²

is submitted to Molecular Pharmaceutics

¹⁰ PhD Candidate, Department of Chemistry, The University of Rhode Island, Kingston, RI 02881. Email: sbell@chm.uri.edu

¹¹ Adjunct Professor, Department of Chemistry, The University of Rhode Island, Kingston, RI, 02881. Email: brian.bronk@sanofi.com

¹² Professor, Department of Chemistry, The University of Rhode Island, Kingston, RI, 02881. Email: weuler@chm.uri.edu

Designing Pregnancy Centered Medications: Insights and Recommendations

The first three chapters detail the evaluation of a series of sulfonylurea analogs in cell-based transport assays to determine if they are substrates for the ATP binding cassette transporter proteins, Pgp and BCRP. The cell lines used in the study were Madin-Darby Canine Kidney cells, stably transfected for Pgp or BCRP gene overexpression, described and characterized in literature and summarized in Chapters 1 and 2.

Glyburide is the most prescribed oral sulfonylurea medication and has been shown to be actively transported by the ABC transporter proteins, specifically Pgp and BCRP, but also by various other transporters. Our work examined the interaction of the sulfonylurea analogs with Pgp and BCRP, and determined the molecular features driving the specific protein activity. We confirmed that the sulfonylureas are substrates of both Pgp and BCRP and built pharmacophore and QSAR models explaining the Pgp and BCRP activities in the two and three-dimensional space.

The study of Glyburide and the ABC transporters has presented a unique and exciting opportunity to learn about tailoring drug delivery for pregnant women. As discussed previously, Glyburide has demonstrated unique placental transport due to the active transport by the ABC transporters, minimally crossing the placenta and leaving the placenta against the concentration gradient. The treatment of Gestational Diabetes Mellitus with Glyburide is an interesting case for drug delivery to the receptor (pancreatic β -cells), allowing the mother to maintain and control insulin levels for proper function, while limiting the exposure of the drug to the fetus (through placental transport). Numerous studies have been performed to evaluate the pharmacokinetics

and pharmacodynamics of Glyburide during pregnancy detailing: the fetal exposure, umbilical cord concentrations, the safety compared to insulin, and placental transport assays. However, there has not been extensive research to understand the molecular properties responsible for driving the interaction with the ABC transporters responsible for the placental transport, for instance, with Pgp instead of BCRP.

Our research demonstrated that the sulfonylurea molecules need to have specific physical-chemical parameters to have ABC transporter activity, in Pgp and BCRP. These parameters, among many others, speak to the size, shape, and lipophilicity of the molecule, governed by the placement of ligands at the appropriate locations on the molecule. As discussed in chapters 2 and 3, the sulfonylurea analogs with similar or larger molecular weight or molecular volume as compared to Glyburide were more likely to be substrates for both Pgp and BCRP. Conversely, sulfonylurea analogs that were much smaller in molecular weight and volume, or were missing the arylsulfonylurea and benzamido core structure, were not substrates of either Pgp or BCRP. We found that these results were consistent with the structure activity relationship of the first and second-generation sulfonylureas, with the smaller, first-generation sulfonylureas being weak substrates of the SUR1 receptor. The main difference between the first and second-generation sulfonylureas lies in the “core” structure found to increase potency of the second-generation sulfonylureas. This required core structure is presented in Figure 42, with the benzamido ligand highlighted in light blue, and the arylsulfonylurea highlighted in dark blue.

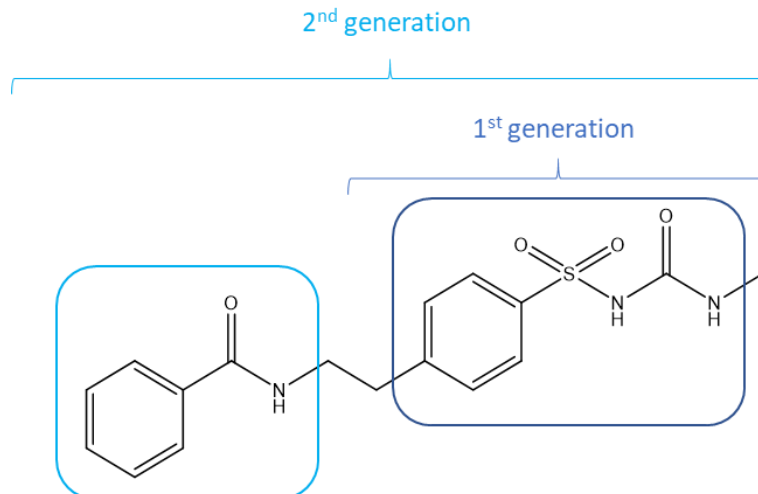


Figure 42. Diagram of core structure for each sulfonylurea generation highlighting the arylsulfonylurea (dark blue) and the benzamido (light blue) ligand.

Based on the Activity Cliff modeling reported in Chapter 3, our research has shown that adding ligands to increase the hydrophobicity and steric hinderance (bulky groups) to the substituted benzamido ring and to the amide ligand of the aryl sulfonylurea sections of the molecule increase the activity for both Pgp and BCRP. Also, we have shown that increasing the positive charge on the cyclohexyl ligand attached to the arylsulfonylurea also increases activity for both Pgp and BCRP. We found the differences in the Pgp or BCRP activities were connected to two locations on the Glyburide molecule: the sulfonylurea and amide moieties on either side of the central aryl ring. Specifically, that an increase the positive charge or negative charge at these specific locations (figure 43), would make the molecules more likely to be BCRP or Pgp substrates, respectively.

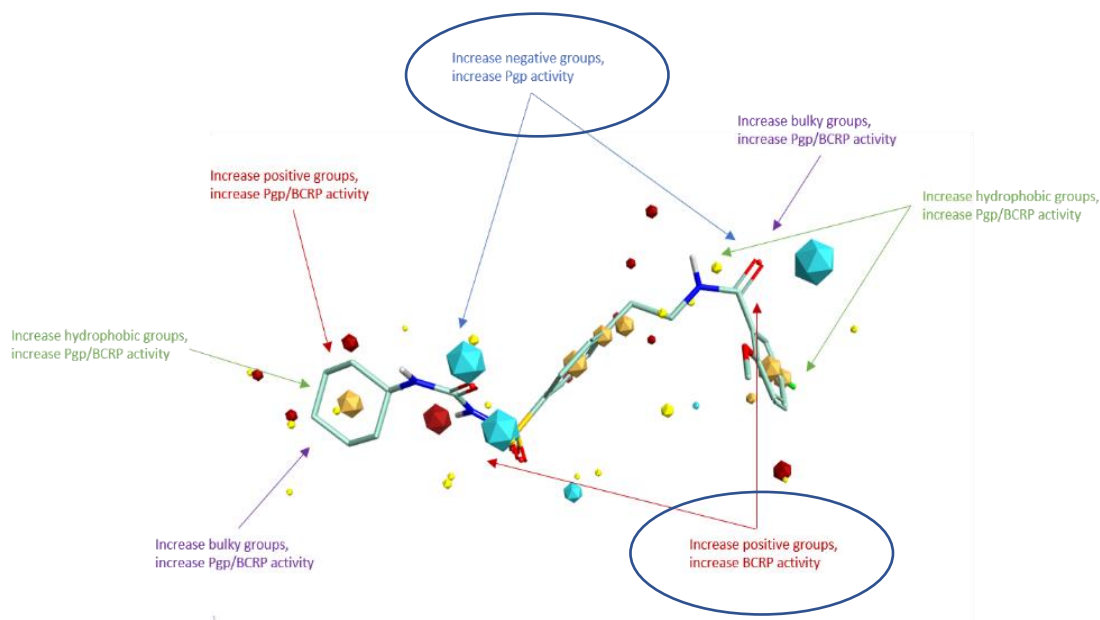


Figure 43. Summary of Activity Atlas modeling for the Pgp and BCRP models on Glyburide. *Note: blue circles indicate the key feature placement behind the activity differences in each model.*

Based on this work presented in chapters 1-3, we present some recommendations to design medications for pregnant women based on these learnings from our Glyburide case study. First, and assumed, the molecules need to have appropriate safety and PK/PD parameters, for example, high protein binding (>99%), high bioavailability (80-100%), moderate half-life (4 to 10hrs), to afford predictable and well-behaved ADMET (absorption, distribution, metabolism, excretion, toxicology) properties. Similarly, important physical-chemical properties would warrant the molecules to be at least the same size (M_w of ~500g/mol), volume (molecular vol 424.74), and molecular shape (low energy conformer in Figure 44) to interact with binding pockets of the target receptor (in this case, SUR1), as well as the placental ABC transporter

proteins. Specifically, those molecules fitting the Glyburide pharmacophores need an increase in the bulky and hydrophobic ligands on the ends of the molecule, with strategically placed electrostatic groups (negative or positive) in the central core to enhance the ABC transporter activity. Designing molecules that incorporate these molecular features, aligned against the Glyburide pharmacophore for Pgp or BCRP, will increase the respective activity. The preceding are all learnings from our research to direct the sulfonylurea molecules to interact with one protein or the other.

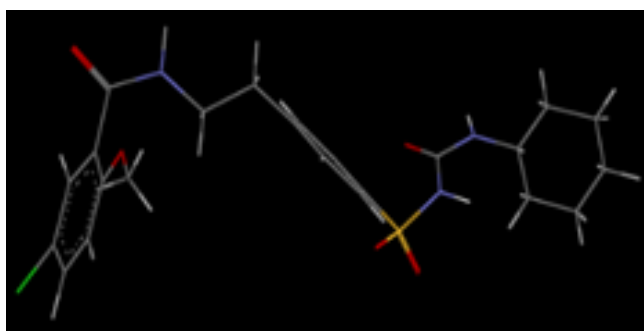


Figure 44. Glyburide low energy conformation used in our research.

For the purpose of keeping drugs out of the placenta, interactions with more than one ABC transporter protein would provide a potentially superior solution. For conditions requiring treatment in transporter rich areas, for example the blood brain barrier, this approach will not work due to the need to cross the tight junctions containing the numerous transporters designed for redundant protection. However, for those disease states that have receptor targets outside of the area protected by the ABC proteins, this approach may be appropriate. Therefore, to design pregnancy centered medications, we need to maintain the fetal protection by designing the molecules that interact with numerous placental transporters. This would allow for protection of the fetus by the

natural and redundant system of the ABC Transporter proteins, inherent in pregnant women and ever increasing over the course of gestation. By design, the molecules would interact with more than one ABC transporter, allowing for redundant protection of the fetus if an issue arose with one of the transporters in the mother, for example, Pgp deficiency or mutation in the BCRP protein reducing the activity.

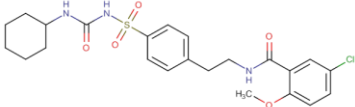
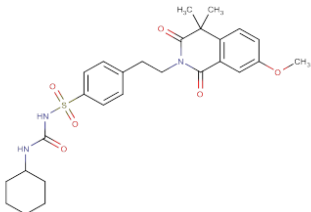
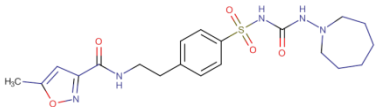
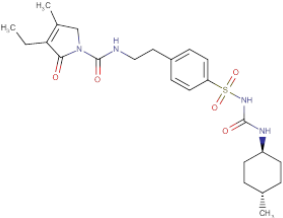
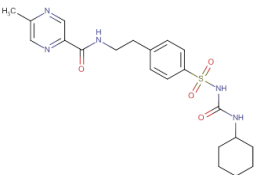
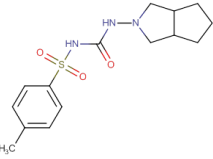
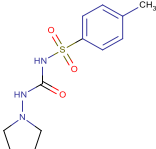
To better define this idea, future research efforts will focus on evaluating the substrate activity of the sulfonylurea analogs in other ABC transporter proteins known to be present in the fetal-placental barrier.

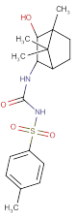
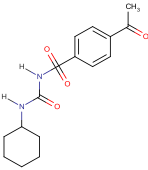
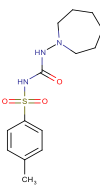
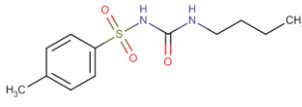
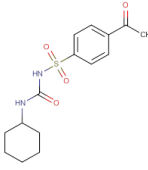
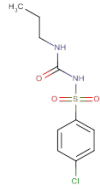
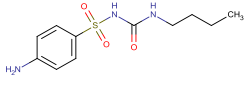
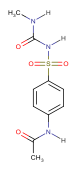
Following the work presented in this thesis, the two and three-dimensional QSAR models would be built for the new sulfonylurea-ABC protein interactions, and the respective pharmacophores generated. Aligning the pharmacophore models of each ABC transporter against the lowest energy conformation of Glyburide will allow for the overlap the key points from each molecule to the overall key pharmacophore features. Then, comparing the numerous models against each-other in the Activity Analysis software will help describe the needed features for each interaction. And finally, this concept will be tested in a more “global mode”, using our sulfonylurea activity models to predict and describe the key pharmacophore features and activities of other molecular classes.

As you can imagine, the treatment options for pregnant women is severely limited due to the fact that most drugs will cross the placenta and present a safety risk to the fetus. Therefore, designing drugs not to cross the placenta would allow doctors to treat pregnant women’s conditions without harming the fetus. This would expand the treatment options and positively impact the lives and conditions of an entire subset of

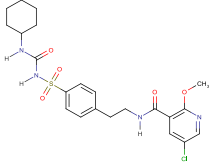
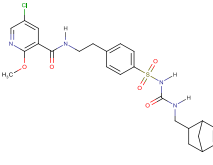
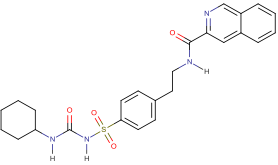
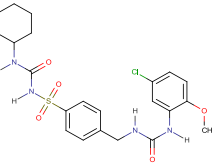
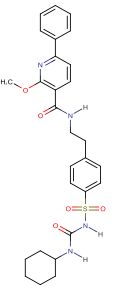
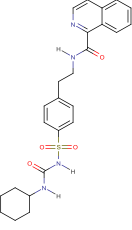
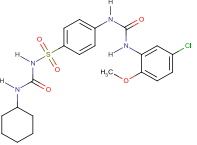
the population currently overlooked, with the potential to revolutionize treatment options.

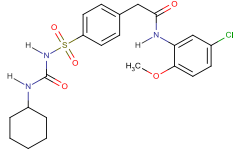
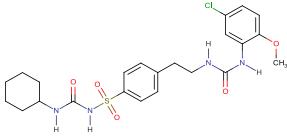
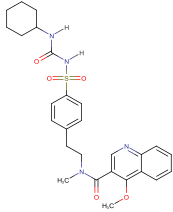
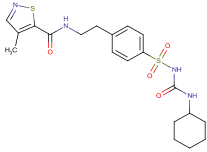
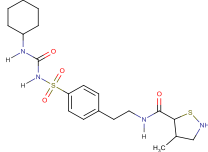
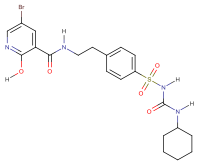
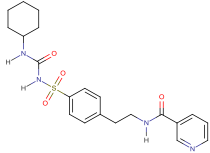
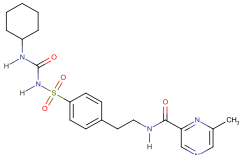
APPENDIX I

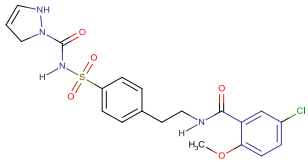
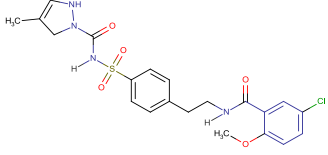
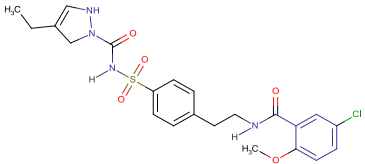
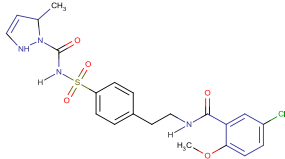
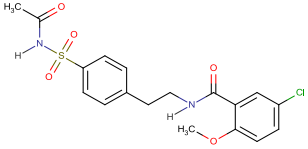
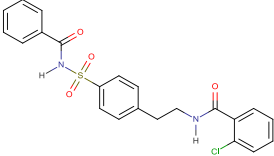
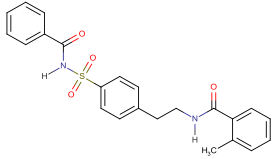
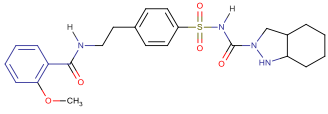
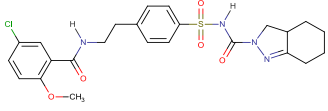
Molecule Number	Structure	Pgp P _{app}	log Pgp P _{app}
1		6.39	0.806
2		2.75	0.439
3		6.21	0.793
4		5.51	0.741
5		2.3	0.362
6		0.93	-0.032
7		0.9	-0.046

8		0.99	-0.004
9		0.53	-0.276
10		0.82	-0.086
11		0.76	-0.119
12		0.7	-0.155
13		0.65	-0.187
14		0.74	-0.131
15		0.55	-0.260

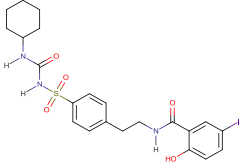
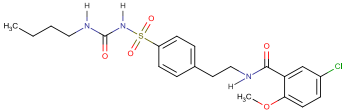
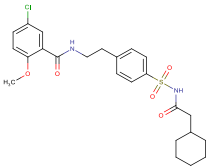
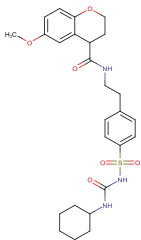
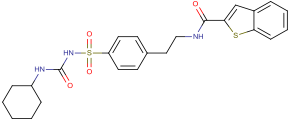
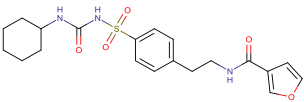
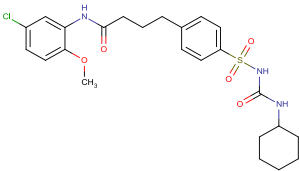
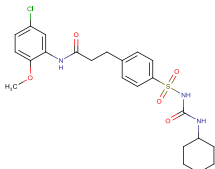
16		0.56	-0.259
17		5.40	0.732
18		10.2	1.01
19		4.17	0.620
20		2.99	0.476
22		9.3	0.968
23		2.43	0.386
24		1.33	0.124

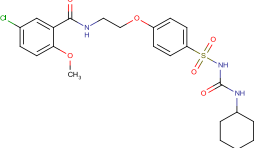
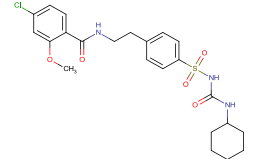
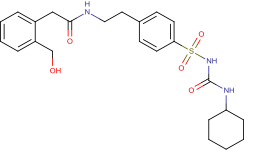
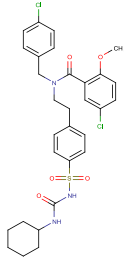
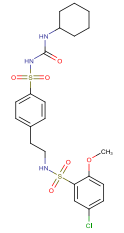
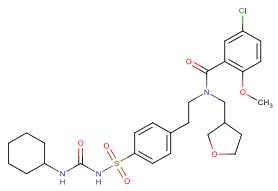
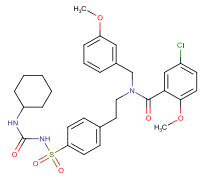
25		9.73	0.988
26		8.45	0.927
27		3.83	0.583
28		12.8	1.107
29		5.41	0.733
30		2.04	0.310
31		8.52	0.930

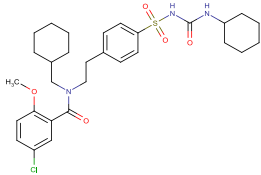
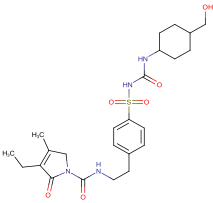
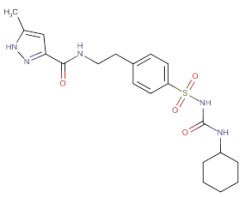
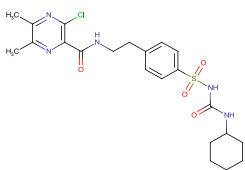
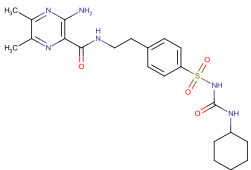
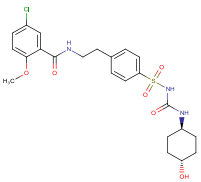
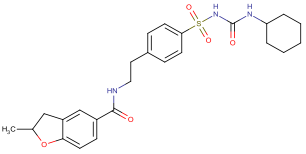
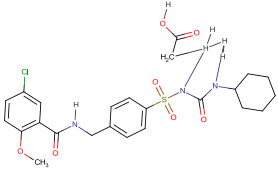
32		12.9	1.111
33		21	1.322
34		15.3	1.185
35		3.37	0.528
36		1.56	0.193
37		5.08	0.706
38		0.443	-0.354
39		1.62	0.210

40		0.682	-0.166
41		1.76	0.246
42		2.24	0.350
43		1.52	0.182
44		1.09	0.04
45		1.34	0.127
46		1.54	0.186
47		3.57	0.553
48		12.4	1.09

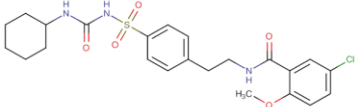
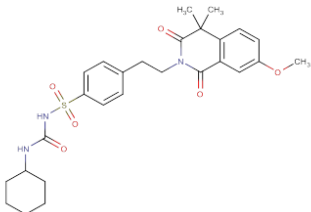
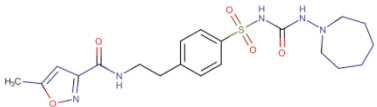
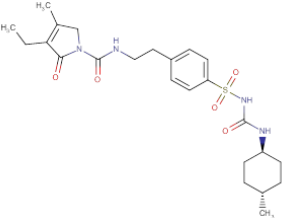
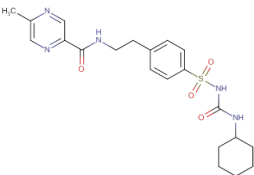
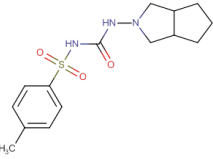
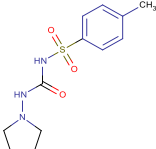
49		3.05	0.484
50		5.89	0.770
51		2.89	0.461
52		4.37	0.640
53		12.5	1.097
54		9.38	0.972
55		1.36	0.134
56		57.4	1.759

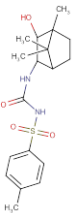
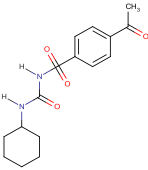
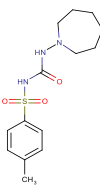
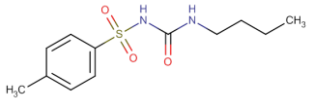
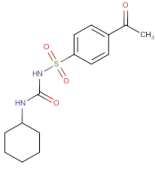
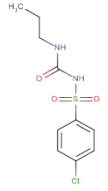
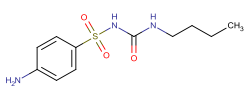
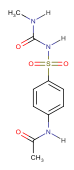
57		5.35	0.728
58		7.64	0.883
59		6.7	0.826
60		16.5	1.217
61		3.62	0.559
62		3.08	0.489
63		9.74	0.989
64		7.81	0.893

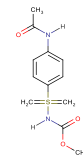
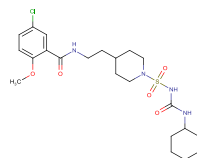
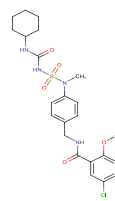
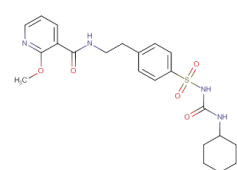
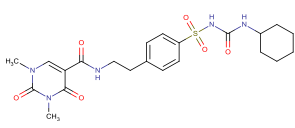
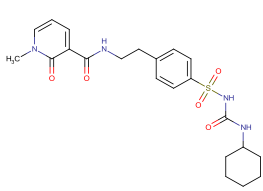
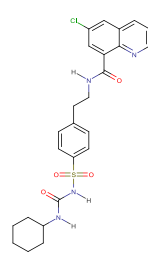
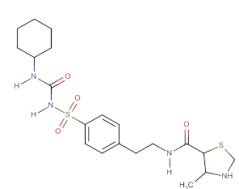
65		14.3	1.155
66		11.7	1.068
67		1.72	0.236
68		28.4	1.453
69		25.5	1.407
70		7.45	0.872
71		18.1	1.258

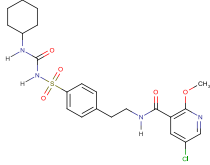
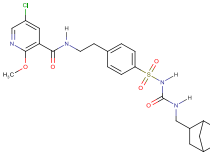
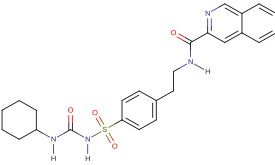
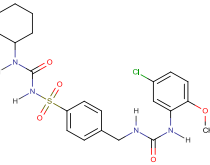
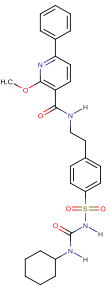
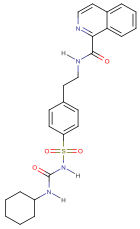
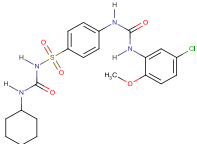
72		24.3	1.386
73		1.34	0.127
74		1.06	0.025
75		2.93	0.467
76		4.29	0.632
77		0.848	-0.072
78		12.4	1.093
79		6.07	0.783

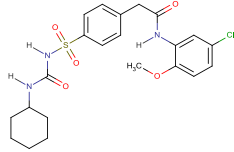
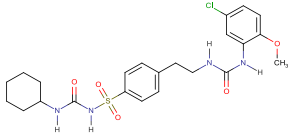
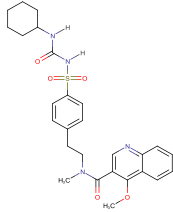
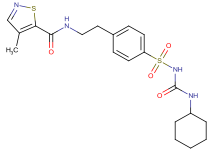
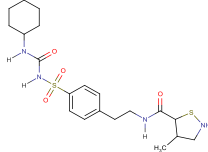
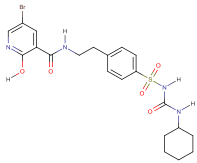
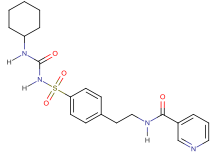
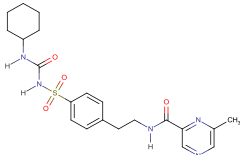
APPENDIX II

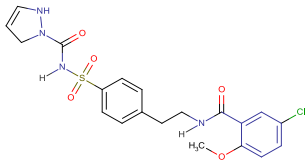
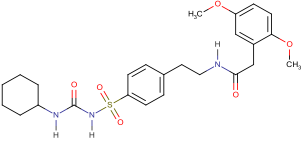
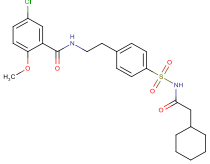
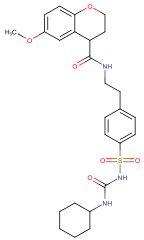
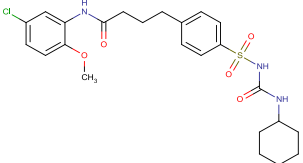
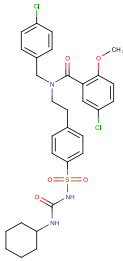
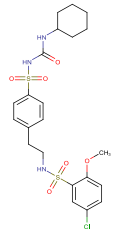
Molecule Number	Structure	BCRP P_{app}	log BCRP P_{app}
1		2.78	0.444
2		1.9	0.278
3		3.21	0.506
4		3.45	0.537
5		1.14	0.056
6		1.01	0.004
7		0.88	-0.055

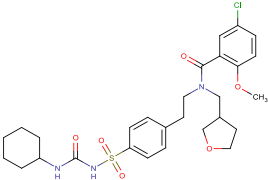
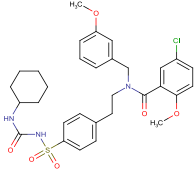
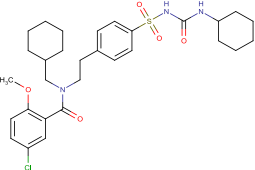
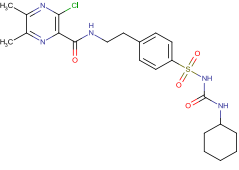
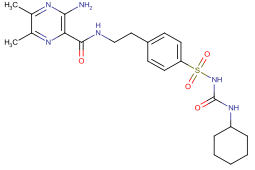
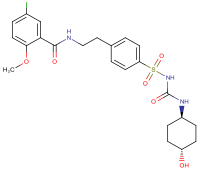
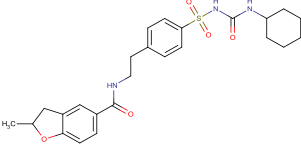
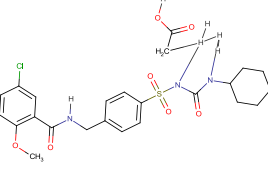
8		0.87	-0.060
9		0.67	-0.173
10		0.54	-0.267
11		0.55	-0.259
12		0.59	-0.229
13		0.72	-0.142
14		0.91	-0.040
15		0.44	-0.356

16		0.5	-0.301
17		2.32	0.365
18		3.72	0.570
19		2.41	0.382
20		1.76	0.246
22		2.4	0.380211242
23		6.54	0.815577748
24		1.65	0.217483944

25		4.18	0.621176282
26		3.67	0.564666064
27		2.72	0.434568904
28		5.43	0.73479983
29		3.34	0.523746467
30		1.49	0.173186268
31		3.37	0.527629901

32		4.28	0.631443769
33		3.32	0.521138084
34		7.67	0.884795364
35		3.9	0.591064607
36		1.87	0.271841607
37		2.75	0.439332694
38		0.877	- 0.057000407
39		1.76	0.245512668

40		0.881	-0.055
56		13.1	1.117
59		3.7	0.568
60		8.33	0.920
63		1.3	0.113
68		13.4	1.127
69		6.00	0.778

70		4.54	0.657
71		7.45	0.872
72		12.4	1.093
75		2.3	0.361
76		3.13	0.495
77		0.73	-0.136
78		4.11	0.613
79		3.88	0.588

APPENDIX III

Molecular descriptor classes in VLifeMDS QSAR

A. Physicochemical descriptors class: (total 239 descriptors)

Physicochemical descriptors are based on the physicochemical properties of molecule. Sub classes of physicochemical descriptors are as follows.

1. Individual
2. Retention Index (chi)
3. Atomic valence connectivity index (chiv)
4. Path Count
5. Chi Chain
6. Chiv Chain
7. Chain Path Count
8. Cluster
9. Path Cluster
10. Kappa
11. Element Count
12. Dipole Moment
13. Electrostatic
14. Distance Based Topological
15. Estate numbers
16. Estate Contributions
17. Information Theory Index
18. Extended Topochemical Atom (ETA) based descriptors
19. Hydrophobicity XlogpA
20. Hydrophobicity XlogpK
21. Hydrophobicity SlogpA
22. Hydrophobicity SlogpK
23. Polar Surface Area

Various physicochemical descriptors are as follows.

1. Sub class: Individual
 - i. Mol.Wt: This descriptor signifies molecular weight of a compound.
 - ii. Volume: This descriptor signifies volume of a compound.
 - iii. H-AcceptorCount: Number of hydrogen bond acceptor atoms
 - iv. H-DonorCount: : Number of hydrogen bond donor atoms
 - v. RotatableBondCount: Number of rotatable bonds
 - vi. XlogP: This descriptor signifies ratio of solute concentration in octanol & water and generally termed as Octanol Water partition Coefficient. This is atom based evaluation of logP as described in Wang et al.)

- vii. **slogp**: This descriptor signifies log of the octanol/water partition coefficient (including implicit hydrogens). This property is an atomic contribution model [Crippen 1999] that calculates logP from the given structure; i.e., the correct protonation state
- viii. **smr**: This descriptor evaluates molecular refractivity (including implicit hydrogens) which also measure of molecular size. This property is an atomic contribution model [Crippen 1999] that assumes the correct protonation state (washed structures).
- ix. **polarizabilityAHC**: This descriptor evaluates molecular polarizability using sum of atomic polarizabilities using the atomic hybrid component (AHC).
- x. **polarizabilityAHP**: This descriptor evaluates molecular polarizability using atomic hybrid polarizability (AHP).

2. Sub class: Chi

- i. **chi0**: This descriptor signifies a retention index (zero order) derived directly from gradient retention times
- ii. **chi1**: This descriptor signifies a retention index (first order) derived directly from gradient retention times
- iii. **chi2**: This descriptor signifies a retention index (second order) derived directly from gradient retention times.
- iv. **chi3**: This descriptor signifies a retention index (third order) derived directly from gradient retention times
- v. **chi4**: This descriptor signifies a retention index (fourth order) derived directly from gradient retention times.
- vi. **chi5**: This descriptor signifies a retention index (fifth order) derived directly from gradient retention times.

3. Sub class: Chiv

- i. **chiV0**: This descriptor signifies atomic valence connectivity index (order 0) from [Hall 1991] and [Hall 1997]. This is calculated as the sum of $1/\sqrt{v_i}$ over all heavy atoms i with $v_i > 0$.
- ii. **chiV1**: This descriptor signifies atomic valence connectivity index (order 1) from [Hall 1991] and [Hall 1997]. This is calculated as the sum of $1/\sqrt{v_i v_j}$ over all bonds between heavy atoms i and j where $i < j$.
- iii. **chiV2**: This descriptor signifies atomic valence connectivity index (order 2) from [Hall 1991] and [Hall 1997].
- iv. **chiV3**: This descriptor signifies atomic valence connectivity index (order 3) from [Hall 1991] and [Hall 1997].
- v. **chiV4**: This descriptor signifies atomic valence connectivity index (order 4) from [Hall 1991] and [Hall 1997].
- vi. **chiV5**: This descriptor signifies atomic valence connectivity index (order 5) from [Hall 1991] and [Hall 1997].

4. Sub class: Path Count

- i. **0PathCount**: This descriptor signifies total number of fragments of zero order (atoms) in a compound.
- ii. **1PathCount**: This descriptor signifies total number of fragments of first order (bonds) in a compound.
- iii. **2PathCount**: This descriptor signifies total number of fragments of second order (two bond path) in a compound.

- iv. 3PathCount: This descriptor signifies total number of fragments of third order (three bond path) in a compound.
- v. 4PathCount: This descriptor signifies total number of fragments of fourth order (four bond path) in a compound.
- vi. 5PathCount: This descriptor signifies total number of fragments of fifth order (five bond path) in a compound.

5. Sub class: Chi Chain

- i. chi3chain: This descriptor signifies a retention index for three membered ring.
- ii. chi4chain: This descriptor signifies a retention index for four membered ring.
- iii. chi5chain: This descriptor signifies a retention index for five membered ring.
- iv. chi6chain: This descriptor signifies a retention index for six membered ring.

6. Sub class: ChiV Chain

- i. chiV3chain: This descriptor signifies atomic valence connectivity index for three membered ring.
- ii. chiV4chain: This descriptor signifies atomic valence connectivity index for four membered ring.
- iii. chiV5chain: This descriptor signifies atomic valence connectivity index for five membered ring.
- iv. chiV6chain: This descriptor signifies atomic valence connectivity index for six membered ring.

7. Sub class: Chain Path count

- i. 3ChainCount: This descriptor signifies total number three membered rings in a compound.
- ii. 4ChainCount: This descriptor signifies total number four membered rings in a compound.
- iii. 5ChainCount: This descriptor signifies total number five membered rings in a compound.
- iv. 6ChainCount: This descriptor signifies total number six membered rings in a compound.

8. Sub class: Cluster

- i. chi3Cluster: This descriptor signifies simple 3rd order cluster chi index in a compound.
- ii. chiV3Cluster: This descriptor signifies valence molecular connectivity index of 3rd order cluster.
- iii. 3ClusterCount: This descriptor signifies total number of fragments of third order cluster in a molecule.

9. Sub Class: Path Cluster

- i. chi4pathCluster: This descriptor signifies molecular connectivity index of 4th order pathcluster.
- ii. chiV4pathCluster: This descriptor signifies valence molecular connectivity index of 3rd order pathcluster.
- iii. 4pathClusterCount: This descriptor signifies total number of fragments of fourth order pathcluster in a molecule.

10. Sub Class: Kappa

- i. kappa1: This descriptor signifies first kappa shape index: $(n-1)^2 / m^2$ [Hall 1991]
- ii. kappa2: This descriptor signifies second kappa shape index: $(n-1)^2 / m^2$ [Hall 1991]
- iii. kappa3: This descriptor signifies third kappa shape index: $(n-1)(n-3)^2 / p^2$ for odd n, and $(n-3)(n-2)^2 / p^2$ for even n [Hall 1991]

- iv. k1alpha: This descriptor signifies first alpha modified shape index: $s (s-1)^2 / m^2$ where $s = n + a$ [Hall 1991]
- v. k2alpha: This descriptor signifies second alpha modified shape index: $s (s-1)^2 / m^2$ where $s = n + a$ [Hall 1991]
- vi. k3alpha: This descriptor signifies third alpha modified shape index: $(n-1) (n-3)^2 / p^3$ for odd n, and $(n-3) (n-2)^2 / p^3$ for even n where $s = n + a$ [Hall 1991]

11. Sub Class: Element Count

- i. HydrogensCount: This descriptor signifies number of hydrogen atoms in a compound.
- ii. CarbonsCount: This descriptor signifies number of carbon atoms in a compound.
- iii. SulfursCount : This descriptor signifies number of sulphur atoms in a compound.
- iv. OxygensCount: This descriptor signifies number of oxygen atoms in a compound.
- v. NitrogensCount: This descriptor signifies number of nitrogen atoms in a compound.
- vi. ChlorinesCount: This descriptor signifies number of chlorine atoms in a compound.
- vii. FluorinesCount: This descriptor signifies number of fluorine atoms in a compound.
- viii. BrominesCount: This descriptor signifies number of bromine atoms in a compound.
- ix. IodinesCount: This descriptor signifies number of iodine atoms in a compound.

12. Sub Class: Dipole Moment

- i. XcompDipole : This descriptor signifies the x component of the dipole moment (external coordinates).
- ii. YcompDipole : This descriptor signifies the y component of the dipole moment (external coordinates).
- iii. ZcompDipole : This descriptor signifies the z component of the dipole moment (external coordinates).
- iv. DipoleMoment: This descriptor signifies dipole moment calculated from the partial charges of the molecule.
- v. Quadrupole1: This descriptor signifies magnitude of first tensor of quadrupole moments.
- vi. Quadrupole2: This descriptor signifies magnitude of second tensor of quadrupole moments.
- vii. Quadrupole3: This descriptor signifies magnitude of third tensor of quadrupole moments.

13. Sub class: Electrostatic

- i. vdWSurfaceArea: This descriptor signifies total van der Waals surface area of the molecule.
- ii. +vePotentialSurfaceArea: This descriptor signifies total van der Waals surface area with positive electrostatic potential of the molecule.
- iii. -vePotentialSurfaceArea: This descriptor signifies total van der Waals surface area with negative electrostatic potential of the molecule.
- iv. Most+vePotential: This descriptor signifies the highest value of +ve electrostatic potential on van der Waals surface area of the molecule.
- v. Most-vePotential: This descriptor signifies the highest value of -ve electrostatic potential on van der Waals surface area of the molecule.
- vi. AveragePotential: This descriptor signifies average of the total electrostatic potential on van der Waals surface area of the molecule.

- vii. **Average+vePotential:** This descriptor signifies the average of the total +ve electrostatic potential on van der Waals surface area of the molecule.
- viii. **Average-vePotential:** This descriptor signifies the average of the total -ve electrostatic potential on van der Waals surface area of the molecule.
- ix. **Most+ve&-vePotentialDistance:** This descriptor signifies the distance between points having the highest value of +ve and highest value of -ve electrostatic potential on van der Waals surface area of the molecule.

14. Sub Class: Distance based Topological

- i. **DistTopo:** This descriptor signifies distance based topological index.
- ii. **ConnectivityIndex:** This signifies a numeric descriptor derived from molecular topology.
- iii. **WienerIndex** : This descriptor signifies the sum of the numbers of edges in shortest paths in a chemical graph between all pairs of non-hydrogen atoms in a molecule.
- iv. **RadiusOfGyration:** This descriptor signifies size descriptor for the distribution of atomic masses in a molecule.
- v. **MomInertiaX** : This descriptor signifies moment of inertia at X-axis
- vi. **MomInertiaY** : This descriptor signifies moment of inertia at Y-axis
- vii. **MomInertiaZ** : This descriptor signifies moment of inertia at Z-axis
- viii. **BalabanIndexJ:**

$$J = (E/\mu + 1) \sum (ds_i, ds_j)$$

Where ds_i, ds_j = sum of the row i and j of the distance matrix

E = number of edges

μ = Number of rings in a molecule.

- ix. **BalabanB:**

$$B = \sum_{i=1}^N d_i^2$$

Where d_i = Number of vertices deleted at each step

N = Number of all vertices

- x. **BalabanC:**

$$C = (1/2)(B - 2N + U)$$

Where B = Balaban B index

N = Number of all vertices

$$U = [1 - (-1)^N]$$

- xi. **BalabanQ:**

$$Q = 3V_4 + V_3$$

Where V_3 = Number of vertices of degree 3

V_4 = Number of vertices of degree 4

- xii. **BalabanCdash:**

$$C^I = \frac{B - 2N + U}{(N - 2)^2 - 2 + U}$$

Where B = Balaban B index

N = Number of all vertices and U = [1 - (-1)^N]

xiii. BalabanQdash:

$$Q^I = \frac{3V_4 + V_3}{2(N - 2)(N - 3)}$$

Where V₃ = Number of vertices of degree 3

V₄ = Number of vertices of degree 4

N = Number of all vertices

xiv. HosoyaIndex: This descriptor signifies the topological index or Z index of a graph is the total number of matching in it plus 1 ("plus 1" accounts for the number of matchings with 0 edges).

$$Z = \sum_k p(G, k)$$

Where, p(G,k) = Number of ways in which K edges from all bonds of a graph G may be chosen so that no two of them are adjacent

15. Sub class: Estate Numbers

- i. SsCH3count: This descriptor defines the total number of -CH₃ group connected with single bond
- ii. SdCH2count: This descriptor defines the total number of -CH₂ group connected with double bond
- iii. SssCH2count : This descriptor defines the total number of -CH₂ group connected with two single bonds
- iv. StCHcount: This descriptor defines the total number of -CH group connected with triple bond
- v. SdsCHcount: This descriptor defines the total number of -CH group connected with one double and one single bond.
- vi. SaaCHcount: This descriptor defines the total number of carbon atoms connected with a hydrogen along with two aromatic bonds.
- vii. SsssCHcount: This descriptor defines the total number of -CH group connected with three single bond.
- viii. SddCcount: This descriptor defines total number of carbon atoms (= C =) with two double bonds present in the molecule.
- ix. StsCcount: This descriptors defines total number of carbon atoms (- C □) with a triple bond and a single bond present in the molecule.
- x. SdsCcount: This descriptor defines the total number of carbon connected with one double and two single bond.
- xi. SaasCcount: This descriptor defines the total number of carbon connected with one single bond along with two aromatic bonds.
- xii. SaaaCcount: This descriptor defines the total number of carbon connected with three aromatic bonds.
- xiii. SssssCcount: This descriptor defines the total number of carbon connected with four single bonds.

- xiv. S₅NH₃count: This descriptor defines the total number of –NH₃ group connected with one single bond.
- xv. S₅NH₂count: This descriptor defines the total number of –NH₂ group connected with one single bond.
- xvi. S₅₅NH₂count : This descriptor defines the total number of –NH₂ group connected with two single bonds.
- xvii. S_dNHcount: This descriptor defines the total number of –NH group connected with one double bond.
- xviii. S₅₅NHcount: This descriptor defines the total number of –NH group connected with two single bonds.
- xix. S_{aa}NHcount: This descriptor defines the total number of –NH group connected with two aromatic bonds.
- xx. S_tNcount: This descriptor defines the total number of nitrogen connected with triple bond.
- xxi. S₅₅₅NHcount: This descriptor defines the total number of –NH group connected with three single bonds.
- xxii. S_{d5}Ncount: This descriptor defines the total number of nitrogen connected with one single and one double bond.
- xxiii. S_{aa}Ncount: This descriptor defines the total number of nitrogen connected with two aromatic bonds.
- xxiv. S₅₅₅Ncount: This descriptor defines the total number of nitrogen connected with three single bonds.
- xxv. S_{dd5}N(nitro)count: This descriptor defines the total number of nitro group connected with one single and two double bonds.
- xxvi. S_{aa5}N(Noxide)count : This descriptor defines the total number of nitro oxide group connected with one single along with two aromatic bonds.
- xxvii. S₅₅₅₅N(onium)count : This descriptor defines the total number of N- onium group connected with four single bonds.
- xxviii. S₅OHcount: This descriptor defines the total number of –OH group connected with one single bond.
- xxix. S_dOcount: This descriptor defines the total number of oxygen connected with one double bond.
- xxx. S₅₅Ocount: This descriptor defines the total number of oxygen connected with two single bonds.
- xxxi. S_{aa}Ocount: This descriptor defines the total number of oxygen connected with two aromatic bonds.
- xxxii. S₅PH₂count: This descriptor defines the total number of –PH₂ group connected with one single bond.
- xxxiii. S₅₅PHcount: This descriptor defines the total number of –PH group connected with two single bonds.
- xxxiv. S₅₅₅Pcount: This descriptor defines the total number of phosphorous atom connected with three single bonds.
- xxxv. S_{d555}Pcount: This descriptor defines the total number of phosphorous atom connected with three single bonds and one double bond.
- xxxvi. S₅₅₅₅₅Pcount: This descriptor defines the total number of phosphorous atom connected with five single bonds.

- xxxvii. S₂SHcount: This descriptor defines the total number of -SH group connected with one single bond.
- xxxviii. S_dScount: This descriptor defines the total number of sulphur atom connected with one double bond.
- xxxix. S_{ss}Scount: This descriptor defines the total number of sulphur atom connected with two single bonds.
 - xl. S_{aa}Scount: This descriptor defines the total number of sulphur atom connected with two aromatic bonds.
 - xli. S_{ds}S(sulfone)count : This descriptor defines the total number of sulphone group connected with two single and one double bond.
 - xl.ii. S_{dds}S(sulfate)count: This descriptor defines the total number of sulphate group connected with two single and two double bonds.
- xl.iii. S₂Clcount: This descriptor defines the total number of chlorine atom connected with one single bond.
- xl.iv. S₂Brcount: This descriptor defines the total number of bromine atom connected with one single bond.
- xl.v. S₂Icount: This descriptor defines the total number of iodine atom connected with one single bond.
- xl.vi. S₂Fcount: This descriptor defines the total number of fluorine atom connected with one single bond.

16. Sub class: Estate contributions

- i. S₂CH₃E-index: Electrotological state indices for number of -CH₃ group connected with one single bond.
- ii. S_dCH₂E-index: Electrotological state indices for number of -CH₂ group connected with one double bond.
- iii. S_{ss}CH₂E-index: Electrotological state indices for number of -CH₂ group connected with two single bonds.
- iv. S_tCH₂E-index: Electrotological state indices for number of -CH₂ group connected with one triple bond
- v. S_{ds}CH₂E-index: Electrotological state indices for number of -CH₂ group connected with one double and one single bond.
- vi. S_{aa}CH₂E-index: Electrotological state indices for number of -CH₂ group connected with two aromatic bonds.
- vii. S_{sss}CH₂E-index: Electrotological state indices for number of -CH₂ group connected with three single bonds.
- viii. S_{dd}CE-index: Electrotological state indices for number of carbon atom connected with two double bonds.
- ix. S_{ts}CE-index: Electrotological state indices for number of carbon atom connected with one triple and one single bond.
- x. S_{ds}CE-index : Electrotological state indices for number of carbon atom connected with one double and two single bonds.
- xi. S_{aa}CE-index : Electrotological state indices for number of carbon atom connected with one single bond along with two aromatic bonds.

- xii. SaaaCE-index : Electrotological state indices for number of carbon atom connected with three aromatic bonds.
- xiii. SssssCE-index: Electrotological state indices for number of carbon atom connected with four single bonds.
- xiv. S₅NH3E-index: Electrotological state indices for number of –NH₃ group connected with one single bond.
- xv. S₅NH2E-index: Electrotological state indices for number of –NH₂ group connected with one single bond.
- xvi. S₅₅NH2E-index: Electrotological state indices for number of –NH₂ group connected with two single bond.
- xvii. S_dNHE-index : Electrotological state indices for number of –NH group connected with one double bond.
- xviii. S₅₅NHE-index : Electrotological state indices for number of –NH group connected with two single bonds.
- xix. SaaNHE-index: Electrotological state indices for number of –NH group connected with two aromatic bonds.
- xx. S_tNE-index: Electrotological state indices for number of nitrogen atom connected with one triple bonds.
- xxi. S₅₅₅NHE-index: Electrotological state indices for number of –NH group connected with three single bonds.
- xxii. S_{d5}NEindex: Electrotological state indices for number of nitrogen atom connected with two double and one single bond.
- xxiii. SaaNE-index: Electrotological state indices for number of nitrogen atom connected with two aromatic bonds.
- xxiv. S₅₅₅NE-index: Electrotological state indices for number of nitrogen atom connected with three single bonds.
- xxv. S₅₅₅N(nitro)E-index : Electrotological state indices for number of –nitro group connected with two double and one single bond.
- xxvi. Saa5N(Noxide)E-index: Electrotological state indices for number of nitro-oxide group connected with two aromatic and one single bond.
- xxvii. S₅₅₅₅N(onium)E-index: Electrotological state indices for number of N-onium group connected with four single bonds.
- xxviii. S₅OHE-index: Electrotological state indices for number of –OH group connected with one single bond.
- xxix. S_dOE-index: Electrotological state indices for number of oxygen atom connected with one double bond.
- xxx. S₅₅OE-index: Electrotological state indices for number of oxygen atom connected with two single bonds.
- xxxi. SaaOE-index: Electrotological state indices for number of oxygen atom connected with two aromatic bonds.
- xxxii. S₅PH2E-index : Electrotological state indices for number of –PH₂ group connected with one single bond.
- xxxiii. S₅₅PHE-index : Electrotological state indices for number of –PH group connected with two single bonds.

- xxxiv. SsssPE-index: Electrotopological state indices for number of phosphorous atom connected with three single bonds.
- xxxv. SdsssPE-index: Electrotopological state indices for number of phosphorous atom connected with three single bonds along with one double bond.
- xxxvi. SsssssPE-index: Electrotopological state indices for number of phosphorous atom connected with five single bonds.
- xxxvii. SsSHE-index: Electrotopological state indices for number of -SH group connected with one single bond.
- xxxviii. SdSE-index: Electrotopological state indices for number of sulphur atom connected with one double bond.
- xxxix. SssSE-index: Electrotopological state indices for number of sulphur atom connected with two single bonds.
 - xl. SaaSE-index: Electrotopological state indices for number of sulphur atom connected with two aromatic bonds.
 - xli. SdssS(sulfone)E-index: Electrotopological state indices for number of sulfone group connected with two single bonds.
 - xl.ii. SdssS(sulfate)E-index: Electrotopological state indices for number of sulfate group connected with two single bonds and two double bonds.
- xl.iii. SsClE-index: Electrotopological state indices for number of chlorine connected with one single bond.
- xl.ii. SsBrE-index: Electrotopological state indices for number of bromine connected with one single bond.
- xl.v. SsIE-index: Electrotopological state indices for number of iodine connected with one single bond.
- xl.vi. SsFE-index: Electrotopological state indices for number of fluorine connected with one single bond.

17. Sub class: Information theory based

- i. Ipc: This is a type of information theory based descriptors.
- ii. IpcAverage: This is a type of information theory based descriptors.
- iii. Id: This is a type of information theory based descriptors.
- iv. IdAverage: This is a type of information theory based descriptors.
- v. Idw: This is a type of information-based descriptors.
- vi. IdwAverage: This is a type of information-based descriptors.
- vii.

18. Sub Class: Extended Topochemical Atom (ETA) based descriptors

- i. VolumeCount: Measure of molecular bulk and represents lipophilicity of a given molecule. [K Roy 2011]
- ii. ElectronegativityCount: Measure of electronegative atom count [K Roy 2011]
- iii. ElectronegativityCountEH: Measure of electronegative atom count excluding hydrogen atoms [K Roy 2011]
- iv. Psil: A measure of hydrogen-bonding propensity of the molecules and/or polar surface area [K Roy 2011]

- v. AlphaR: Indicates sum of alpha value of all non-hydrogen atoms in a reference alkane. The reference alkane is when all heteroatoms in the molecular graph are replaced by carbon and multiple bonds are replaced by single bond, corresponding molecular graph may be considered as the reference alkane [K Roy 2011]
- vi. DeltaAlphaA: A measure of count of non-hydrogen heteroatoms [K Roy 2011]
- vii. DeltaAlphaB: A measure of count of hydrogen bond acceptor atoms and/or polar surface area [K Roy 2011]
- viii. EpsilonR: A measure of electronegativity without considering the heteroatoms and multiple bonds in a molecule. [K Roy 2011]
- ix. EpsilonSS: A measure of electronegativity of saturated carbon skeleton including Hydrogen. [K Roy 2011]
- x. Epsilon3: Measure of electronegative atom count including hydrogen atoms with respect to the saturated hydrocarbon(reference alkane) created from the molecule/fragment under consideration [K Roy 2011]
- xi. Epsilon4: Measure of electronegative atom count including hydrogen atoms with respect to the saturated hydrocarbon(reference alkane) created from the molecule/fragment under consideration [K Roy 2011]
- xii. DeltaEpsilonA: A measure of contribution of unsaturation and electronegative atom count [K Roy 2011]
- xiii. DeltaEpsilonB: A measure of contribution of unsaturation [K Roy 2011]
- xiv. DeltaEpsilonC: A measure of contribution of electronegativity [K Roy 2011]
- xv. DeltaPsiA: A measure of hydrogen-bonding propensity of the molecules [K Roy 2011]
- xvi. DeltaPsiB: A measure of hydrogen-bonding propensity of the molecules [K Roy 2011]

19. Sub class: Hydrophobicity XlogpA

- i. XAHydrophobicArea: vdW surface descriptor showing hydrophobic surface area. (By Audry Method using Xlogp)
- ii. XAHydrophilicArea: vdW surface descriptor showing hydrophilic surface area. (By Audry Method using Xlogp)
- iii. XAMostHydrophobic: Most hydrophobic value on the vdW surface. (By Audry Method using Xlogp)
- iv. XAMostHydrophilic: Most hydrophilic value on the vdW surface. (By Audry Method using Xlogp)
- v. XAAverage: Average hydrophobicity function value. (By Audry Method using Xlogp)
- vi. XAAverageHydrophobicity: Average hydrophobic value on the vdW surface. (By Audry Method using Xlogp)
- vii. XAAverageHydrophilicity: Average hydrophilic value on the vdW surface. (By Audry Method using Xlogp)
- viii. XAMostHydrophobicHydrophilicDistance: This descriptor signifies distance between most hydrophobic and hydrophilic point on the vdW surface. (By Audry Method using Xlogp)

20. Sub class: Hydrophobicity XlogpK

- i. XKHydrophobicArea: vdW surface descriptor showing hydrophobic surface area. (By Kellogg Method using Xlogp)

Tutorial: QSAR

- ii. XKHydrophilicArea: vdW surface descriptor showing hydrophilic surface area. (By Kellog Method using Xlogp)
- iii. XKMostHydrophobic: Most hydrophobic value on the vdW surface. (By Kellog Method using Xlogp)
- iv. XKMostHydrophilic: Most hydrophilic value on the vdW surface. (By Kellog Method using Xlogp)
- v. XKAverage: Average hydrophobicity function value. (By Kellog Method using Xlogp)
- vi. XKAverageHydrophobicity: Average hydrophobic value on the vdW surface. (By Kellog Method using Xlogp)
- vii. XKAverageHydrophilicity: Average hydrophilic value on the vdW surface. (By Kellog Method using Xlogp)
- viii. XKMostHydrophobicHydrophilicDistance: This descriptor signifies distance between most hydrophobic and hydrophilic point on the vdW surface. (By Kellog Method using Xlogp)

21. Sub class: Hydrophobicity SlogpA

- i. SAHydrophobicArea: vdW surface descriptor showing hydrophobic surface area. (By Audry Method using Slogp)
- ii. SAHydrophilicArea: vdW surface descriptor showing hydrophilic surface area. (By Audry Method using SlogP)
- iii. SAMostHydrophobic: Most hydrophobic value on the vdW surface. (By Audry Method using Slogp)
- iv. SAMostHydrophilic: Most hydrophilic value on the vdW surface. (By Audry Method using Slogp)
- v. SAAverage: Average hydrophobicity function value. (By Audry Method using Slogp)
- vi. SAAverageHydrophobicity: Average hydrophobic value on the vdW surface. (By Audry Method using Slogp)
- vii. SAAverageHydrophilicity: Most hydrophilic value on the vdW surface. (By Audry Method using Slogp)
- viii. SAMostHydrophobicHydrophilicDistance: This descriptor signifies distance between most hydrophobic and hydrophilic point on the vdW surface. (By Audry Method using Slogp)

22. Sub class: Hydrophobicity SlogpK

- i. SKHydrophobicArea: vdW surface descriptor showing hydrophobic surface area. (By Kellog Method using Slogp)
- ii. SKHydrophilicArea: vdW surface descriptor showing hydrophilic surface area. (By Kellog Method using Slogp)
- iii. SKMostHydrophobic: Most hydrophobic value on the vdW surface. (By Kellog Method using Slogp)
- iv. SKMostHydrophilic: Most hydrophilic value on the vdW surface. (By Kellog Method using Slogp)
- v. SKAverage: Average hydrophobicity function value. (By Kellog Method using Slogp)
- vi. SKAverageHydrophobicity: Average hydrophobic value on the vdW surface. (By Kellog Method using Slogp)
- vii. SKAverageHydrophilicity: Average hydrophilic value on the vdW surface. (By Kellog Method using Slogp)

- viii. SKMostHydrophobicHydrophilicDistance: This descriptor signifies distance between most hydrophobic and hydrophilic point on the vdW surface. (By Kellog Method using Slogp)

23. Sub class: Polar Surface Area

- i. PolarSurfaceAreaExcludingPandS: This descriptor signifies total polar surface area excluding phosphorous and sulphur.
- ii. PolarSurfaceAreaIncludingPandS: This descriptor signifies total polar surface area including phosphorous and sulphur.

B. Alignment Independent (AI) descriptors class: (more than 700 descriptors)

Alignment Independent descriptors are calculated as discussed in Baumann's paper [1]. For calculation of AI descriptors every atom in the molecule was assigned at least one and at most three attributes. The first attribute is 'T-attribute' to thoroughly characterize the topology of the molecule. The second attribute is the atom type. The atom symbol is used here. The third attribute is assigned to atoms taking part in a double or triple bond. After all atoms have been assigned their respective attributes, selective distance count statistics for all combinations of different attributes are computed [1]. A selective distance count statistic 'XY2' (e.g. 'TOPO2N3') counts all the fragments between start atom with attribute 'X' (e.g. '2' double bonded atom) and end atom with attribute 'Y' (e.g. 'N') separated by the graph distance 3. The graph distance can be defined as the smallest number of atoms along the path connecting two atoms in molecular structure. In this study to calculate AI descriptors, we have used following attributes: 2 (double bonded atom), 3(triple bonded atom), C, N, O, S, H, F, Cl, Br and I and the distance range of 0 to 7.

Some other examples are as follows:

- i. T_2_O_7: This is the count of number of double bounded atoms (i.e. any double bonded atom, T_2) separated from Oxygen atom by 7 bonds in a molecule.
- ii. T_2_N_5: This is the count of number of double bounded atoms (i.e. any double bonded atom, T_2) separated from Nitrogen atom by 5 bonds.
- iii. T_N_N_5: This is the count of number of Nitrogen atoms (single double or triple bonded) separated from any other Nitrogen atom (single double or triple bonded) by 5 bonds in a molecule.
- iv. T_2_2_6: This is the count of number of double bounded atoms (i.e. any double bonded atom, T_2) separated from any other double bounded atom by 6 bonds in a molecule.
- v. T_C_O_1: This is the count of number of Carbon atoms (single double or triple bonded) separated from any Oxygen atom (single or double bonded) by 1 bond distance in a molecule.
- vi. T_O_Cl_5: This is the count of number of Oxygen atoms (single double or triple bonded) separated from Chlorine atom by 5 bond distance in a molecule.

Similarly around 700 alignment independent descriptors can be generated considering topology of the molecule, atom type & bond.

C. Atom type count descriptors class: (total 99 descriptors)

The atom type count descriptors are based on MMFF atom types and their count in each molecule. In MMFF, there are 99 atom types and hence 99 descriptors indicating number of times that atom type has occurred in a given molecule are generated.

Reference:

- [1] A.T. Balaban, Chem. Phys. Letters, 89, 399-404, (1982).
- [2] D. Plavsic, M. Soskic, N. Lers, J. Chem. Inf. Comput. Sci., 38, 889-892,(1998).
- [3] H. Wiener, J. Am. Chem. Soc. 69, 17 (1947).

- [4] M. Randic, in *Encyclopedia of Computational Chemistry*, P.v.R. Schleyer, N. L. Allinger, T. Clark, J. Gasteiger, P. A. Kollman, H. F. Schaefer III, P. R. Schreiner Eds, John Wiley & Sons, Chinchester, 1998, pp. 3018-3032
- [5] D. Bonchev and Trinajstic, *J. Chem. Phys.*, 67, 4517-4533, (1977).
- [6] L.B. Kier and L.H. Hall, *Eur. J. Med. Chem.*, 12, 307 (1977).
- [7] L.H. Hall and L.B. Kier in *Reviews of Computational Chemistry*, Vol. 2, D.B. Boyd and K. Lipkowitz, eds. (1991).
- [8] L.B. Kier, *Quant. Struct-Act. Relat.*, 4, 109 (1985).
- [9] L.H. Hall, B.K. Mohny and L.B. Kier, *J. Chem. Inf. Comput. Sci.*, 31, 76 (1991).
- [10] L.H. Hall and L.B. Kier, *J. Chem. Inf. Comput. Sci.*, 35, 1039-1045 (1995).
- [11] R. Wang, Y. Fu, L. Lai, *J. Chem. Inf. Comput. Sci.*, 37, 615-621 (1997).
- [12] F.C. Wireko, G. E. Kellogg, D. J. Abraham, *J. Med. Chem.*, 34, 758 (1991).
- [13] E. Audry, J.P. Dubost, J.C. Colleter, P. Dallet, *Eur. J. Med. Chem-Chim. Ther.* 21, 71-72, (1986).
- [14] S.A. Wildman, G.M. Crippen, *J. Chem. Inf. Comput. Sci.* 39, 868-873, (1999).
- [15] K. Baumann, *J. Chem. Inf. Comput. Sci.*, 42, 26-35 (2002).
- [16] K. Roy, Das, R. SAR and QSAR in *Environmental Res.*, 22(5-6), 451-472 (2011).

About VLife

VLife is an independent research organization providing enabling software solutions and project-based research services for pharmaceutical, biotech, chemical and agri biotechnology sectors. At VLife, we devise and develop innovative approaches that clearly focus on and directly address various risks in R & D. VLife is equipped with proven technologies that significantly mitigate these risks by allowing better decision making at every step in the discovery process.

REFERENCES

- ¹ Krentz, A.J., and Bailey, C.J. Oral Antidiabetic Agents: Current Role in Type 2 Diabetes Mellitus. **2005**, *Drugs*, 65(3), 385-411.
- ² Loubatieres, A. Effects of Sulfonylureas on the Pancreas. *The Diabetic Pancreas*, Springer Boston, MA, **1977**, 489-515.
- ³ Bolen, S., Feldman, L., Vassy, J., Wilson, L., Yeh, H.C., Marinopoulos, S., Wiley, C., Selvin, E., Wilson, R., Bass, E.B. and Brancati, F.L. Systematic review: comparative effectiveness and safety of oral medications for type 2 diabetes mellitus. **2007**, *Annals of internal medicine*, 147(6), 386-399.
- ⁴ Yang, N.J.Y., Hinner, M.J. Getting Across the Cell Membrane: An Overview for Small Molecules, Peptides and Proteins. *Methods Mol Biol*, **2016**, 1266, 29-53.
- ⁵ Plumpe, H. Sulfonylureas and Related Compounds: Chemistry and Structure-Activity Relationships. Oral Antidiabetics, in: Kuhlmann J., Puls W. (eds) *Oral Antidiabetics. Handbook of Experimental Pharmacology*, **1996**, vol 119. Springer, Berlin, Heidelberg
- ⁶ Vila-Carriles, W.H., Zhao, G., Bryan, J. Defining a binding pocket for the sulfonylureas in ATP-sensitive potassium channels, *The FASEB Journal*, **2007**, 21, 18-25.
- ⁷ Kudaravalli, J., Vijayalakshmi, G., and Kishore, K.K. Safety and Efficacy of Sulfonylurea Drugs in Type 2 Diabetes Mellitus. *Apollo Medicine*, **2013**, Vol 10(2), 165-168.
- ⁸ Vila-Carriles, W.H., Zhao, G., Bryan, J. Defining a binding pocket for the sulfonylureas in ATP-sensitive potassium channels, *The FASEB Journal*, **2007**, 21, 18-25.
- ⁹ Ahr, H.J. *et al.* Oral Antidiabetics In: Kuhlmann J, Puls W, editors. *Handbook of experimental pharmacology: oral Antidiabetics*. Berlin: Springer Verlag, 1995: 7-42.
- ¹⁰ Krentz, A.J. and Bailey, C.J., "Oral Antidiabetic Agents: Current Role in Type 2 Diabetes Mellitus."
- ¹¹ Langer, O. Oral Anti-Hyperglycemic Agents for the Management of Gestational Diabetes Mellitus. *Obstetrics and Gynecology Clinics of North America*, **2007**, 34, 255-274.
- ¹² Rajan, A.S. *et al.* ion Channels and Insulin Secretion. *Diabetes Care*, **1990**, 13(3), 340-363.
- ¹³ Lebovitz, H.E. Insulin secretagogues: old and new. **1999**, *Diabetes Reviews*, 7(3), pp.139-153.
- ¹⁴ Masia, R., Caputa, G., Nichols, CG. Regulation of kATP channel expression and activity by the SUR1 nucleotide binding fold 1. *Channels (Austin)*, **2007**, Jul-Aug 1 (4), 315-323.
- ¹⁵ Ashcroft, F.M. Mechanism of the Glycaemic Effects of Sulfonylureas. *Horm Metab Res*, **1996**, 28(9), 456-463.
- ¹⁶ Langer, O. Oral Anti-Hyperglycemic Agents for the Management of Gestational Diabetes Mellitus. *Obstetrics and Gynecology Clinics of North America*, **2007**, 34, 255-274.

-
- ¹⁷ Aittonieni, J., Fotinou, C., Craig, T.J., Proks, P., and Ashcroft, F.M. Review: SUR1 a unique ATP-binding cassette protein that functions as an ion channel regulator. *Philos Trans R Soc Lond B Biol Sci*, **2009**, 364(1514), 257-267.
- ¹⁸ <http://www.forbes.com/sites/johnfarrell/2013/04/25/harvard-scientists-discover-hormone-that-could-help-treat-diabetes/#7b0a0bf95c27>, Sept 2017.
- ¹⁹ Lebovitz, H.E. Insulin Secretagogues: Sulfonylureas, Meglitinides, and Phenylalanine Derivatives in: LeRoith, D., Taylor, S.I., Olefsy, J.M., editors. *Diabetes Mellitus: A Fundamental and Clinical Text*, 3rd edition, Lippincott William and Wilkins, 2004, 1107-1121.
- ²⁰ Blair, M. Diabetes Mellitus Review. *Urologic Nursing*, **2016**, 36 (1), 27-36.
- ²¹ Scheen, A.J., Pathophysiology of Type 2 Diabetes. *Acta Clinica Belgica*, **2003**, 58-6, 335-341.
- ²² Tahrani, A.A Barnett, A.H., Bailey, C.J. Pharmacology and therapeutic implications of current drugs for type II Diabetes Mellitus. *Nature Reviews Endocrinology*, 2016, v12, n10.
- ²³ Refuerzo, J.S. Oral Hypoglycemic Agents in Pregnancy. *Obstetrics and Gynecology Clinics of North America*, **2011**, 227-234.
- ²⁴ Olokoba, A., Olusegun, A., and Olokoba, L.B. Type 2 Duabetes Mellitus: A Review of Current Trends. *Oman Medical Journal*, **2012**, Vol. 27, No. 4, 269-273.
- ²⁵ Lee-Parritz, A. Contemporary Management of Gestational Diabetes. *Current Opinion in Endocrinology, Diabetes and Obesity*, **2011**, 18, 395-400.
- ²⁶ Moore, T. Glyburide for the Treatment of Gestational Diabetes: A Critical Appraisal. *Diabetes Care*, **2007**, 30 Suppl 2, 5209-5213.
- ²⁷ Gedeon, C., Behravan, J., Kpren, G., Piquette-Miller, M. Transport of Glyburide by Placental ABC Transporters: Implications in Fetal Drug Exposure. Placenta, Breast cancer resistance protein: mediating the trans-placental transfer of glyburide across the human placenta. *Placenta*, **2006**, 27 (11-12), 1096-1102.
- ²⁸ Kimber-Trojnar, Z., Marciniak, B., Trojnar, M., Oleszczuk, J. Glyburide for the treatment of gestational diabetes mellitus. *Pharmacological Reports*, **2008**, 60, 308-318.
- ²⁹ Refuerzo, J.S. Oral Hypoglycemic Agents in Pregnancy. *Obstetrics and Gynecology Clinics of North America*, **2011**, 227-234.
- ³⁰ Poomalar, G. K. Changing trends in management of gestational diabvetes mellitus. *World Journal of Diabetes*, **2015**, 6(2), 284-295.
- ³¹ Reece, E.A., Homko, C. Review: Insulins and Oral Hypoglycemic Agents in Pregnancy. *J Matern Fetal Neonatal Med*. **2006**, 19(11):679-86.
- ³² Lee-Parritz, A. Contemporary Management of Gestational Diabetes. *Current Opinion in Endocrinology, Diabetes and Obesity*, **2011**, 18, 395-400.
- ³³ Shuster, D.L., Hebert, M.F., Mao, Q. Glyburide Disposition During Pregnancy. *Gestational Diabetes*, **2011**, In Tech-Open Access.
- ³⁴ Langer, O. Oral Anti-Hyperglycemic Agents for the Management of Gestational Diabetes Mellitus. *Obstetrics and Gynecology Clinics of North America*, **2007**, 34, 255-274.
- ³⁵ Webster, W.S., Freeman, J.A. Prescription Drugs and Pregnancy. *Expert Opinion Pharmacotherapy* 2003, 4 (6) 949-961

-
- ³⁶ Griffiths, S.K., and Campbell, J.P. Placental Structure, Function, and Drug Transfer. Continuing Education in Anaesthesia Critical Care and Pain. **2015**, Vol 15(2), 84-89.
- ³⁷ Hemhauer, S.J., Patrikeeva, S.L., Nanovskaya, T.N., Hankins, G.D.V., Ahmed, M.S. Role of human placental apical transporters in the efflux of glyburide, rosiglitazone, and metformin. *Am J Obstet Gynecol.* **2010**, 202(4) 383 e1-7
- ³⁸ Lebovitz, H.E. Insulin Secretagogues: Sulfonylureas, Meglitinides, and Phenylalanine Derivatives in: LeRoith, D., Taylor, S.I., Olefsy, J.M., editors. *Diabetes Mellitus: A Fundamental and Clinical Text*, 3rd edition, Lippincott William and Wilkins, 2004, 1107-1121.
- ³⁹ Lee-Parritz, A. Contemporary Management of Gestational Diabetes. *Current Opinion in Endocrinology, Diabetes and Obesity*, **2011**, 18, 395-400.
- ⁴⁰ Gedeon, C., Behravan, J., Kpren, G., Piquette-Miller, M. Transport of Glyburide by Placental ABC Transporters: Implications in Fetal Drug Exposure. Placenta, Breast cancer resistance protein: mediating the trans-placental transfer of glyburide across the human placenta. *Placenta*, **2006**, 27 (11-12), 1096-1102
- ⁴¹ Shuster, D.L., Hebert, M.F., Mao, Q. Glyburide Disposition During Pregnancy. *Gestational Diabetes*, **2011**, In Tech-Open Access.
- ⁴² Nagandla, K., Somsubhra, D., Sachchithanantham, K. Oral Hypoglycemic Agents in Pregnancy: An Update. *The Journal of Obstetrics and Gynecology of India*, March-April **2013**, 63 (2), 82-87.
- ⁴³ Kalra, B., Gupta, Y., Singla, R., Kalra, S. Use of Oral Anti-Diabetic Agents in Pregnancy: A Pragmatic Approach. *North American Journal of Medical Sciences*, **2015**, 7 (1), 6-12.
- ⁴⁴ Luna, B., and Feinglos, M. Oral Agents in the Management of Type 2 Diabetes Mellitus. *Am Fam Physician*, **2001**, 63(9), 1747-1756.
- ⁴⁵ Gedeon, C., Koren, G. Designing Pregnancy Centered Medications: Drugs Which Do Not Cross the Human Placenta. *Placenta*, **2006**, 27, 861-868
- ⁴⁶ Scheen, A.J., Pathophysiology of Type 2 Diabetes. *Acta Clinica Belgica*, **2003**, 58-6, 335-341.
- ⁴⁷ Placental ABC Transporters: Implications in Fetal Drug Exposure. Placenta, Breast cancer resistance protein: mediating the trans-placental transfer of glyburide across the human placenta. *Placenta*, **2006**, 27 (11-12), 1096-1102.
- ⁴⁸ Scheen, A.J., Pathophysiology of Type 2 Diabetes. *Acta Clinica Belgica*, **2003**, 58-6, 335-341.
- ⁴⁹ Kimber-Trojnar, Z., Marciniak, B., Trojnar, M., Oleszczuk, J. Glyburide for the treatment of gestational diabetes mellitus. *Pharmacological Reports*, **2008**, 60, 308-318.
- ⁵⁰ Hemhauer, S.J., Patrikeeva, S.L., Nanovskaya, T.N., Hankins, G.D.V., Ahmed, M.S. Role of human placental apical transporters in the efflux of glyburide, rosiglitazone, and metformin. *Am J Obstet Gynecol.* **2010**, 202(4) 383 e1-7
- ⁵¹ Langer, O., Conway, D., Berkus, M.D., Xenakis, E.M.J., Gonzales, O. A Comparison of Glyburide and Insulin in Women with Gestational Diabetes Mellitus. *The New England Journal of Medicine*, **2000**, 343 (16), 1134-1138.

-
- ⁵² Hebert, M.F., et al for the Obstetric-Fetal Pharmacology Research Unit Network. Are We Optimizing Gestational Diabetes Treatment with Glyburide? The Pharmacological Basis for Better Clinical Practice. *Clinical Pharmacology and Therapeutics*, **2009**, 85 (6), 607-614.
- ⁵³ Swarcz, R., Rosenn, B., Aleska, K., Koren, G. Transplacental transfer of Glyburide: is it clinically significant? *American Journal of Obstetrics and Gynecology*, **2013**, 208 (Suppl 1), S25.
- ⁵⁴ Langer, O. Oral hypoglycemic agents in pregnancy: their time has come. *The Journal of Maternal-Fetal and Neonatal Medicine*, **2002**, 12, 376-383.
- ⁵⁵ Balsells, M. *et al.* Glibenclamide, metformin, and insulin treatment of gestational diabetes: a systemic review and meta-analysis. *British Medical Journal*, **2015**, 350, h102.
- ⁵⁶ Gedeon, C., Koren, G. Designing Pregnancy Centered Medications: Drugs Which Do Not Cross the Human Placenta. *Placenta*, **2006**, 27, 861-868.
- ⁵⁷ Elliott, B.D., Schenker, S., Langer, O., Johnsons, R., Prihoda, T. Comparative placental transport of oral hypoglycemic agents in humans: A model of human placental drug transfer. *American Journal of Obstetrics and Gynecology*, **1994**, 171 (3), 653-660
- ⁵⁸ Gedeon, C., Anger, G., Lubetsky, A., Piquette-Miller, M., Koren, G. Breast Cancer Resistance Protein: Mediating the Trans-Placental Transfer of Glyburide across the Huma Placenta. **2008**, 29(1), 39-43.
- ⁵⁹ Kraemer, J, Klein, J., Lubetsky, A., and Koren, G. Perfusion studies of glyburide transfer across the human placenta: Implications for fetal safety. *American Journal of Obstetrics & Gynecology*, **2006**, Vol 195, Issue 1, 270- 274.
- ⁶⁰ Gedeon, C., Anger, G., Lubetsky, A., Piquette-Miller, M., Koren, G. Investigating the role of multi-drug resistance protein (MRP) transporters in fetal to maternal glyburide efflux in the human placenta. *Journal of Obstetrics and Gynecology*, **2008**, 5, 455-489.
- ⁶¹ Koren, G. Glyburide and Fetal Safety: transplacental pharmacokinetic considerations. *Reproductive Toxicology*, **2001**, 15, 227-229.
- ⁶² Gedeon, C., Anger, G., Lubetsky, A., Piquette-Miller, M., Koren, G. Investigating the role of multi-drug resistance protein (MRP) transporters in fetal to maternal glyburide efflux in the human placenta. *Journal of Obstetrics and Gynecology*, **2008**, 5, 455-489.
- ⁶³ Gedeon, C., Anger, G., Lubetsky, A., Piquette-Miller, M., Koren, G. Breast Cancer Resistance Protein: Mediating the Trans-Placental Transfer of Glyburide across the Huma Placenta. **2008**, 29(1), 39-43.
- ⁶⁴ Gedeon, C., Behravan, J., Kpren, G., Piquette-Miller, M. Transport of Glyburide by Placental ABC Transporters: Implications in Fetal Drug Exposure. *Placenta, Breast cancer resistance protein: mediating the trans-placental transfer of glyburide across the human placenta. Placenta*, **2006**, 27 (11-12), 1096-1102.
- ⁶⁵ Payen L, Delugin L, Courtois A, Trinquart Y, Guillouzo A, Fardel O. The sulfonylurea glibenclamide inhibits multidrug resistance protein (MRP1) activity in human lung cancer cells. *British Journal of Pharmacology* **2001**, 132:778e84.

-
- ⁶⁶ You, G., Morris, M.E. editors. Overview of Drug Transporter Families in Drug Transporters: Molecular Characterization and Role in Drug Disposition, Wiley and Sons, **2007**, 2-3.
- ⁶⁷ Pawagi, A.B., *et al.* Transmembrane Aromatic Amino Acid Distributions in P-glycoprotein: A Functional Role in Broad Substrate Specificity. *Journal of Molecular Biology*, **1994**, Vol 235(2), 554-564.
- ⁶⁸ Terada, T., and Inui, K. Gene expression and regulation of drug transporters in the intestine and kidney. *Biochemical Pharmacology*, **2007**, Vol 73(3), 440-449.
- ⁶⁹ You, G., Morris, M.E. editors. Overview of Drug Transporter Families in Drug Transporters: Molecular Characterization and Role in Drug Disposition, Wiley and Sons, **2007**, 6-7.
- ⁷⁰ Jones, P.M., O'Mara, M.L., George, A.M. ABC Transporters: a riddle wrapped in a mystery inside an enigma. *Trends in Biochemical Sciences*, **2009**, 34 (10), 520-531.
- ⁷¹ Joshi, A.A., *et al.* Placental ABC Transporters: Biological Impact and Pharmaceutical Significance. *Pharmaceutical Research*, **2016**, 33 (12), 2847-2878.
- ⁷² You, G., Morris, M.E. editors. Overview of Drug Transporter Families in Drug Transporters: Molecular Characterization and Role in Drug Disposition, Wiley and Sons, **2007**, 1-10.
- ⁷³ Sharom, F.J. Multidrug Resistance Protein P-Glycoprotein in You, G., Morris, M.E. editors, *Drug Transporters: Molecular Characterization and Role in Drug Disposition*, Wiley and Sons, **2007**, 223-262.
- ⁷⁴ Nies, A.T., Rius, M., Keppler, D. Multidrug Resistance Proteins of the ABCC Subfamily You, G., Morris, M.E. editors, *Drug Transporters: Molecular Characterization and Role in Drug Disposition*, Wiley and Sons, **2007**, 263-318.
- ⁷⁵ Robey, R., Polgar, O., Deeken, J., To, K.K.W., Bates, S. Breast Cancer Resistance Protein in You, G., Morris, M.E. editors, *Drug Transporters: Molecular Characterization and Role in Drug Disposition*, Wiley and Sons, **2007**, 319-358.
- ⁷⁶ Davidson, A.L., Dassa, E., Orelle, C., and Cehn, J. Structure, Function, and Evolution of Bacterial ATP-Binding Cassette Systems. *Microbiol. Mol. Biol. Rev.*, June **2008**, vol. 72 no. 2 317-3641.
- ⁷⁷ Gottesman, M.M., Fojo, T., Bates, S. Multidrug resistance in cancer: role of ATP-dependent transporters. *Nature Reviews Cancer*, **2002**, 2, 48-58.
- ⁷⁸ Elliott, B.D., Schenker, S., Langer, O., Johnsons, R., Prihoda, T. Comparative placental transport of oral hypoglycemic agents in humans: A model of human placental drug transfer. *American Journal of Obstetrics and Gynecology*, **1994**, 171 (3), 653-660.
- ⁷⁹ Gedeon, C.; Koren, G. Designing Pregnancy Centered Medications: Drugs Which Do Not Cross the Human Placenta. *Placenta*, **2006**, 27, 861-868
- ⁸⁰ Gedeon, C.; Anger, G.; Lubetsky, A.; Piquette-Miller, M.; Koren, G. Investigating the role of multi-drug resistance protein (MRP) transporters in fetal to maternal glyburide efflux in the human placenta. *Journal of Obstetrics and Gynecology*, **2008**, 5, 455-489.
- ⁸¹ Gedeon, C.; Anger, G.; Lubetsky, A.; Piquette-Miller, M.; Koren, G. Breast Cancer Resistance Protein: Mediating the Trans-Placental Transfer of Glyburide across the Human Placenta. **2008**, 29(1), 39-43.

-
- ⁸² Gedeon, C.; Behravan, J.; Kpren, G.; Piquette-Miller, M. Transport of Glyburide by Placental ABC Transporters: Implications in Fetal Drug Exposure. Placenta, Breast cancer resistance protein: mediating the trans-placental transfer of glyburide across the human placenta. *Placenta*, **2006**, 27 (11-12), 1096-1102.
- ⁸³ Cygalova, J.H.; Hofman, J.; Ceckova, M.; Staud, F. Transplacental Pharmacokinetics of Glyburide, Rhodamine ₁₂₃, and BODIPY FL Prazosin: Effect of Drug Efflux Transporters and Lipid Solubility. *The Journal of Pharmacology and Experimental Therapeutics*, **2009**, 331 (3) 1118-1125.
- ⁸⁴ Hemhauer, S.J.; Patrikeeva, S.L.; Nanovskaya, T.N.; Hankins, G.D.V.; Ahmed, M.S. Role of human placental apical transporters in the efflux of glyburide, rosiglitazone, and metformin. *Am J Obstet Gynecol.* **2010**, 202(4) 383 e1-7.
- ⁸⁵ Payen L, Delugin L, Courtois A, Trinquart Y, Guillouzo A, Fardel O. The sulfonylurea glibenclamide inhibits multidrug resistance protein (MRP1) activity in human lung cancer cells. *British Journal of Pharmacology* **2001**, 132:778e84.
- ⁸⁶ Goldstein, P.E., Boom, A., van Geffel, J., Jacobs, P., Masereel, B., Beauwens, R. P-glycoprotein inhibition by glibenclamide and related compounds. *European Journal of Physiology*, **1999**, 437, 652-660.
- ⁸⁷ Pollex, E., Lubetsky, A., Koren, G. The Role of Placental Breast Cancer Resistance Protein in the Efflux of Glyburide across the Human Placenta. *Placenta*, **2008**, 743-747.
- ⁸⁸ Ahr, H.J. *et al.* Oral Antidiabetics In: Kuhlmann J, Puls W, editors. Handbook of experimental pharmacology: oral Antidiabetics. Berlin: Springer Verlag, 1995: 7-42.
- ⁸⁹ Krentz, A.J. and Bailey, C.J., "Oral Antidiabetic Agents: Current Role in Type 2 Diabetes Mellitus."
- ⁹⁰ Langer, O. Oral Anti-Hyperglycemic Agents for the Management of Gestational Diabetes Mellitus. *Obstetrics and Gynecology Clinics of North America*, **2007**, 34, 255-274.
- ⁹¹ Lebovitz, H.E. Insulin Secretagogues: Sulfonylureas, Meglitinides, and Phenylalanine Derivatives in: LeRoith, D., Taylor, S.I., Olefsky, J.M., editors. *Diabetes Mellitus: A Fundamental and Clinical Text*, 3rd edition, Lippincott William and Wilkins, 2004, 1107-1121.
- ⁹² Masia, R.; Caputa, G.; Nichols, CG. Regulation of kATP channel expression and activity by the SUR1 nucleotide binding fold 1. *Channels (Austin)*, **2007**, Jul-Aug 1 (4), 315-323.
- ⁹³ Scheen, A.J.; Pathophysiology of Type 2 Diabetes. *Acta Clinica Belgica*, **2003**, 58-6, 335-341.
- ⁹⁴ Tahrani, A.A.; Barnett, A.H.; Bailey, C.J. Pharmacology and therapeutic implications of current drugs for type 2 Diabetes Mellitus, **2016**, 12, 566-592.
- ⁹⁵ Blair, M. Diabetes Mellitus Review. *Urologic Nursing*, **2016**, 36 (1), 27-36.
- ⁹⁶ Kimber-Trojnar, Z.; Marciniak, B.; Trojnar, M.; Oleszczuk, J. Glyburide for the treatment of gestational diabetes mellitus. *Pharmacological Reports*, **2008**, 60, 308-318.

-
- ⁹⁷ Refuerzo, J.S. Oral Hypoglycemic Agents in Pregnancy. *Obstetrics and Gynecology Clinics of North America*, **2011**, 227-234.
- ⁹⁸ Poomalar, G. K. Changing trends in management of gestational diabetes mellitus. *World Journal of Diabetes*, **2015**, 6(2), 284-295.
- ⁹⁹ Lee-Parritz, A. Contemporary Management of Gestational Diabetes. *Current Opinion in Endocrinology, Diabetes and Obesity*, **2011**, 18, 395-400.
- ¹⁰⁰ Nagandla, K.; Somsubhra, D.; Sachchithanatham, K. Oral Hypoglycemic Agents in Pregnancy: An Update. *The Journal of Obstetrics and Gynecology of India*, March-April **2013**, 63 (2), 82-87.
- ¹⁰¹ Kalra, B.; Gupta, Y.; Singla, R.; Kalra, S. Use of Oral Anti-Diabetic Agents in Pregnancy: A Pragmatic Approach. *North American Journal of Medical Sciences*, **2015**, 7 (1), 6-12.
- ¹⁰² Langer, O.; Conway, D.; Berkus, M.D.; Xenakis, E.M.J.; Gonzales, O. A Comparison of Glyburide and Insulin in Women with Gestational Diabetes Mellitus. *The New England Journal of Medicine*, **2000**, 343 (16), 1134-1138.
- ¹⁰³ Hebert, M.F., et al for the Obstetric-Fetal Pharmacology Research Unit Network. Are We Optimizing Gestational Diabetes Treatment With Glyburide? The Pharmacological Basis for Better Clinical Practice. *Clinical Pharmacology and Therapeutics*, **2009**, 85 (6), 607-614.
- ¹⁰⁴ Swarcz, R.; Rosenn, B.; Aleska, K.; Koren, G. Transplacental transfer of Glyburide: is it clinically significant? *American Journal of Obstetrics and Gynecology*, **2013**, 208 (Suppl 1), S25.
- ¹⁰⁵ Langer, O. Oral hypoglycemic agents in pregnancy: their time has come. *The Journal of Maternal-Fetal and Neonatal Medicine*, **2002**, 12, 376-383.
- ¹⁰⁶ Balsells, M. *et al*. Glibenclamide, metformin, and insulin treatment of gestational diabetes: a systemic review and meta-analysis. *British Medical Journal*, **2015**, 350, h102.
- ¹⁰⁷ Elliott, B.D.; Schenker, S.; Langer, O.; Johnsons, R.; Prihoda, T. Comparative placental transport of oral hypoglycemic agents in humans: A model of human placental drug transfer. *American Journal of Obstetrics and Gynecology*, **1994**, 171 (3), 653-660.
- ¹⁰⁸ Sastry, B.V.R. Techniques to study human placental transport. *Advanced Drug Delivery Reviews*, **1999**, 38, 17-39.
- ¹⁰⁹ Zhang, Y., Bachmeier, C., Miller, D.W. In vitro and in vivo models for assessing drug efflux transporter activity. *Advanced Drug Delivery Reviews*, **2003**, 55, 31-51.
- ¹¹⁰ Heaton, S.J., et al. The use of BeWO cells as an in vitro model for the placental iron transport. *American Journal of Physiology-Cell Physiology*, **2008**, 5, 1445-1453.
- ¹¹¹ Unadkat, J.D., Dahlin, A., Vijay, S. Placental Drug Transporters. *Current Drug Metabolism*, **2004**, 5, 125-131.
- ¹¹² Wang, Q., Rager, J.D., Weinstein, K., Kardos, P.S, Dobson, G.L., Li, J. and Hidalgo, I.J. Evaluation of the MDR-MDCK cell line as a permeability screen for the blood-brain barrier. *Int J Pharm*, **2005**, 288(2), 349-359.

-
- ¹¹³ Zhang, Z. and Benet, L. Characterization of P-glycoprotein Mediated Transport of K02, a Novel Vinylsulfone Peptidomimetic Cysteine Protease Inhibitor, Across MDR1-MDCK and Caco2 cell Monolayers. *Pharmaceutical Research*, **1998**, Vol 15(10), 1520-1524.
- ¹¹⁴ Enokizono J, Kusuhara H, Sugiyama Y. Effect of breast cancer resistance protein (Bcrp/Abcg2) on the disposition of phytoestrogens. *Mol Pharmacol*. **2007**, 72, 967-75
- ¹¹⁵ <https://www.nki.nl/divisions/molecular-oncology/borst-p-group/>, March 2018.
- ¹¹⁶ Irvine JD, Takahashi L, Lockhart K, Cheong J, Tolan JW, Selick HE, and Grove JR (1999) MDCK (Madin-Darby canine kidney) cells: A tool for membrane permeability screening. *J Pharm Sci* 88:28-33.
- ¹¹⁷ Pastan, I., *et al.* *Proc Natl Acad Sci USA*. **1988**, 85, 4486-4490
- ¹¹⁸ Feng *et al*, In vitro P-glycoprotein assays to predict the in vivo interactions of P-glycoprotein with drugs in the central nervous system, *Drug Metab Dispos*, **2008**, 36 (2), 268-275.
- ¹¹⁹ Zhou, L. *et al.* The Effect of Breast Cancer Resistance Protein and P-glycoprotein on the Brain Penetration of Flavipiridol, Imatinib Mesylate, Prazosin, and 2-Methoxy-3-(4-(2-(5-methyl-2-phenyloxazol-4-yl)ethoxy)phenyl)propanoic Acid (PF-407288) in Mice. *Drug Metabolism and Disposition*, **2009**, 27, 946-955.
- ¹²⁰ Srinivasan, B. *et al.* TEER Measurement techniques for *on vitro* barrier model systems. *J of laboratory Automation*, **2015**, 20(2), 107-126.
- ¹²¹ Pfizer internal P-glycoprotein Transport Assay Standard Operating Procedure, **2012**.
- ¹²² Pfizer internal Breast Cancer Resistance Protein Transport Assay Standard Operating Procedure, **2012**.
- ¹²³ Feng *et al*, In vitro P-glycoprotein assays to predict the in vivo interactions of P-glycoprotein with drugs in the central nervous system, *Drug Metab Dispos*, **2008**, 36 (2), 268-275.
- ¹²⁴ Varma, M.V.S *et al*, Mechanism Based Pharmacokinetic Modeling to Evaluate Transporter-Enzyme Interplay in Drug Interactions and Pharmacogenetics of Glyburide, *The AAPS Journal*, **2014**, 16 (4), 736-748.
- ¹²⁵ Di L, *et al.* Development of a New Permeability Assay Using Low- Efflux MDCKII Cells. *Journal of Pharmaceutical Sciences*. 2011, 100(11):4974-4985.
- ¹²⁶ Feng *et al*, In vitro P-glycoprotein assays to predict the in vivo interactions of P-glycoprotein with drugs in the central nervous system, *Drug Metab Dispos*, **2008**, 36 (2), 268-275.
- ¹²⁷ Varma, M.V.S *et al*, Mechanism Based Pharmacokinetic Modeling to Evaluate Transporter-Enzyme Interplay in Drug Interactions and Pharmacogenetics of Glyburide, *The AAPS Journal*, **2014**, 16 (4), 736-748.
- ¹²⁸ VLifeMDS,
http://www.vlifesciences.com/products/VLifeMDS/Product_VLifeMDS.php,
March 2018.
- ¹²⁹ Cherkasov, A. *et al.* QSAR Modeling: Where have you been? Where are you going to? *J Med Chem*, **2014**, 57(12), 4977-5010.
- ¹³⁰ ChemDraw, <http://www.cambridgesoft.com/software/overview.aspx>, March 2018.

-
- ¹³¹ ChemAxon Marvin, <https://www.chemaxon.com/products/marvin>, March 2018.
- ¹³² Halgren, T. A. (1996), Merck molecular force field. II. MMFF94 van der Waals and electrostatic parameters for intermolecular interactions. *J. Comput. Chem.*, 17: 520–552.
- ¹³³ Halgren, T. A. (1996), Merck molecular force field. I. Basis, form, scope, parameterization, and performance of MMFF94. *J. Comput. Chem.*, 17: 490–519.
- ¹³⁴ Halgren, T. A. (1996), Merck molecular force field. III. Molecular geometries and vibrational frequencies for MMFF94. *J. Comput. Chem.*, 17: 553–586.
- ¹³⁵ Halgren, T. A. and Nachbar, R. B. (1996), Merck molecular force field. IV. conformational energies and geometries for MMFF94. *J. Comput. Chem.*, 17: 587–615.
- ¹³⁶ Zhu, Hongbo, "IMPLEMENTATION AND APPLICATION OF THE MMFF94 FORCE FIELD" (2014). Student Research Projects, Dissertations, and Theses - Chemistry Department. 45.
- ¹³⁷ Yuriev *et al*, Investigation of structure-activity relationships in a series of glibenclamide analogs, *European Journal of Medicinal Chemistry*, **2004**, 39, 835-847.
- ¹³⁸ L. Lins, R. Brasseur, W.J. Malaisse, *Biochem. Pharmacol.* 50, 1995, 1879–1884
- ¹³⁹ Byrn *et al*, Conformation of Glybriuide in the Solid State and in Solution. *Journal of Pharmaceutical Sciences*, **1986**, Vol. 75 (6), 596-600.
- ¹⁴⁰ W. Grell, R. Hurnaus, G. Griss, R. Sauter, E. Rupprecht, M. Mark, P. Luger, H. Nar, H. Wittneben, P. Muller, *J. Med. Chem.* 41, **1998**, 5219–5246.
- ¹⁴¹ T.J. Hou, Z.M. Li, Z. Li, J. Liu, X.J. Xu, *J. Chem. Inf. Comput. Sci.* 40, **2000**, 1002–1009.
- ¹⁴² Kelsi, H. and Grewal, R.K. Interaction of mouse intestinal P-glycoprotein with the oral antidiabetic drugs and its inhibitors. *Indian J Exp Biol*, **2015**, 53(9), 611-616.
- ¹⁴³ Meyer *et al*. Structural requirements of sulfonylureas and analogues for interaction with sulfonylurea receptor subtypes, *British Journal of Pharmacology*, **1999**, 128, 27-34.
- ¹⁴⁴ Goldstein, P.E., Boom, A., van Geffel, J., Jacobs, P., Masereel, B., Beauwens, R. P-glycoprotein inhibition by Glibenclamide and related compounds. *European Journal of Physiology*, **1999**, 437, 652-660.
- ¹⁴⁵ Abbasii, M.M., *et al*. Inhibition of P-glycoprotein expression and function by anti-diabetic drugs gliclazide, metformin, and pioglitzone *in vitro* and *in situ*, *Research in Pharmaceutical Sciences*, **2016**, 11 (3), 177-186.
- ¹⁴⁶ Roy, K. and Das, R.N. A Review on Principles, Theory and Practices of 2D-QSAR. *Curr Drug Metab.*, **2014**, 15(4), 346-379.
- ¹⁴⁷ Molecular Descriptor Classes in VLifeMDS QSAR, Tutorial QSAR, **2017**. http://www.vlifesciences.com/services/QSAR_Modeling.php
- ¹⁴⁸ Sutter, J.M. and Kalivas, J.H. Comparison of Forward Selection, Backward Elimination, and Generalized Simulated Annealing for Variable Selection. **1993**, *Microchemical Journal*, Vol 47(1-2), 60-66.

-
- ¹⁴⁹ Schneider, A., Hommel, G., and Blettner, M. Linear Regression Analysis: Part 14 of a Series on Evaluation of Scientific Publications, *Dtsch Arztebl Int.* **2010**, 107(44), 776-782.
- ¹⁵⁰ Obtaining 3D QSAR models by kNN-MFA methods using VLifeMDS QSAR, VLifeMDS Product Documentation, Tutorial QSAR, **2017**.
http://www.vlifesciences.com/services/QSAR_Modeling.php
- ¹⁵¹ Obtaining conventional QSAR model by Partial Least Squares Regression method using VLifeMDS, Tutorial QSAR, **2017**.
http://www.vlifesciences.com/services/QSAR_Modeling.php
- ¹⁵² Schneider, A., Hommel, G., and Blettner, M. Linear Regression Analysis: Part 14 of a Series on Evaluation of Scientific Publications, *Dtsch Arztebl Int.* **2010**, 107(44), 776-782.
- ¹⁵³ Obtaining Conventional QSAR models using VLifeMDS. VLifeMDS Product Documentation, Tutorial QSAR, **2017**.
http://www.vlifesciences.com/services/QSAR_Modeling.php
- ¹⁵⁴ Noolvi, M.N.; Patel, H.M. A Comparative QSAR analysis and molecular docking studies of quinazoline derivatives as tyrosine kinase (EGFR) inhibitors: a rational approach to anticancer drug design, *Journal of Saudi Chemical Society*, **2013**, 17, 361-379.
- ¹⁵⁵ Jun Shao, *Journal of the American Statistical Association* Vol. 88, No. 422 (Jun., 1993), pp. 486-494.
- ¹⁵⁶ Obtaining Conventional QSAR models using VLifeMDS. VLifeMDS Product Documentation, Tutorial QSAR, **2017**.
http://www.vlifesciences.com/services/QSAR_Modeling.php
- ¹⁵⁷ Obtaining Conventional QSAR models using VLifeMDS. VLifeMDS Product Documentation, Tutorial QSAR, **2017**.
http://www.vlifesciences.com/services/QSAR_Modeling.php
- ¹⁵⁸ Obtaining Conventional QSAR models using VLifeMDS. VLifeMDS Product Documentation, Tutorial QSAR, **2017**.
http://www.vlifesciences.com/services/QSAR_Modeling.php
- ¹⁵⁹ Schneider, A., Hommel, G., and Blettner, M. Linear Regression Analysis: Part 14 of a Series on Evaluation of Scientific Publications, *Dtsch Arztebl Int.* **2010**, 107(44), 776-782.
- ¹⁶⁰ Streitwieser, A. and Taft, R.W., eds. Wiley Interscience, 1972, *Progress in Phys Organic Chem* volume 9, pg 64.
- ¹⁶¹ Molecular Descriptor Classes in VLifeMDS QSAR, Tutorial QSAR, **2017**.
http://www.vlifesciences.com/services/QSAR_Modeling.php
- ¹⁶¹ Gasteiger J, Marsili M. Iterative partial equalization of orbital electronegativity—a rapid access to atomic charges. *Tetrahedron.* **1980**, 36(22), 3219–3228.
- ¹⁶³ Noolvi, M.N.; Patel, H.M. A Comparative QSAR analysis and molecular docking studies of quinazoline derivatives as tyrosine kinase (EGFR) inhibitors: a rational approach to anticancer drug design, *Journal of Saudi Chemical Society*, **2013**, 17, 361-379
- ¹⁶⁴ IUPAC definition, <http://www.sbcs.qmul.ac.uk/iupac/medchem/ix.html#p7>. March 2018.

-
- ¹⁶⁵ Bessadock *et al.* Recognition of Sulfonylurea Receptor (ABCC8/9) Ligands by the Multidrug Resistance Transporter P-glycoprotein (ABCB1), *Journal of Biological Chemistry*, **2011**, 286 (5), 3552-3569.
- ¹⁶⁶ Tokyo Transporter database, <http://togodb.dbcls.jp/tpssearch>, 2017.
- ¹⁶⁷ Goldstein, P.E., Boom, A., van Geffel, J., Jacobs, P., Masereel, B., Beauwens, R. P-glycoprotein inhibition by glibenclamide and related compounds. *European Journal of Physiology*, **1999**, 437, 652-660.
- ¹⁶⁸ Abbasi *et al.* Inhibition of P-glycoprotein expression and function by anti-diabetic drugs gliclazide, metformin, and pioglitazone *in vitro* and *in situ*, *Research in Pharmaceutical Sciences*, **2016**, 11 (3), 177-186.
- ¹⁶⁹ Abbasi *et al.* Inhibition of P-glycoprotein expression and function by anti-diabetic drugs gliclazide, metformin, and pioglitazone *in vitro* and *in situ*, *Research in Pharmaceutical Sciences*, **2016**, 11 (3), 177-186.
- ¹⁷⁰ Meyer, Miriam *Br J Pharmacol.* 1999 Sep; 128(1): 27-34.
- ¹⁷¹ Vila-Carriles, W.H., Zhao, G., Bryan, J. Defining a binding pocket for the sulfonylureas in ATP-sensitive potassium channels, *The FASEB Journal*, **2007**, 21, 18-25.
- ¹⁷² Bessadock *et al.* Recognition of Sulfonylurea Receptor (ABCC8/9) Ligands by the Multidrug Resistance Transporter P-glycoprotein (ABCB1), *Journal of Biological Chemistry*, **2011**, 286 (5), 3552-3569.
- ¹⁷³ Rosenberg, M.F., *et al.* Three-dimensional structure of the human breast cancer resistance protein (BCRP/ABCG2) in an inward-facing conformation. *Acta Crystallogr D Biol Crystallogr*, **2015**, 71(8), 1725-1735.
- ¹⁷⁴ Aller, S.G., *et al.* Structure of P-glycoprotein Reveals a Molecular Basis for Poly-Specific Drug Binding, *Science*, **2009**, 323(5922), 1718-1722.
- ¹⁷⁵ Chang, C. and Ekins, S. Pharmacophores for Human ADME/Tox- Related Proteins. **2006**, In *Pharmacophores and Pharmacophore Searches* (eds R. Mannhold, H. Kubinyi, G. Folkers, T. Langer and R. D. Hoffmann).
- ¹⁷⁶ Elliott, B.D., Schenker, S., Langer, O., Johnsons, R., Prihoda, T. Comparative placental transport of oral hypoglycemic agents in humans: A model of human placental drug transfer. *American Journal of Obstetrics and Gynecology*, **1994**, 171 (3), 653-660.
- ¹⁷⁷ Gedeon, C.; Koren, G. Designing Pregnancy Centered Medications: Drugs Which Do Not Cross the Human Placenta. *Placenta*, **2006**, 27, 861-868
- ¹⁷⁸ Gedeon, C.; Anger, G.; Lubetsky, A.; Piquette-Miller, M.; Koren, G. Investigating the role of multi-drug resistance protein (MRP) transporters in fetal to maternal glyburide efflux in the human placenta. *Journal of Obstetrics and Gynecology*, **2008**, 5, 455-489.
- ¹⁷⁹ Gedeon, C.; Anger, G.; Lubetsky, A.; Piquette-Miller, M.; Koren, G. Breast Cancer Resistance Protein: Mediating the Trans-placental Transfer of Glyburide across the Human Placenta. **2008**, 29(1), 39-43.
- ¹⁸⁰ Gedeon, C.; Behravan, J.; Kpren, G.; Piquette-Miller, M. Transport of Glyburide by Placental ABC Transporters: Implications in Fetal Drug Exposure. *Placenta*, Breast cancer resistance protein: mediating the trans-placental transfer of glyburide across the human placenta. *Placenta*, **2006**, 27 (11-12), 1096-1102

-
- ¹⁸¹ Cygalova, J.H.; Hofman, J.; Ceckova, M.; Staud, F. Transplacental Pharmacokinetics of Glyburide, Rhodamine ₁₂₃, and BODIPY FL Prazosin: Effect of Drug Efflux Transporters and Lipid Solubility. *The Journal of Pharmacology and Experimental Therapeutics*, **2009**, 331 (3) 1118-1125.
- ¹⁸² Pollex, E., Lubetsky, A., Koren, G. The Role of Placental Breast Cancer Resistance Protein in the Efflux of Glyburide across the Human Placenta. *Placenta*, **2008**, 743-747.
- ¹⁸³ Payen L, Delugin L, Courtois A, Trinquart Y, Guillouzo A, Fardel O. The sulfonylurea glibenclamide inhibits multidrug resistance protein (MRP1) activity in human lung cancer cells. *British Journal of Pharmacology* **2001**, 132:778e84.
- ¹⁸⁴ Abbasii *et al.* Inhibition of P-glycoprotein expression and function by anti-diabetic drugs gliclazide, metformin, and pioglitzone *in vitro* and *in situ*, *Research in Pharmaceutical Sciences*, **2016**, 11 (3), 177-186.
- ¹⁸⁵ References for GLY and other SUs
- ¹⁸⁶ Abbasii, M.M., *et al.* Inhibition of P-glycoprotein expression and function by anti-diabetic drugs gliclazide, metformin, and pioglitzone *in vitro* and *in situ*, *Research in Pharmaceutical Sciences*, **2016**, 11 (3), 177-186.
- ¹⁸⁷ Glipizide ref
- ¹⁸⁸ Lins, L., Brasseur, R., and Malaisse, W.J. *Biochem. Pharmacol.* 50, 1995, 1879–1884
- ¹⁸⁹ ChemDraw, <http://www.cambridgesoft.com/software/overview.aspx>.
- ¹⁹⁰ ChemAxon Marvin, <https://www.chemaxon.com/products/marvin>
- ¹⁹¹ Lins, L., Brasseur, R., and Malaisse, W.J. *Biochem. Pharmacol.* 50, 1995, 1879–1884
- ¹⁹² Cruz-Montegudo, M. *et al.* Activity Cliffs in drug discovery: Dr Jekyll or Mr Hyde? *Drug Discovery Today*, **2014**, 19 (8), August, 1069-1080.
- ¹⁹³ Tedesco, G. Tackling selectivity with Activity Atlas, **2012**, www.cresset-group.com.
- ¹⁹⁴ Hu, Ye, Dagmar Stumpfe, and Jürgen Bajorath. “Advancing the Activity Cliff Concept.” *FI000Research 2* (**2013**): 199. *PMC*.
- ¹⁹⁵ Cheesewright, T.; Macke, M.; Rose, S.; and Vinter, A.; Molecular Field Extrema as Descriptors of Biological Activity: Definition and Validation. *J. Chem. Inf. Model*, 2006, 46, 665-676.
- ¹⁹⁶ <https://www.cresset-group.com/tag/activity-atlas/> reference for coefficient calculations. Sept, 2017.
- ¹⁹⁷ Refs for 1st vs 2nd generation efflux
- ¹⁹⁸ Gottesman, M. Mechanism of Cancer Drug Treatment, *Annu Rev Med*, **2002**, 53, 615-627.
- ¹⁹⁹ Refs for Pgp/BCRP specific interactions
- ²⁰⁰ Matsson, P. *et al.* A global Drug Inhibition Pattern for the Human ATP-Binding Cassette Transporter Breast Cancer Resistance Protein (ABCG2). *Journal of Pharmacology and Experimental Therapeutics*, **2007**, 323 (1), 19-30.
- ²⁰¹ Kelin, *et al.* An inventory of the Human ABC Proteins. *Biochimica et Biophysica Acta*, **1999**, 1461, 237-262.

²⁰² Higgins, C.F. ABC transporters: physiology, structure and mechanism – an overview. *Res Microbiol*, **2001**, 152, 205-210.